FINAL REPORT

Reducing Air Pollution Exposure in Passenger Vehicles and School Buses

Contract Number 11-310

Prepared by
Dr. Yifang Zhu (Principal Investigator)
and Dr. Eon Lee

UCLA Fielding School of Public Health
Department of Environmental Health Sciences

April 10, 2015

Prepared for the California Air Resources Board and
the California Environmental Protection Agency

I.   DISCLAIMER

The statements and conclusions in this Report are those of the contractor and not necessarily those of the California Air Resources Board (ARB). The mention of commercial products, their source, or their use in connection with material reported herein is not to be construed as actual or implied endorsement of such products.

II.   ACKNOWLEDGMENT

III. TABLE OF CONTENTS

IV. LIST OF FIGURES

V. LIST OF TABLES

VI. ABSTRACT

Exposures to vehicle-emitted $PM_{2.5}$, black carbon (BC), and ultrafine particles (UFPs), have been associated with adverse health effects. As a potential strategy to mitigate in-cabin exposure, the authors developed a novel high efficiency cabin air (HECA) filter for passenger vehicles and an on-board HECA filtration system for school buses. Their performance was evaluated in twelve passenger vehicles and six school buses, respectively. UFP number concentration and size distribution as well as BC and $PM_{2.5}$ levels were concurrently monitored inside and outside of each vehicle under three driving conditions: stationary, on local roadways, and on freeways. For passenger vehicles, data were collected with no filter, the in-use original equipment manufacturer (OEM) filter, and two prototypes of HECA filters (i.e., HECA A and B filters). For school buses, data were collected with and without operating the filtration system equipped with HECA B filters. For passenger vehicles, the HECA B filters offered in-cabin concentration reductions of 90 ± 8% for UFPs on average across all driving conditions, much higher than the OEM filters (50 ± 11% on average). Similarly, the HECA B filters offered an 81 ± 15% reduction for BC and 66 ± 28% for $PM_{2.5}$ across all driving conditions. In comparison, across all driving conditions, in-use OEM filters only provided 31 ± 17% and 29 ± 20% reduction for BC and $PM_{2.5}$, respectively. For school buses, across all driving conditions, in-cabin UFP and BC levels were reduced by 88 ± 6% and 84 ± 5% on average, respectively, when the on-board HECA filtration system was operating. The HECA system achieved 55 ± 22% reductions on average for $PM_{2.5}$ and successfully kept its levels below 12 µg/m^3.

VII. EXECUTIVE SUMMARY

BACKGROUND
Exposures to high levels of traffic-related particulate matter (PM) such as ultrafine particles (UFPs, diameter ≤ 100 nm), black carbon (BC), and $PM_{2.5}$ (aerodynamic diameter ≤ 2.5 μm) have been associated with pulmonary and cardiovascular health risks (Gilmour et al., 2004; Oberdorster, 2001; Weichenthal et al., 2013). Since children are in the developing stage for their pulmonary function and immune system, they are particularly vulnerable to traffic-related pollutants (Sabin et al., 2005; Song et al., 2013). The on-road UFP concentrations typically range from 10,000 to 500,000 particles/cm^3 (Zhu et al., 2007), one or two orders of magnitude higher than typical ambient levels in an urban environment. Despite the short average commuting time among Californians (1.3 h/day) (Klepeis et al., 2001), in-cabin exposure alone accounts for up to 45–50% of the total daily exposure to UFPs (Fruin et al., 2008; Zhu et al., 2007). High pollutant levels have been observed inside school buses not only under normal driving conditions (Behrentz et al., 2004; Sabin et al., 2005), but also under idling (Zhang et al., 2013). Children commuting in school buses may experience exposure levels even higher than regular commuters in passenger cars.

Modern passenger vehicles are commonly equipped with cabin air filters (Qi et al., 2008); however, their overall protection against UFPs is limited to 40–60% under outdoor air (OA) mode and the filtration efficiency varies as a function of particle size (Qi et al., 2008; Xu et al., 2011). Operating the automotive ventilation system under recirculation (RC) mode can achieve a protection of ~ 90% using original equipment manufacturer (OEM) filters (Pui et al., 2008; Zhu et al., 2007). However, under RC mode, passenger-exhaled CO_2 can accumulate rapidly in the vehicle cabin due to limited air exchange (Lee and Zhu, 2014; Zhu et al., 2007). Exposures to high CO_2 concentration of 1,000 ppm can significantly reduce decision-making-performances (Satish et al., 2012). Therefore, it is important to reduce both UFPs and CO_2 concentrations simultaneously inside vehicles. Retrofitting school buses is promising for tailpipe emission control but not necessarily true for in-cabin exposure reduction (Hammond et al., 2007; Rim et al., 2008; Trenbath et al., 2009; Zhang and Zhu, 2010). Mitigating children's exposure to particulate pollutants inside school buses with the application of high efficiency cabin air (HECA) filters directly addresses the ARB's concern with protecting children's health. The overall objective of this study is to develop cost effective techniques to reduce in-cabin fine and ultrafine particle levels and provide data that can be used by ARB to incorporate into future in-cabin air pollution exposure guidelines or regulations.

METHODS
Two types of HECA filters (A and B) were developed in collaboration with an industrial partner. The developed filter was manufactured with nano-fibers much smaller in diameter (A: 1−3 μm and B: 0.4−0.8 μm) than typical fibers (2−5 μm) used in commercial cabin air filters. The HECA A filter prototypes were designed to increase particle removal efficiency and maintain an acceptable pressure drop. The HECA B filter prototypes were

developed to maximize particle removal efficiency. Field measurements were conducted to evaluate to what extent the developed HECA filters can reduce passenger exposures to UFPs, $PM_{2.5}$ and BC. In the first phase, 12 passenger vehicles of different models and types from several automobile manufacturers were selected and evaluated. The HECA filters were retrofitted in the existing passenger vehicle ventilation system. In-cabin UFP reductions were compared under three driving conditions (i.e., stationary, on local roadway, and on freeway) under four different filtration scenarios: no filter, in-use OEM filter, and two prototypes of HECA filters (i.e., A and B filters). In the second phase, a prototype on-board filtration system was developed specifically for school buses using the HECA B filter. Its performance was evaluated in six school buses under various field conditions.

RESULTS and DISCUSSION
Substantial reductions of particulate pollutants were observed in passenger vehicles with the HECA filters and in school buses with operating the on-board HECA filtration system. For passenger vehicles, the developed HECA filters removed in-cabin particulate pollutants more effectively than OEM filters. For both passenger vehicles and school buses, the application of HECA filtration was effective in removing UFPs and BC (80–90% for UFPs and 65–90% for BC on average under different driving conditions). The effectiveness was relatively lower for $PM_{2.5}$ (30–75% on average under different driving conditions). This is likely due to the different size ranges of these particulate pollutants. The removal efficiency of fibrous filters depends largely on particle diameters. It is well known, particles of smaller sizes (e.g., UFPs and BC) are likely removed by Brownian diffusion. $PM_{2.5}$, on the other hand, is more likely removed by impaction due to particle inertia. It is also important to note that the concentration units used for $PM_{2.5}$ and BC are in mass concentration; whereas, UFPs are measured in number concentrations. The mass concentration can be more sensitive to changes of a few large particles than many small particles. In particular, under OA mode of passenger vehicles, the application of HECA filtration achieved high UFP mitigation while avoiding the CO_2 accumulation problem. Throughout the measurements in 12 passenger vehicles, the in-cabin CO_2 concentration remained in the range of 620–930 ppm, significantly lower than the typical level of 2,500–4,000 ppm observed in the RC mode.

CONCLUSIONS
The application of HECA filters substantially reduced the level of particulate pollutants in both passenger vehicles and school buses. In passenger vehicles, a simple retrofit application of the HECA filter reduced the in-cabin particulate pollutant concentrations by 89%, 82%, and 64% on average for UFPs, BC, and $PM_{2.5}$, respectively. The on-board HECA filtration system achieved similar results in school buses. The application of this technology also kept in-cabin CO_2 concentrations below 1,000 ppm under OA mode. In-cabin $PM_{2.5}$ was also reduced from approximately 35 $\mu g/m^3$ to 10 $\mu g/m^3$. This proof-of-concept study concludes that the HECA technology can significantly reduce human exposures to UFPs, BC, and $PM_{2.5}$ in passenger vehicles and school buses. Practical application of the HECA filter, however, requires long-term evaluations under a broader range of vehicle models and driving conditions.

1. INTRODUCTION

Epidemiological studies have reported deleterious health effects of traffic emissions (Pope et al., 1995) that contain particulate matter (PM) of different sizes such as $PM_{2.5}$ (aerodynamic diameter ≤ 2.5 μm), black carbon (BC), and ultrafine particles (UFPs, diameter ≤ 100 nm). Exposures to high levels of UFPs, BC, and $PM_{2.5}$ have been associated with pulmonary and cardiovascular health risks (Gilmour et al., 2004; Oberdorster, 2001; Weichenthal et al., 2013). UFPs have been shown to induce oxidative stress, mitochondria damage, and acute pulmonary inflammation (Kroll et al., 2013; Li et al., 2003; Strak et al., 2012). Children are a particularly vulnerable sub-population (Sabin et al., 2005; Song et al., 2013) because they are in the developing stage for pulmonary function and immune system. In addition, exposures to particulate pollutants were also found to be associated with poor academic performance among school-age children (Mohai et al., 2011).

Previous studies have shown that traffic emissions significantly increase in-cabin concentrations of UFP, BC, and $PM_{2.5}$ on local arterial roadways and freeways (Hitchins et al., 2000; Morawska et al., 2008; Tainio et al., 2005). The on-road UFP concentration typically ranges from 10,000 to 500,000 particles/cm^3 (Zhu et al., 2007), one or two orders of magnitude higher than a typical ambient level in an urban environment. Despite the short average commuting time among Californians (1.3 h/day) (Klepeis et al., 2001), in-cabin exposure alone accounts for up to 45–50% of the total daily exposure to UFPs (Fruin et al., 2008; Zhu et al., 2007). In addition to the pollutants originating from surrounding traffic, school buses' own exhaust can also penetrate into the bus cabin, the so-called self-pollution (Behrentz et al., 2004; Ireson et al., 2011; Marshall and Behrentz, 2005; Sabin et al., 2005). High pollutant levels have been observed not only under driving conditions, but also under idling (Zhang et al., 2013). Children commuting in school buses may be exposed to even higher pollutant concentrations than regular commuters in passenger vehicles (Zhu et al., 2007).

Previous in-cabin air pollution exposure studies have focused primarily on PM in a larger size range, e.g., PM_{10} (aerodynamic diameter ≤ 10 μm) and $PM_{2.5}$, metals, and gas-phase pollutants such as carbon monoxide (CO), nitric oxides (NOx), and volatile organic compounds (VOCs) (Chan and Chung, 2003; Chan and Liu, 2001; Leung and Harrison, 1999). These investigators found ventilation settings and vehicle types had little effect on in-cabin pollutant levels. In contrast, recent studies focusing on UFPs have found commuter exposure was strongly related to their choice of ventilation setting (Knibbs et al., 2010). Based on field measurements inside three passenger cars, the overall passenger protection against UFPs was found to vary between 20% and 90% with respect to vehicle type and age and in-cabin ventilation settings (Zhu et al., 2007). Maximum protection (~ 85%) inside passenger cars was obtained under recirculation (RC) mode (Zhu et al., 2007).

There are many factors affecting commuter exposure to fine and ultrafine particles. These include on-roadway particle concentrations, air exchange rate (AER), particle penetration factors, deposition rate inside vehicles, and in-cabin filter efficiency (Xu and

Zhu, 2009). On-roadway levels, affected by emissions from surrounding vehicles, are by far the most important factor determining in-cabin exposure. Besides on-roadway pollutant levels, AER and vehicle ventilation setting are also important factors affecting in-cabin UFP levels. A wide range of vehicle AER, from 1.6 h^{-1} to 71 h^{-1}, has been reported depending on vehicle speed, window position, ventilation system, and AC settings (Fletcher and Saunders, 1994; Ott and Siegmann, 2006). With closed windows and passive ventilation, the AER was linearly related to the vehicle speed over a range from 15 to 72 mph. Opening a single window by 7.6 cm increased the AER by 8–16 times. AER values at higher fan settings under outside air (OA) mode have been reported to be 73% higher than at lowest fan setting (Knibbs et al., 2009a; Knibbs et al., 2009b). AERs could be an order of magnitude higher under OA mode than under RC mode and were primarily driven by blower fan speed not vehicle speed (Fruin et al., 2011). Greater variation of AERs was also reported for running buses. Rim and colleagues (2008) found the AERs in school buses with windows closed were 2.9 ~ 5.1 h^{-1} when driving on a typical route in suburban Austin, TX. In the study of Sabin et al. (2005), the school bus AERs with windows closed were between 15.2 and 94.6 h^{-1}, depending on driving speeds. When windows were open, the AER became even greater, varying from 14.0 to 224.7 h^{-1}.

Previously the authors have developed a theoretical model to investigate the particle in-cabin to on-roadway (I/O) concentration ratios for passenger vehicles (Xu and Zhu, 2009). They found the most significant drivers of I/O ratios were ventilation conditions and filtration efficiency of cabin filters (Xu and Zhu, 2009). Under three different ventilation conditions, (1) Fan off-RC off, (2) Fan on-RC off, and (3) Fan on-RC on, the modeled UFP I/O ratios were found to be 0.40, 0.25 and 0.10, respectively (Xu and Zhu, 2009). These results agree well with experimental data collected inside passenger vehicles (Zhu et al., 2007). Although recirculating cabin air decreases in-cabin UFP levels, a rapid build-up of in-cabin CO_2 levels will occur under this ventilation condition because there is a minimal air exchange between the in-cabin and the outside. In some cases, CO_2 from exhaled breath of passengers can build up within a few minutes and exceed Cal-OSHA exposure limits in cars when vents are set to RC on and windows are closed (Zhu et al., 2007). Although CO_2 is non-toxic at the atmospheric concentration, exposure to high CO_2 concentration was associated with a variety of health effect, such as dry eyes, sore throat and nose, wheeze and other respiratory illnesses (Apte et al., 2000). In sensitive population, the health effect of high CO_2 exposure is more severe. Patients with bipolar disorder were more anxious and breathed more deeply and rapidly when exposed to high CO_2 levels (MacKinnon et al., 2007). In comparison to 600 ppm CO_2, human exposed to CO_2 level of 1000 ppm had decreased decision-making performances in four categories (i.e., basic activity, applied activity, information usage, and breath of approach). Exposures to 2500 ppm CO_2 significantly reduced the decision-making performances in four more categories (i.e., focused activity, task orientation, initiative, and basic strategy) (Satish et al., 2012). To overcome the CO_2 build up issue, sufficient air exchange between in-cabin and outside is needed. Under "vent open–OA mode" condition, improving cabin filter efficiency is a promising low-cost strategy to reduce in-cabin $PM_{2.5}$ and UFP exposures.

Tremendous progress has been made to reduce vehicular emissions by tightening emission standards and retrofitting school buses. Retrofitting school buses with diesel oxidation catalysts and crankcase filtration systems have been widely used. The effectiveness of the retrofit technologies is promising for tail-pipe emission control but not necessarily true for in-cabin exposure reduction (Hammond et al., 2007; Rim et al., 2008; Trenbath et al., 2009; Zhang and Zhu, 2010). However, the potential to further reduce population exposure to vehicle-related pollutants by reducing the proportion of on-roadway pollutants penetrating into and remaining inside vehicles is largely overlooked. Currently, most of the modern passenger vehicles are equipped with cabin air filters; however, the overall protection against UFPs is limited to 40–60% under OA mode and the filtration efficiency varies as a function of particle size (Qi et al., 2008; Xu et al., 2011). A large number of school buses are not equipped with any mechanical ventilation or filtration systems. Although some newer school buses have an air-conditioning unit with an air filter, the purpose of the filter is primarily for removing large debris to protect the mechanical ventilation system.

This study aims to achieve a reduction of passenger exposures to particulate pollutants under OA mode ventilation in a wide range of passenger vehicles. In addition to controlling in-cabin UFP level, this method can solve the CO_2 accumulation problem by using the OA mode ventilation. The authors developed high-efficiency cabin air (HECA) filtration to replace the automotive cabin air filter in passenger vehicles. Field measurements were conducted in 12 vehicles of different models and types from several automobile manufacturers. In-cabin UFP reductions were compared under three driving conditions (i.e., stationary, on local roadway, and on freeway) with four different filtration scenarios: no filter, in-use original equipment manufacturer (OEM), and two prototypes of HECA filters. The authors also developed a prototype on-board filtration system using the same type of HECA filters, but specifically designed for school buses. Field measurements were conducted to evaluate its effectiveness in reducing children's exposure to particulate pollutants in six school buses under various field scenarios, including stationary, local roadway, and freeway driving conditions.

The overall objective of this study is to develop effective techniques to reduce in-cabin fine and ultrafine particle levels and to provide data that can be used by ARB to incorporate into future in-cabin air pollution exposure guidelines or regulations. The specific objective of this study is summarized as followed:

- To determine to what extent an in-cabin HECA filter can reduce fine and ultrafine particle levels inside passenger vehicles.
- To identify important factors affecting HECA filter's performance inside vehicles.
- To determine to what extent operating an on-board HECA filtration system could reduce fine and ultrafine particle levels in school buses.
- To identify important factors affecting the on-board HECA filtration system inside school buses.

3

2. MATERIALS AND METHODS

2.1 Development of High-Efficiency Cabin Air (HECA) Filters

Since high efficiency filters are not currently marketed for passenger vehicles, two types of automotive HECA filters (noted here as HECA A and HECA B) were developed in collaboration with an industrial partner. The two HECA filters were similar to OEM cabin air filters in terms of their structure, i.e., the pleated panel type, but differed in the filtration media. Whereas OEM filters are typically composed of a single layer of glass fibers, the developed HECA filters were manufactured with a double layer, with synthetic fibers on the upstream side and glass fibers on the downstream side. The application of synthetic fibers with different physicochemical properties (e.g., diameter, material, and density) on the upstream layer allows the HECA filters to achieve significantly higher filtration efficiency than OEM filters. The HECA A filters were designed to maintain a pressure drop equivalent to the OEM filters (~36 mm H_2O under the standard minimum efficiency reporting value (MERV) testing condition) by increasing the intrinsic surface area, while maintaining the same filtration material volume by using fibers of smaller diameters (1–3 µm). The HECA B filters were designed to maximize the filtration efficiency using 0.4–0.8 µm diameter fibers with a slightly higher pressure drop (~50 mm H_2O under the standard MERV testing condition). The testing was conducted with air-flow rate of 3,344 m^3/h and face velocity of 2.5 m/s in temperature and relative humidity controlled (i.e., 23°C and 50% RH) condition. Figures 1 and 2 present the SEM images of the two HECA filters, respectively.

Because currently there is no standard efficiency rating for OEM filters, the HECA filters were graded using the MERV standard developed by American Society of Heating, Refrigerating and Air-Conditioning Engineers (ASHRAE) for building heating, ventilating, and air-conditioning (HVAC) systems (ASHRAE, 2007). When challenged with potassium chloride particles of 0.3 µm diameter in a standardized lab environment (ASHRAE, 2007), the HECA A and B filters achieved an averaged filtration efficiency of 92% and 99%, respectively. This is equivalent to a MERV rating of 15 and 16, respectively (See Figures 3 and 4). The tests were conducted with particles at a constant air flow rate and face velocity of 3,344 m^3/h and 2.5 m/s, respectively. In Figure 3, the filtration efficiencies of the HECA A filter increases from 87% at the first loading to 95% at the fifth loading for 0.3 µm particles. However, as shown in Figure 4, the HECA B filter consistently provides filtration efficiency at 99% during the testing.

Figure 1. Scanning electron microscope (SEM) image of HECA A filter with synthetic fibers of 1–3 μm in diameter.

Figure 2. Scanning electron microscope (SEM) image of HECA B filter with synthetic fibers of 400–800 nm in diameter.
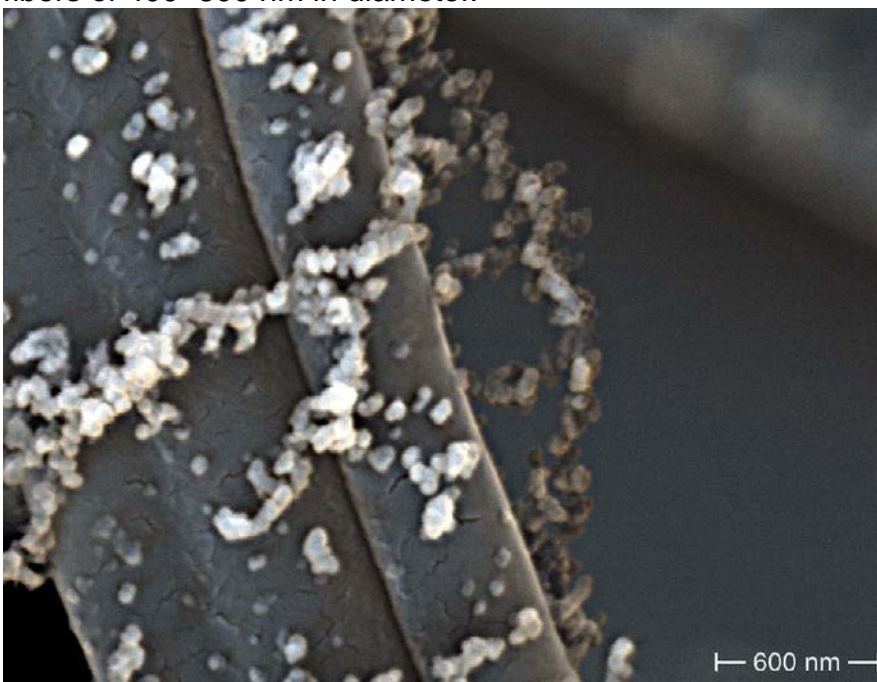
Figure 3. Particle size-specific filtration efficiency of HECA A filter (MERV 15) from ASHRAE 52.2 standard lab testing.
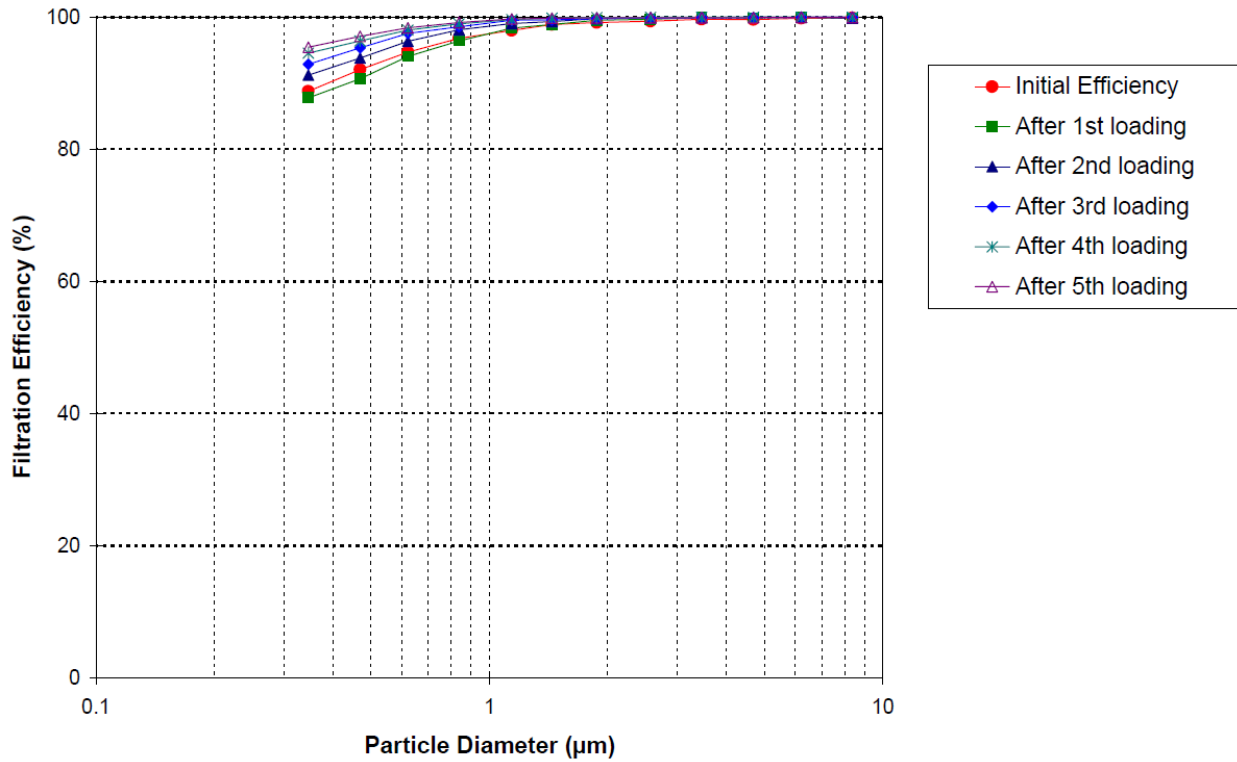
Figure 4. Particle size-specific filtration efficiency of HECA B filter (MERV 16) from ASHRAE 52.2 standard lab testing.
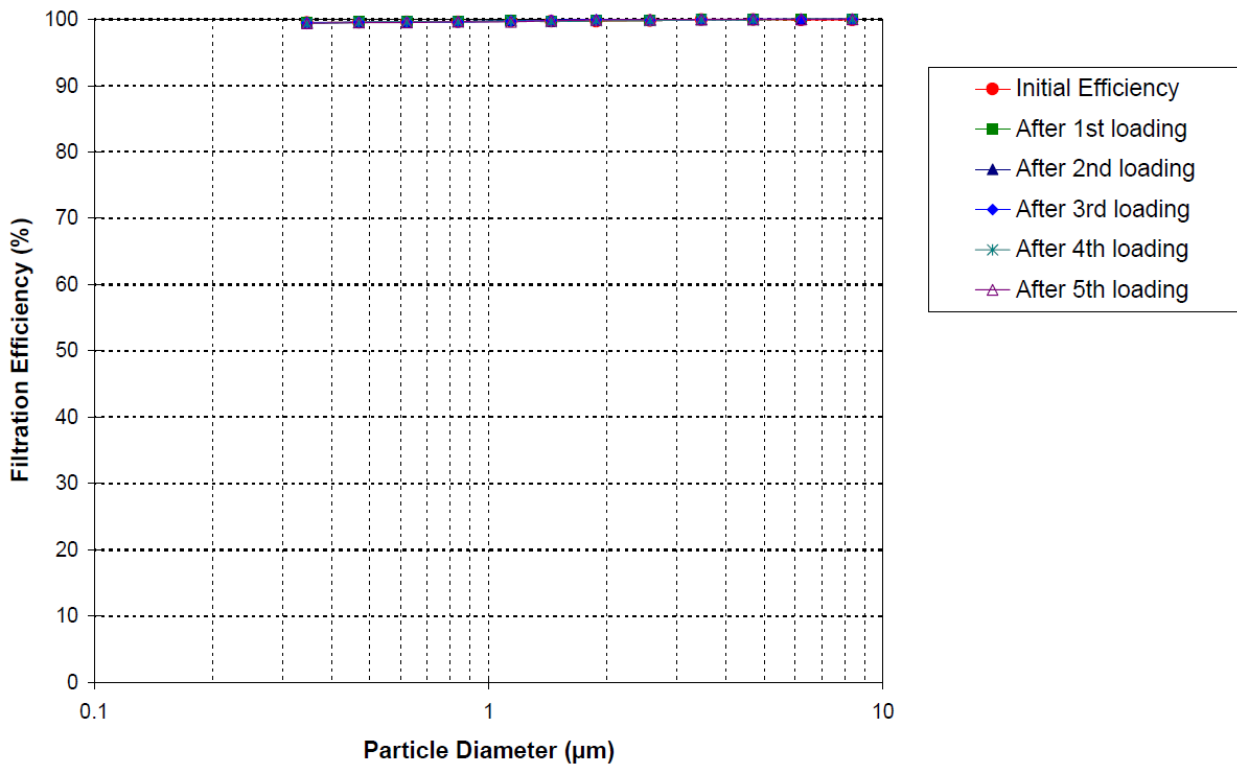
2.2 On-board HECA Filtration System for School Buses

An on-board HECA filtration system was developed by using the same type of HECA B filters used in passenger vehicles. The HECA B filter is equivalent to MERV 16. The filtration system was powered by school bus battery. Two HECA units were installed in the back of school bus cabin as shown in Figure 5. Through the diffusers located on the sides of each unit, cabin air was drawn in and filtered by the HECA filters. Filtered air was then delivered at a constant airflow rate to the bus cabin.

Two types of air delivery systems were used in this study to achieve an even distribution of filtered air inside school buses of different sizes. Note that the cabin volume of the selected school buses ranged from 22 – 54 m^3, which is an order of magnitude greater than passenger vehicles (i.e., 3 – 7 m^3 in cabin volume). Filtered air was delivered at a constant airflow rate either of ~ 1,360 m^3/h through jet diffusers or ~ 1,160 m^3/h through air distribution ducts as shown in Figure 5. The jet diffuser supplied the filtered air at an air velocity of ~ 8 m/s. The air distribution ducts delivered the filtered air through a number of punch-holes (1 cm in diameter). Decreasing numbers of punch-holes were applied with respect to the extended distance from the filtration system to provide a consistent air velocity (~ 1 m/s) at each punch-hole diffuser. The use of air distribution duct provided even distribution of filtered air inside a large school bus (i.e., school bus E in Table 2) and the jet diffusers were used for other school buses.

Figure 5. HECA filtration system prototypes with two air delivery systems: (a) jet diffusers and (b) air distribution ducts.

2.3 Selection of Testing Vehicles

Passenger Vehicle

Twelve passenger vehicles of different models and types from different manufacturers and countries of origin were selected to investigate the in-cabin exposure reductions resulting from the application of the HECA filters. As listed in Table 1, the vehicle selection included two hatchbacks, six sedans, two SUVs, and two minivans. It should be noted, the size of OEM filter is not proportional to the cabin volume. The OEM filters across different vehicle models were similar in size (approximately 10 x 10 inches), but slightly different in dimension. The authors were able to locate filter housings for most of the originally proposed vehicles except for the BMW 3 series. Therefore, a Toyota Camry was substituted for the BMW 3 series. In addition, due to limited availability, the Toyota 4Runner in the original proposal was replaced by another SUV model from the same manufacturer (i.e., Toyota Highlander). The two substitute vehicle models serve the purpose of this study well since their AERs agree with those of the originally proposed as shown in Appendix A. These 12 vehicle models were selected among popular vehicle models in California. According to the California Department of Transportation, in southern California, small cabin vehicles (passenger cars and pickups) account for 63% of the total fleet and large cabin vehicles (SUVs and vans) account for 37%. The cabin volume size ranged from 2.92 to 7.03 m^3 (U.S. EPA, 2012). To minimize the potential variability that can result from vehicle aging, no vehicles older than three years were selected for testing. The accumulated mileage of the vehicles ranged from 1,339 to 74,174 km. The cabin air filter housing was most commonly found behind the glove box, but a few vehicle models also had cabin air filters under the dashboard or hood, as noted in Table 1. All test models were equipped with an in-use OEM filter except for the 2012 Chevrolet Impala. The cabin air filter housing of this vehicle model was successfully located; however, there was no in-use cabin air filter in the cabin air filter housing. Thus, this vehicle model was only evaluated for no filter, HECA A, and HECA B filter scenarios.

Table 1. A summary of the test vehicle models and specifications

Vehicle Type	Maker	Model	Year	Mileage (km)	Cabin Filter Locations	Cabin Volume (m^3)	Testing Date	Temp. (°C)	RH (%)
Hatch-back	Ford	Focus	2012	51,347	Glove Box	2.94	8/1/2012	29±3	44±8
	Toyota	Prius	2012	9,102	Glove Box	3.88	10/22/2012	21±2	61±12
Sedan	Chevrolet	Impala	2012	1,339	Glove Box	4.01	11/5/2012	29±2	24±8
	Honda	Accord	2011	51,194	Glove Box	3.83	11/15/2012	21±2	41±13
	Hyundai	Sonata	2013	21,712	Glove Box	3.41	11/29/2012	19±4	74±11
	Nissan	Sentra	2012	30,398	Under Dash	3.50	11/27/2012	21±3	59±11
	Toyota	Camry	2012	1,931	Glove Box	3.78	10/31/2012	23±2	54±9
	Volkswagen	Jetta	2012	14,917	Under Hood	3.55	11/21/2012	22±3	54±9
SUV	Ford	Explorer	2013	16,510	Glove Box	4.89	11/7/2012	24±4	56±13
	Toyota	Highlander	2012	10,611	Glove Box	4.43	11/19/2012	22±2	55±8
Minivan	Honda	Odyssey	2010	38,622	Glove Box	7.03	9/11/2012	27±2	68±10
	Toyota	Sienna	2011	74,174	Glove Box	5.76	11/13/2012	26±3	14±7

School Bus

The effectiveness of the HECA filtration system prototype was evaluated inside six school buses of different types. Two small, two medium, and two large size school buses were originally proposed. In this study, however, only one small bus was tested because small size school buses are relatively less popular in California. Table 2 shows the characteristics of the six school buses recruited in this study. The selected school buses include a small school bus (i.e., Bus A), two medium-size school buses (i.e., Buses B and C), and three large-size school buses (i.e., Buses D, E, and F). The selected school buses have a wide range of manufacturers (i.e., Thomas, International, and Bluebird) and model years (i.e., 2006 to 2013). The bus selection took into account different locations of engine (i.e., front and rear) and exhaust tail-pipe (i.e., rear right, rear left, and side left). School buses with different fuel types (i.e., diesel, propane, and CNG) were also considered. All diesel-fuel buses tested in this study were equipped with a diesel particulate filter. The selected buses have passenger capacity from 22 to 80. The internal cabin volume was estimated from the measurements of cabin length, width, and height. Note that the passenger capacity is not necessarily proportional to the estimated internal volume of the cabin. Test school bus E was equipped with air distribution ducts, while the others used jet diffusers because the use of different air delivery system did not make significant differences even in large school buses.

Table 2. A summary of the test school bus models and specifications

Test Bus ID	School Bus Maker	Year	Passenger Capacity	Internal Volume (m^3)[*]	Fuel Type[**]	Engine Location	Exhaust Location	Testing Date	Temp. (°C)	RH (%)
A	Thomas	2006	22	22.3	Diesel	Front	Rear Right	12/5/2013	16±1	42±6
B	International	2007	42	35.9	Diesel	Front	Rear Left	1/3/2014	18±2	60±20
C	Bluebird	2013	48	32.3	Propane	Front	Side Left	11/26/2013	16±2	36±12
D	International	2007	63	53.8	Diesel	Rear	Side Left	12/16/2013	28±3	16±9
E	Bluebird	2010	78	52.4	CNG	Rear	Rear Left	11/19/2013	16±3	63±8
F	Thomas	2011	80	50.6	Diesel	Rear	Rear Left	1/7/2014	20±2	30±10

[*] Internal cabin volumes were estimated from measurements of internal dimensions.
[**] Diesel powered buses were all equipped with diesel particulate filters.

2.4 Testing Route Selections

Passenger Vehicle

The selected 12 passenger vehicles were tested under three different driving conditions: stationary, on local roadway, and on freeway. Each test vehicle was evaluated once for 5 to 8 hours and field sampling was conducted in the similar time frame of 9 AM to 7 PM. Stationary sampling was conducted in an underground parking lot, located at Westwood Boulevard and Olympic Boulevard in Los Angeles to minimize any meteorological effects. A stable background particle concentration of 20,000–25,000 cm^{-3} was observed at this stationary site. As seen in Figure 6, local-roadway tests were conducted on a 3-mile sector of Westwood Blvd between Wilshire Blvd and National Blvd in Los Angeles, CA. The freeway testing route included a 22-mile segment of I-405 between the I-10 and I-710 freeways. The test segment of I-405 has heavy traffic of approximately 67,000 vehicles/day, including passenger cars and commercial trucks. Hourly traffic volume flow rate was reasonably stable (i.e., 3,623 ± 99 vehicles/h) throughout all testing periods. Ambient temperature and relative humidity were 23 ± 4 °C and 50 ± 19%, respectively. In-cabin air temperature and relative humidity were 21 ± 3 °C and 70 ± 6%, respectively. The averaged driving speed of test vehicles was 69 ± 37 km/h on the freeway sampling route and 18 ± 16 km/h on the local roadway sampling route.

Figure 6. Test routes selected for passenger cars. The testing routes were selected for local roadway and freeway scenarios. Stationary sampling site is indicated by the red dot.

School Bus

The school bus phase of this project was initially proposed to conduct field sampling for two hours in the morning and two hours in the afternoon with children on board. However, per discussion with ARB staffs, the original proposal was revised to conduct continuous field sampling for a longer time period without children on board. The revised plan serves better for the project goal to evaluate the performance of the on-board filtration system.

Each of the six school buses was driven for six to seven hours between 9 AM and 5 PM on two typical bus routes as well as idled at a background site close to the Pacific Ocean (i.e., stationary sampling site). Under each condition, measurements were conducted to evaluate to what extent the HECA filtration system reduces in-cabin concentrations for UFPs, BC, and $PM_{2.5}$. Idling tests were conducted in an open terrain area approximately 400 m downwind from the Pacific Coast Highway (PCH, CA-1), which runs along the Pacific coastline in the Pacific Palisade area of greater Los Angeles. The background particle concentrations were at 3,000−5,000 cm^{-3}. The testing routes were selected from existing charter and local routes in Los Angeles, CA. The selected test routes included major freeways (i.e., I-10, I-110, and I-405) and local arterial roadways. Although the local testing route included freeways, i.e., I-405 (3 km) and I-10 (10 km), sampling on these freeways did not exceed more than 5% of the total sampling time under this scenario. In comparison, the freeway testing route (i.e., charter route) included I-10 (21 km), I-110 (13 km), and I-405 (27 km). The selected routes represent a typical commute on freeways and typical pick-up/drop-off scenarios in residential areas (See Figure 7 for details). Pick-up / drop-off activities of one minute each were simulated on local (9 stops) and freeway (3 stops) routes. Ambient temperature and relative humidity were 20 ± 5 °C and 42 ± 19%, respectively. In-cabin air temperature and relative humidity were 28 ± 4 °C and 30 ± 11%, respectively. The averaged driving speed of test school buses was 60 ± 28 km/h on the freeway route and 26 ± 20 km/h on the local roadway route.

Figure 7. Test routes selected for school buses. The testing routes were selected for local roadway and freeway scenarios. Stationary sampling site is indicated by the red dot.
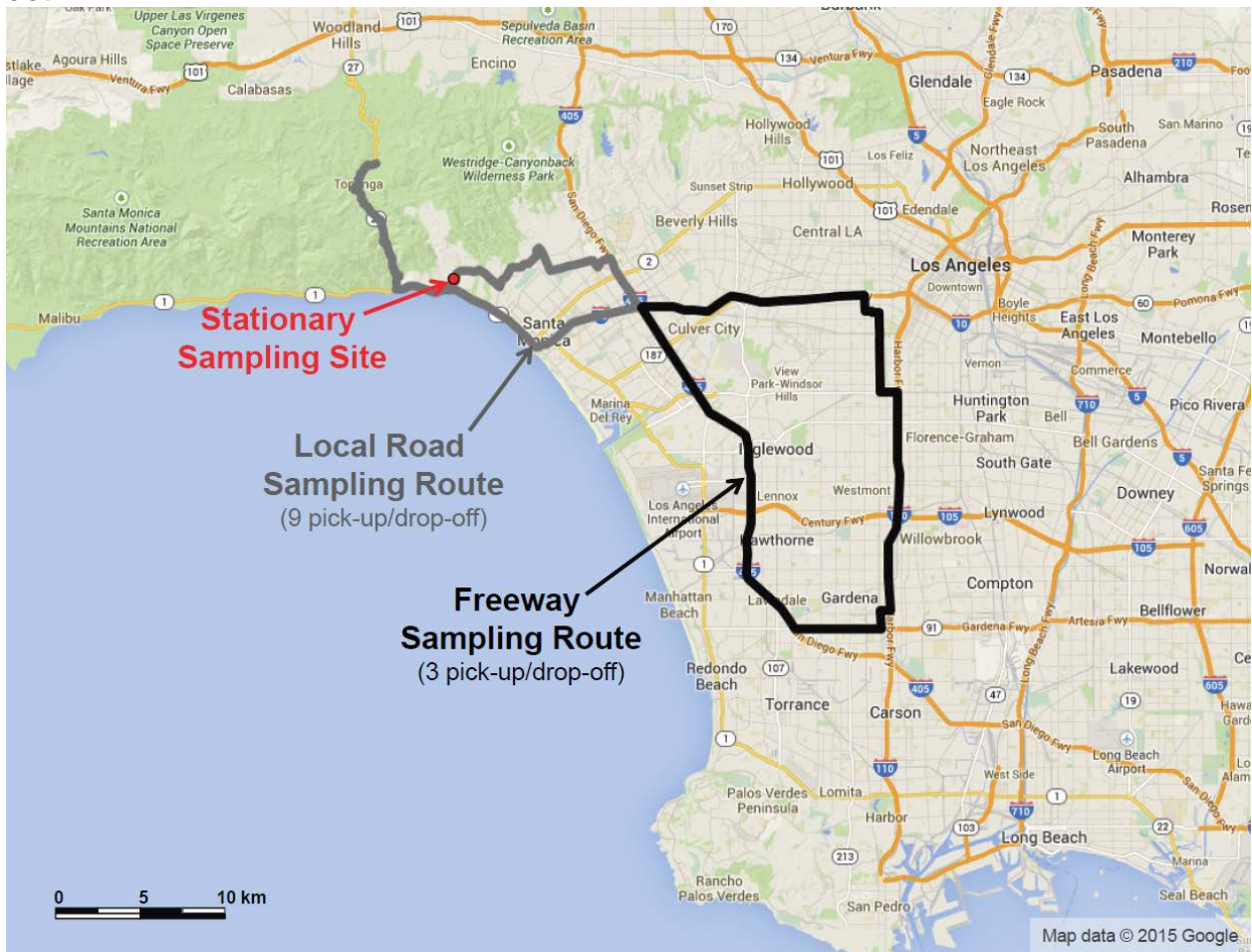
2.5 Field Measurements for Passenger Vehicles

The passenger vehicle sampling plan was reviewed and approved by ARB staff and is provided in the Appendix B. During the field measurements, the in-cabin and on-road concentrations were concurrently monitored by two sets of instruments for UFPs, BC, $PM_{2.5}$, and CO_2. While both sets of instruments were located inside the passenger cabin, one set monitored at the center of the passenger cabin (near the driver's breathing zone) and the other set sampled the air outside of the vehicle at the same location across different test vehicles as seen in Figure 8. The on-roadway aerosols were sampled through a 3 mm (id) isokinetic probes mounted on the car window. The window gaps were sealed with heavy duty duct tape (or masking tape) similar to a previous study (Zhu et al., 2007). A similar probe was used for in-cabin air sampling to compensate any diffusion loss in the sampling lines. In addition to measuring particulate pollutants, AER was estimated and ranged from 22 to 102 h^{-1} across different vehicle models with medium fan setting under OA mode ventilation. Because the AER was too high, the CO_2 decay method cannot be applied. Instead, AER was estimated by measuring ventilation inlet air flow rate and then divided it by the cabin volume.

Two condensation particle counters (CPCs) were deployed to measure the in-cabin (Model 3785, TSI Inc., St. Paul, MN) and on-road (Model 3786, TSI Inc., St. Paul, MN) UFP concentrations. Similarly, two DustTrak (Model 8520, TSI Inc., St. Paul, MN) and two Q-trak monitors (Model 8554, TSI Inc., St. Paul, MN) simultaneously measured the in-cabin and on-road concentrations of $PM_{2.5}$ and CO_2. Although CO data were also collected by the Q-trak, the data were invalid even after several lab calibrations. This is likely because the CO levels were too low and below the instrument detection limit. The BC concentrations inside and outside of the cabin were also recorded with two aethalometers (Models AE-22 and AE-42, Magee Scientific Co., Berkeley, CA). Along with pollutant concentration measurements, the ventilation air-flow rate was continuously monitored with a ventilation meter (Q-trak model 7565-X with model 960, TSI Inc., Shoreview, MN). The hot-wire anemometer probe of the ventilation meter was secured on a single air inlet diffuser in the middle, while all other diffusers were closed and sealed. For all test vehicles, air conditioning was on. It is important to measure ventilation inlet air flow rates because the application of HECA filters can reduce ventilation air flow rates due to a potentially higher pressure drop than OEM filters. All of the instruments were calibrated prior to their deployment for field sampling and set to a logging interval of 1 s, except for the aethalometers, which were set to their minimum logging interval of 1 min.

In addition, particle size distributions were collected using two sets of scanning mobility particle sizers (SMPSs, Model 3080 with Model 3085, TSI Inc., Lakeshore, MN) inside the SUVs and minivans, which provide enough space for the SMPS system. The in-cabin and on-road particle size distributions in the size range of 7.37–289 nm were concurrently collected. The applied scanning and retrace times were 100 and 20 s, respectively.

Four different filtration scenarios (i.e., no filter, in-use OEM, HECA A, and HECA B) were examined under the three different driving conditions for 15–20 min each. The collected data covered 144 different experimental conditions and included more than 130,000 pairs of one-second concentration data concurrently acquired for both in-cabin and on-road for each pollutant. Under the medium fan setting in OA mode, data were collected for each test vehicle model under three different driving conditions: stationary, on local roadway, and on freeway. Data collection was conducted in the order of freeway, stationary, and local roadway.

Each vehicle model was evaluated with two occupants inside for entire local and freeway driving scenarios; whereas, an averaged number of occupants was 1.3 during stationary sampling periods. Table 1 summarizes the sampling dates and ambient conditions for each passenger vehicle. The same sets of instruments with the same configuration were used to monitor in-cabin and on-road air quality for all test vehicles.

Figure 8. A picture of on-road and in-cabin sampling probe locations in a tested passenger vehicle. Air samples were collected at the same location in the 12 passenger vehicles selected in this study.

2.6 Field Measurements for School Buses

The school bus sampling plan was reviewed and approved by ARB staff and is provided in the Appendix C. A stand-alone air purifier originally proposed was replaced with an on-board HECA filtration system, which were specifically designed for school bus applications. Field measurements were conducted with and without operating the on-board HECA filtration system. To assess in-cabin pollutant reductions, UFP number concentration and size distribution as well as BC and $PM_{2.5}$ levels were monitored concurrently inside and outside of six school buses. In addition to measuring particulate pollutants, AER was estimated using the CO_2 gas concentration decay. The estimated AER increased at a higher bus driving speed. For instance, AER increased from 2 h^{-1} at 0 km/h to 10 h^{-1} at 80 km/h. Detailed AER data are reported in Appendix D.

Two comparable sets of instruments were deployed for concurrent sampling of the in-cabin and on-road air. Both sets of instruments were located inside the school bus cabin. One set monitored at the breathing zone (i.e., 1 m above the floor) in the back of the school bus cabin. The other set sampled the on-road air through a 3 mm isokinetic probes mounted on a slightly open (~ 1 cm) window. The window gap was sealed with heavy duty duct tape similar to previous studies (Lee and Zhu, 2014; Zhu et al., 2008). Another sampling probe of the same length was used for in-cabin air sampling to compensate for any diffusion loss in the sampling lines.

Two sets of SMPSs (Model 3081, TSI Inc., Lakeshore, MN) were deployed to measure particle size distributions and total particle number concentrations. The in-cabin and on-road particle size distribution data in the size range of 7.37–289 nm were concurrently collected. The applied scanning and retrace times were 100 and 20 s, respectively. Two DustTrak (Model 8520, TSI Inc., Lakeshore, MN) and two Qtrak monitors (Model 8554, TSI Inc., Lakeshore, MN) simultaneously measured the in-cabin and on-road concentrations of $PM_{2.5}$ and CO_2, respectively. Similarly, the BC concentrations inside and outside of the cabin were recorded with two aethalometers (Models AE-22 and AE-42, Magee Scientific Co., Berkeley, CA). All of the instruments were calibrated prior to their deployment for field sampling and data logging intervals were set to 1 s for all instruments except for the aethalometers, which were set to their minimum logging interval of 1 min.

In addition, two CPCs (Model 3007, TSI Inc., Lakeshore, MN) also measured UFP concentrations at the breathing zone (1 m above floor) in the front and the middle of each school bus. Since each school bus had different length, the authors applied percentile distance by considering the distance from the first-row to the last-row seats as 100 percentile. As shown in Figure 9, the front monitoring location was set at 25 percentile distance from the first-row seats. Similarly, the middle sampling point was located at 50 percentile distance, and the rear sampling point at 75 percentile. These data will be analyzed in a future study focusing on spatial distribution of UFPs inside school buses.

For each bus, data were collected under three different driving conditions: stationary, local roadway, and freeway conditions. Data collection was conducted in the order of freeway, stationary, and local roadway. Two different filtration scenarios (i.e., with and without operating the HECA system) were examined for 60–70 min each under local and freeway driving conditions. Stationary data were collected for 20 – 25 min when the school bus was idling and parked heading leeward of the sea breeze. Note that the stationary emission reduction benefits presented in this report may overstate for uses in California because school bus idling is prohibited under ARB's Airborne Toxic Control Measure (ATCM) and limited to 30 seconds before departing from a school and no more than 5 consecutive minutes or 5 minutes in an hour in any location other than school (more information is available at: http://www.arb.ca.gov/toxics/sbidling/sbidling.htm). Local roadway conditions were evaluated while driving on major arterial roadways, whereas freeway conditions were evaluated on major freeways (i.e., I-10, I-110, and I-405) in Los Angeles, CA. In-cabin and on-road pollutants were concurrently monitored and logged.

The data were collected from 36 different experimental conditions. Each test school bus was evaluated with two passengers and one school bus driver inside during the entire period of testing. Table 2 summarizes the sampling dates and ambient conditions for each testing day. The same sets of instruments with the same configuration were used throughout the study.

Figure 9. A picture of on-road and in-cabin sampling probe locations for a tested school bus.
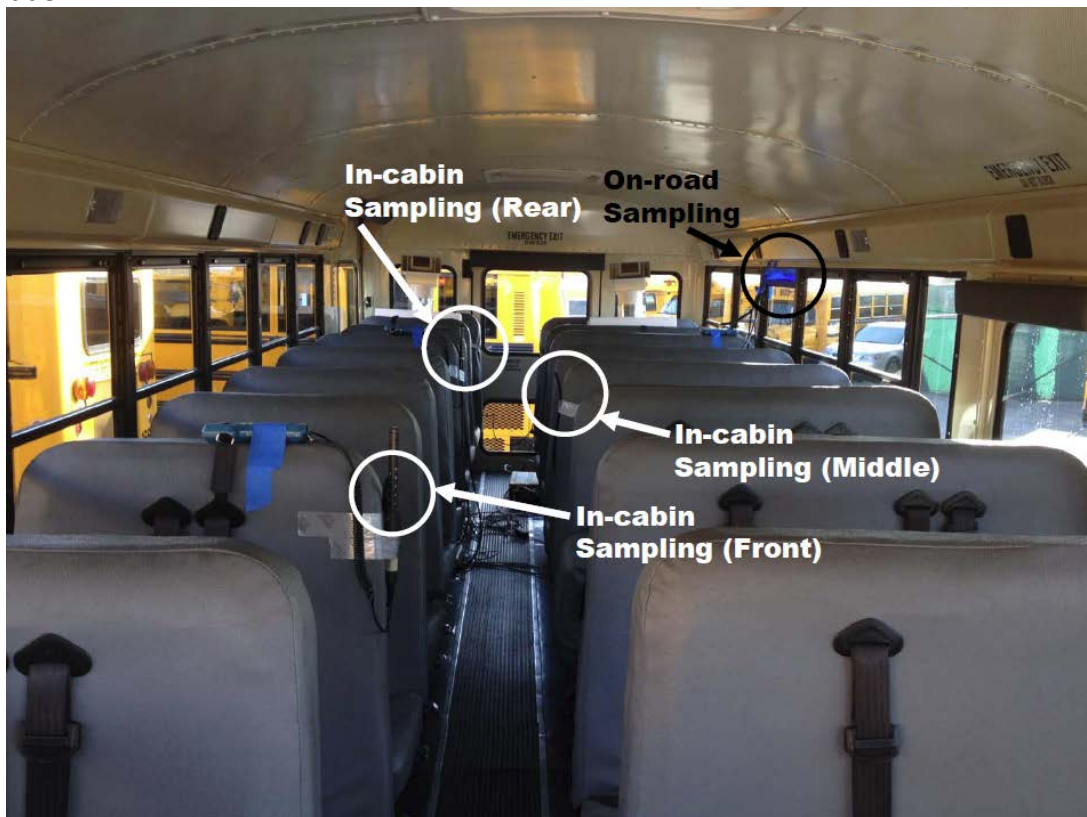
2.7 Acquisition of Data and Quality Assurance

Each pair of instruments was collocated before and after the field sampling for data quality assurance. Good correlations with little bias of the collected data were observed both for passenger vehicles and school buses.

For the passenger vehicle tests, the collocation data for UFP, BC, and $PM_{2.5}$ were well correlated with R^2 of 0.98, 0.78, and 0.96, respectively (see Appendix E). UFP and $PM_{2.5}$ collocated data were within 5% of each other and R^2 was higher than 0.95. As shown in Appendix E, two collocated aethalometers had less correlation ($R^2 = 0.78$) and more bias (~ 14%) for BC. This occurred not because of instrument bias, but because of an insufficient number of collocated data points. For school bus tests, the collocated data from different units of the same instruments showed good correlations for all three types of pollutants (see Appendix F). Additional BC collocated data from the same two aethalometers present a good correlation ($R^2 = 0.93$) with less bias (~ 9%).

The instruments that measured $PM_{2.5}$ (Model 8520, TSI Inc. Shoreview, MN) could be affected by ambient conditions (e.g., temperature and relative humidity) during the day of testing although the collocated data show a good correlation ($R^2 > 0.95$) and little bias (< 5%) for both in-cabin and on-road $PM_{2.5}$ measurements. The in-cabin and on-road temperature differences were less than 3°C on average during data collection for passenger vehicles and less than 7°C on average for school buses. The differences between ambient and in-cabin relative humidity were also low (i.e., < 9% on average) for both passenger vehicles and school buses. Therefore, no post-data processing or data adjustment was conducted to adjust the measurements of UFP, BC, and $PM_{2.5}$ in this study.

The instruments used in this study provided high time resolution data with one-second sampling intervals, except for SMPSs (two minutes) and aethalometers (one minute). The collected data were thoroughly checked and unrealistic data points, caused by instrument malfunction, were removed from further analysis. Then, one-second raw instrument data were averaged to one-minute to minimize unnecessary data fluctuations. The one-minute averaged data were used for data analyses and data presentation in this study. During data analyses, paired t-tests were conducted to verify if the measured differences were statistically significant when HECA filters were applied in passenger vehicles (in Figure 12). Similarly, the Mann-Whitney U-test was conducted to determine the statistical significance of the measured differences from school bus testing (in Figure 14).

3. RESULTS AND DISCUSSION

3.1 Particle Size Distributions

Passenger Vehicle
Figure 10 shows an overview of the in-cabin and on-road particle size distributions averaged across each sampling period for each filter type under different driving conditions, namely (a) stationary, (b) local, and (c) freeway. The solid lines represent the particle size distribution data collected for the on-road air, whereas the dot and dash lines represent the in-cabin particle size distributions with no filter, in-use OEM filter, HECA A filter, and HECA B filter.

The three driving conditions provided distinctively different on-road particle size distributions. For the stationary condition, the on-road particle size distributions had a mode diameter of ~ 80 nm, which was larger than ~ 30 nm observed on the freeway. Due to the abundant presence of nucleation mode particles, the on-freeway condition exhibited a typical bi-modal size distribution (Figure 10c). In comparison, the data collected on local roadways showed a mixture of the stationary and freeway particle size distributions. The particle size distribution had three distinctive modes (Figure 10b) because measured particle size distribution experienced changes in the mode diameter and resulted in multiple mode diameters in the average size distribution. The multiple modes reflect the complexity of the changing traffic density and vehicle emissions due to the stop-and-go traffic pattern on local streets.

The in-cabin reductions were commonly found across a wide range of particle sizes for all driving conditions. In comparison with the on-road concentrations, the data from different filtration scenarios demonstrate a substantial reduction of in-cabin particle concentrations across the measured particle size range for all three driving conditions. Even with no filters, the reduction was observable. Installation of in-use OEM filters offered additional particle removal for all conditions, but the reduction remained small in magnitude. Upon retrofitting with HECA B filters, the in-cabin particle concentration was further decreased especially for particles in the nucleation mode as in the case of freeway driving shown in Figure 10c.

Figure 10. Averaged particle size distribution data are plotted with normalized particle number concentration (dN/dLogDp) across particle diameter (Dp). The plotted data are acquired from passenger vehicle tests for both on-road and in-cabin environments under different filtration scenarios.
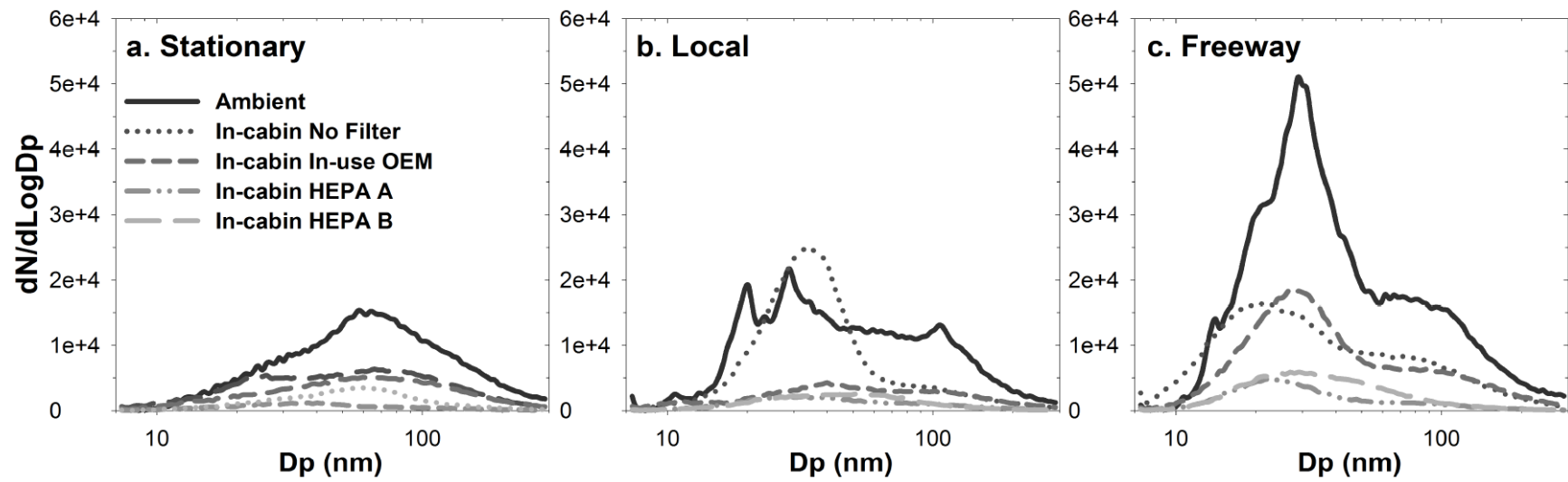
School Bus
Figure 11 plotted particle size distributions under stationary, local, and freeway driving conditions. Similar to Figure 10, the on-road concentrations were higher than in-cabin concentrations even with the HECA filtration system off. Freeway measurements were higher than local or stationary measurements across the measured size range. Throughout different driving scenarios (i.e., stationary, local, and freeway), the size-resolved data indicate high concentrations of nucleation mode particles below 20 nm. It is important to note that these nucleation mode particles are likely from the test school bus itself rather than surrounding vehicle emissions because that high concentration of nucleation mode particles was observed even during stationary sampling in clean background environments.

In this study, stationary sampling was conducted at a site approximately 400 m downwind of the Pacific coastline. Ambient concentrations at the coast ranged from 3,000 to 5,000 cm^{-3} and there was no major source of UFPs except for tail-pipe emissions from the test school bus. Zhang et al. (2013) found that the changes of wind direction can influence air quality monitoring in and around school buses. Considering the effects of wind direction, the authors placed the sampling probe on the opposite side of the exhaust tail-pipe. For example, if the exhaust was located at the right-rear end, the authors placed sampling probes through a left-side window of the school bus. The observed nucleation-mode particles outside of the bus are likely from the bus own emissions.

Even when the pollutant levels were high on freeways, the HECA filtration system maintained UFP concentration at a substantially low level inside the buses. Figure 11 shows particle size distributions measurements with and without operating the HECA filtration system. High levels of in-cabin UFP concentrations were detected due to infiltration and self-pollution without operating the HECA filtration system. With the HECA filtration system was on, particle concentrations were reduced dramatically.

Figure 11. Averaged particle size distribution data are plotted with normalized particle number concentration (dN/dLogDp) across particle diameter (Dp). The plotted data are acquired from school bus tests for the on-road and in-cabin environments with and without operating the on-board HECA filtration system. The normalized particle number concentration data are the averages of measurements from all six school bus models with respect to particle diameter.
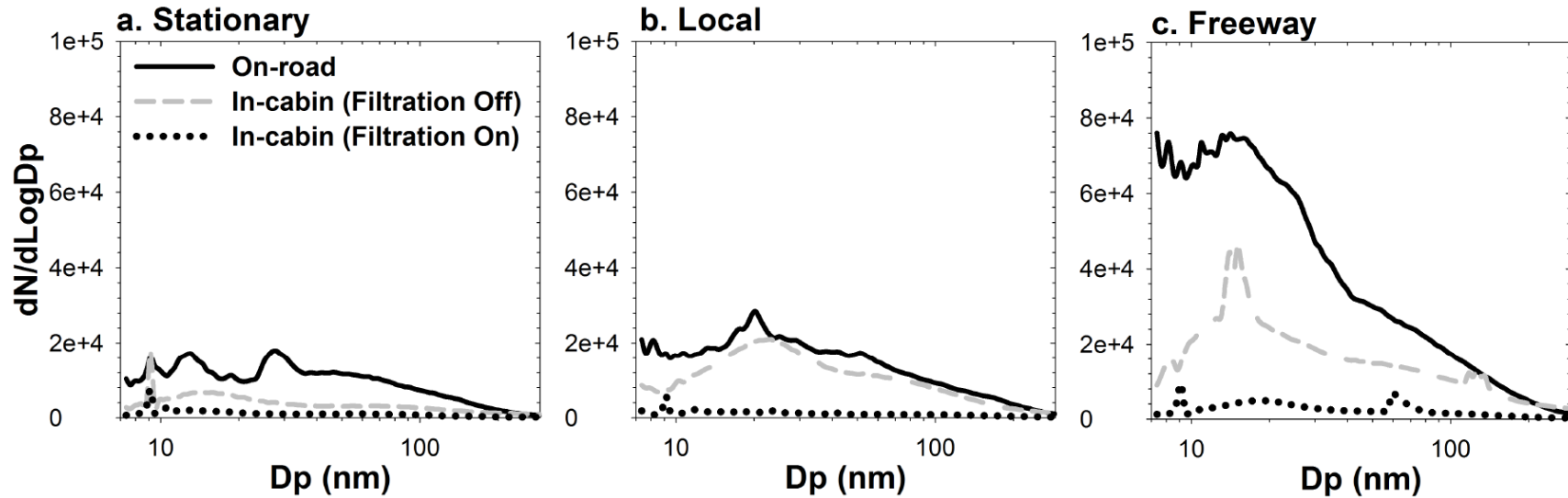
3.2 Effects of HECA Filtration on Reducing Passenger Exposure

Passenger Vehicle
Figure 12 provides average in-cabin pollutant reductions relative to the on-road concentration for UFPs, BC and PM$_{2.5}$. The reduction was calculated from the concurrently measured in-cabin/on-road (I/O) concentration ratio,

$$\text{In-cabin Reduction (\%)} = \left(1 - \frac{\text{In-cabin Concentration}}{\text{On-road Concentration}}\right) \cdot 100 \qquad (1)$$

The data points are the means of the 1-min averaged data for each of the 12 test vehicles for (a) UFPs, (b) BC, and (c) PM$_{2.5}$, under different driving conditions and different filtration scenarios. For each plotted data point (i.e., one-minute mean) and error bar (i.e., standard deviation), there were at least 150 observations averaged from more than 9,000 one-second raw data.

Figure 12. In-cabin reductions (%) in passenger vehicles with respect to on-road particle concentration under different scenarios. The in-cabin reductions were estimated by using Equation (1). The symbols and the error bars are the mean and the standard deviation of the averaged in-cabin reductions in test vehicle models. For each driving condition, HECA B and A filters provided significant in-cabin reduction (p < 0.001) in comparison to OEM or no filter scenarios. (See Appendix G for the numerical values plotted here.)
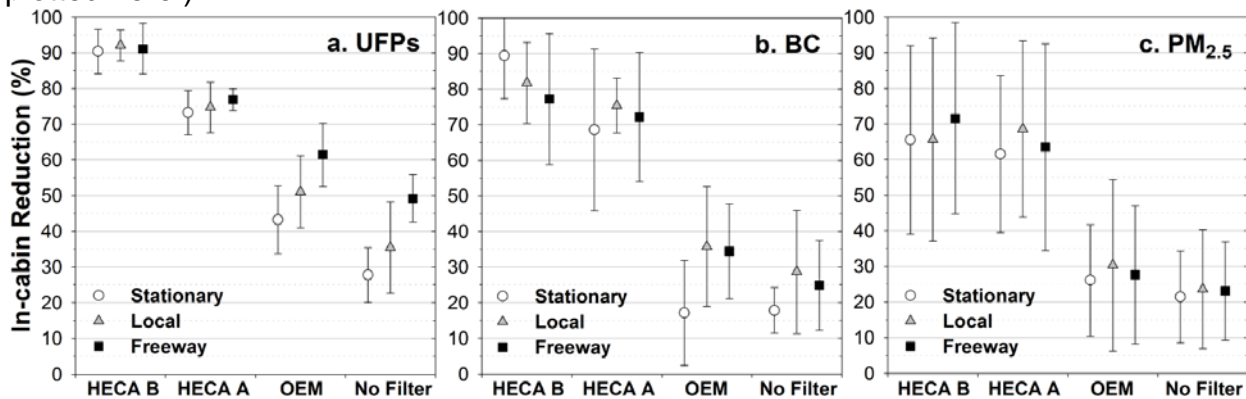
As shown in Figure 12a, under both stationary and realistic driving conditions, the HECA B filter achieved a reduction of 90–92% based on averages for UFPs. The application of the HECA A filter offered a reduction of 73–77% based on averages. In comparison, the no-filter scenario showed a reduction of 28–49% based on averages and the in-use OEM filter had a reduction of 43–61% based on average. In addition to in-cabin UFP reduction, the application of the HECA filters minimized the variability (i.e., error bars) of UFP concentrations across different vehicle models. Note that the reported data in Figure 12 excluded the data from vehicle models, which had substantial amount of bypass flow in the filter housing (i.e., Chevy Impala and Toyota Prius). See Appendix H for the data from individual passenger vehicles. The dimension of HECA filter prototypes

were accurately determined based on the dimension of OEM filters in the market. However, the prototype filters were loosely fitted (~ 1 cm gap around the filter) to the filter housing of Chevy Impala. In case of Toyota Prius, the prototype filters were fitted well to the filter housing; however, the filter housing had a widened opening in the filter housing. In addition, the variability of the data may come from vehicle-specific parameters such as AER, cabin volume size, blower fan capacity (even at the same medium fan settings). Appendices H and I summarize the in-cabin UFP reductions for individual passenger vehicles tested in this study.

Figure 12 also illustrates in-cabin pollutant reductions under each of the three driving conditions (i.e., stationary, local, and freeway). As shown in Figure 12a, the maximum UFP reduction occurred on freeways but the in-cabin reduction was smaller under the stationary condition. One should note that the greater reduction observed in the freeway environment was not because of lower in-cabin UFP concentration during the freeway testing. The overall in-cabin concentrations were still the highest under the freeway condition, followed by the local, and then the stationary condition. Instead, this greater reduction is likely because aerosols from different sources have different size distributions (see Figure 10) and the size-dependent filtration efficiency of the tested filters under different filtration (i.e., HECA B, HECA A, OEM filter, and no filter) and driving conditions.

Figures 12b and 12c present another interesting observation. The in-cabin pollutant reductions were lower for BC and $PM_{2.5}$ than UFPs, and lower on freeway than on local roadway. This is likely due to three factors. First, BC and $PM_{2.5}$ reflect particle mass concentrations; therefore, the diffusion loss of smaller particles has little effect on BC and $PM_{2.5}$ reduction. Second, the mass concentrations of BC and $PM_{2.5}$ represent a wider range of particles with diameters up to approximately 1 μm and 2.5 μm, respectively. Larger particles dominate BC and $PM_{2.5}$ measurements and any unfiltered ones may lead to a decrease of total in-cabin reduction. Finally, the smaller in-cabin reduction under the freeway condition is in part due to the increase of the infiltrated (i.e., unfiltered) proportion of the on-road pollutants, which often occurs at higher driving speeds on freeways. The infiltration effects were less noticeable for UFPs (Figure 12a) because the diffusion loss during the infiltration process was also significant for the nucleation mode UFPs on the freeways. However, the infiltrated on-road BC and $PM_{2.5}$ can lead to a substantial increase in the overall in-cabin particle mass concentration. Due to these three factors, the in-cabin reductions of BC and $PM_{2.5}$ were smaller than UFPs and smaller under the freeway driving than the local driving conditions. See Appendix I for the data from individual passenger vehicles.

The maximum reduction of the in-cabin UFP number concentration occurred on freeways in Figure 12a. The particle size distribution data in Figure 10c offered an explanation. The in-cabin reduction (i.e., 1 – I/O) is sensitive to the on-road particle size distribution, especially for UFP number concentrations. As seen in Figure 10c, the freeway aerosol was dominated by nucleation-mode particles with a mode diameter near 30 nm. These smaller UFPs contribute greatly to the total particle counts. Meanwhile, the filtration efficiency of the HECA B filter is also much higher in this size

range compared with other filters (discussed in details in Figure 15). This is likely due to its smaller fiber diameter which enhances particle collection by diffusion and interception, which is the dominant mode of particle removal especially for nucleation mode particles below 30 nm. Consequently, the HECA B filter was more effective for the nucleation mode particles under the freeway condition. The following section discusses the size-specific UFP removal efficiency in greater details.

Overall, the HECA filters successfully reduced all three particulate pollutants under the experimental conditions. With respect to the on-road concentrations, the HECA B filters offered in-cabin concentration reductions of 90 ± 8% for UFPs on average across all driving conditions, much higher than the OEM filters (50 ± 11% on average). Similarly, the HECA B filters offered an 81 ± 15% reduction for BC and 66 ± 28% for $PM_{2.5}$ across all driving conditions. In comparison, across all driving conditions, in-use OEM filters only provided 31 ± 17% and 29 ± 20% reduction for BC and $PM_{2.5}$, respectively. See Appendix J for in-cabin pollutant reduction data averaged across all driving conditions. The use of the HECA B filter also greatly reduced the variability in the data from different vehicle models and under different driving conditions. Compared to the in-use OEM filters, the HECA filters increased the removal of the three pollutants by a factor of two to three. Table 3 summarizes the measured UFPs, BC, and $PM_{2.5}$ concentrations under all experimental conditions.

Table 3. A summary of the test results for UFP, BC, and $PM_{2.5}$ under three driving conditions and four different filtration scenarios during passenger vehicle tests.

Pollutants		Filtration Scenarios	Stationary		Local		Freeway	
			In-cabin	On-road	In-cabin	On-road	In-cabin	On-road
Particle	UFP ($\#/cm^3$)	No filter	15006 (6125)	22418 (12832)	15368 (5034)	27446 (9849)	28826 (10076)	66292 (26770)
		In-use OEM	12373 (5672)	23292 (12309)	11302 (3933)	26026 (7473)	25916 (11914)	81282 (44536)
		HECA A	6048 (2904)	23715 (13464)	6418 (3039)	27321 (8323)	15558 (5421)	72765 (23677)
		HECA B	2264 (2029)	21508 (9785)	2455 (1792)	30075 (11685)	5726 (2914)	76549 (39837)
	BC (ng/m^3)	No filter	2899 (2169)	2282 (1462)	2473 (2869)	2032 (1181)	4636 (2610)	3589 (1708)
		In-use OEM	2577 (2121)	2102 (1407)	2559 (2819)	2136 (1384)	4275 (2250)	4407 (1795)
		HECA A	1061 (2073)	2192 (1342)	1399 (2725)	2182 (1227)	1433 (2133)	5175 (2055)
		HECA B	1089 (2632)	2724 (1245)	915 (2067)	2412 (1230)	1343 (2809)	3036 (1606)
	$PM_{2.5}$ ($\mu g/m^3$)	No filter	38 (24)	46 (26)	32 (21)	36 (26)	37 (21)	41 (28)
		In-use OEM	28 (25)	47 (24)	33 (25)	40 (34)	33 (19)	44 (29)
		HECA A	15 (15)	34 (25)	10 (5)	38 (33)	11 (7)	40 (28)
		HECA B	12 (13)	28 (17)	10 (7)	38 (31)	9 (6)	37 (26)
Gas	CO_2 (ppm)	No filter	1082 (581)	944 (528)	705 (91)	477 (49)	729 (132)	540 (206)
		In-use OEM	1067 (625)	957 (653)	711 (98)	481 (54)	729 (146)	526 (160)
		HECA A	1268 (663)	1040 (633)	752 (148)	469 (55)	716 (94)	473 (45)
		HECA B	1170 (561)	1022 (577)	792 (132)	470 (54)	746 (111)	472 (48)

* The data are the averages of the field observations and the standard deviations are given in parenthesis.

School Bus

Figure 13 provides average pollutant reductions for UFPs, BC and $PM_{2.5}$ inside school buses. The data plotted in Figure 13 are tabulated in Appendix K. The reduction was calculated using I/O reduction from the concurrently measured in-cabin/on-road (I/O) concentration ratio with and without operating the HECA filtration system,

$$\text{I/O Reduction} = \left\{ 1 - \frac{(I/O)_{HECA-on}}{(I/O)_{HECA-off}} \right\} \cdot 100 \qquad (2)$$

where
$(I/O)_{HECA-on}$: I/O ratio with operating the on-board HECA system
$(I/O)_{HECA-off}$: I/O ratio without operating the on-board HECA system

It should be noted, self-pollution can increase the I/O ratio; however, the I/O Reduction in Equation (2) cancels out the effects of self-pollution occurred with and without operating the filtration system. The data points are the means of the 1-min averaged data for each of the six buses for UFPs, BC, and $PM_{2.5,}$ under different driving conditions. Under both stationary and realistic driving conditions, the on-board HECA filtration system achieved an average reduction of 85–90% for UFPs. The operation of HECA filtration system provided similar results for reducing BC by 80–87% on average, but variable results for $PM_{2.5}$ with 35–75% on average. Appendix K summarizes the in-cabin UFP reductions for individual school buses tested in this study.

Figure 13 also illustrates in-cabin pollutant reductions under each of the three driving conditions (i.e., stationary, local, and freeway). The maximum UFP reduction occurred on freeways but the in-cabin reduction was smaller under the stationary condition. Similar to the observation from passenger vehicles, the greater reduction observed in the freeway environment was not because of lower in-cabin particle concentration during the freeway testing. The overall in-cabin concentrations were still the highest under the freeway condition, followed by the local, and then the stationary condition. Instead, this greater reduction is likely because on-road particles are much smaller in freeway environments (see Figure 11). These smaller particles are removed more effectively by Brownian diffusion. When averaged across all driving conditions, in-cabin UFP and BC levels were reduced by 88 ± 6% and 84 ± 5%, respectively, when the on-board HECA filtration system was operating. The HECA system achieved 55 ± 22% reductions for $PM_{2.5}$. See Appendix L for more detail. Appendices M and N provide the I/O ratios of UFP, BC, and $PM_{2.5}$ data from individual school buses with respect to each experimental condition.

Figure 13. I/O ratio reductions in school buses when operating the on-board HECA filtration systems under different driving scenarios. The I/O reductions were estimated by using the Equation (2). The symbols and the error bars are the mean and the standard deviation of the averaged in-cabin reductions in all six school buses. (See Appendix J for the numerical data plotted here.)
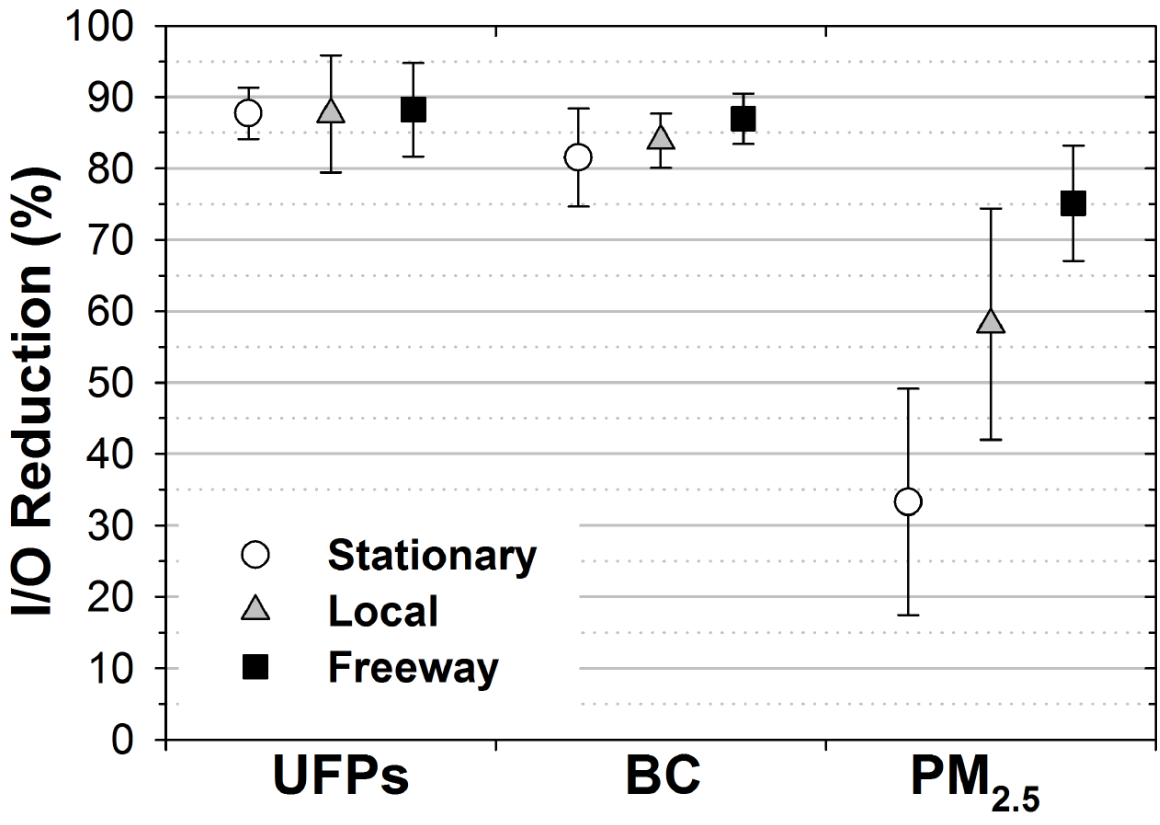
Figure 14 illustrates the measured concentrations of UFPs, BC, and $PM_{2.5}$ inside (white) and outside (grey) of school buses tested in this study. It also compares the measurements with (right) and without (left) operating the on-board HECA filtration system. Overall, on-road concentrations of three particulate pollutants were the highest on freeways, followed by local and stationary conditions. Similar patterns were observed but in a reduced magnitude inside school bus cabins with or without operating the HECA filtration system. The reduction of in-cabin concentration was significant for UFP, BC, and $PM_{2.5}$ ($p < 0.001$) under all driving scenarios in this study.

Under stationary condition without operating the HECA system (i.e., the left panels in Figure 14), UFP concentrations inside the buses were 70% lower than outside (Figure 14a). An in-cabin reduction of 55% was observed for BC and 22% for $PM_{2.5}$ under stationary condition without operating the HECA filtration system (Figures 14b and 14c). With the HECA system off, in-cabin BC concentrations were 50% and 67% higher than on-road concentrations on local streets and freeways, respectively (Figure 14b). Without operating the HECA system, the $PM_{2.5}$ concentrations were also 48% and 17% higher inside the school bus than on local streets and freeways, respectively (Figure 14c). For UFPs, the in-cabin concentrations were frequently (but not always) higher than on-road concentrations particularly in buses E and F, but not necessarily in the others (i.e., buses A, B, C, and D). Note that the on-road measurements are tabulated for individual school buses in Table 4. The in-cabin measurements without and with operating the HECA filtration system are summarized in Tables 5 and 6, respectively. For $PM_{2.5}$, the in-cabin particle concentrations were significantly higher ($p < 0.001$) under both local and freeway conditions. This is presumably because particles may be resuspended from the surface due to human activities (Qian et al., 2012; Tian et al., 2014) and high flowrate of the jet-diffusers. For BC and UFPs, school bus self-pollution may likely contribute to the observed higher in-cabin pollutant levels. The in-cabin BC concentration was often higher than on-road in most school buses tested in this study; however, the similar observation was made for UFP measurements only in two school buses (i.e., buses E and F).

When the HECA filtration system was on (the right panels in Figure 14), in-cabin pollutant concentrations were significantly lower ($p < 0.01$) than on-road levels and were reduced by 94–97% for UFPs (Figure 14a), 80–90% for BC (Figure 14b), and 30–75% for $PM_{2.5}$ (Figure 14c). The authors observed similar reductions when HECA filters were used in passenger vehicles, as shown in Figure 12. The filtration system was more effective during freeway driving than under stationary or local driving conditions. Note that smaller UFPs dominate particle number concentrations on freeways and particle removal efficiency of HECA filters is particularly high for UFPs. The following sections discuss this in more details.

Figure 14. On-road (grey) and in-cabin (white) concentrations of UFP, BC, and $PM_{2.5}$ with and without operating the HECA filtration system inside school buses. The data are presented in stationary, local, and freeway conditions (x-axis). * indicates $p < 0.001$.
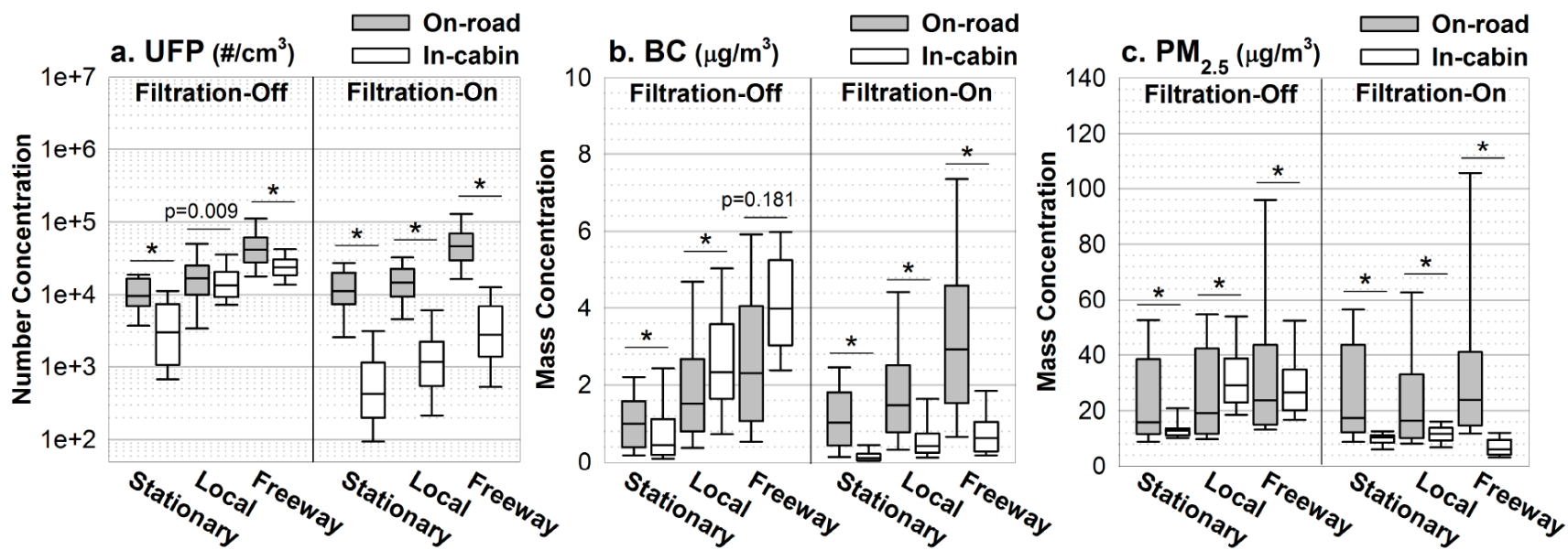
Table 4. A summary of on-road measurements for UFP, PM$_{2.5}$, and BC with and without operating on-board HECA filtration system under different driving conditions in school buses.

Exp. Modes		Stationary			Local			Freeway		
Bus ID	Pollutants	UFP (#/cm^3)	PM$_{2.5}$ (µg/m^3)	BC (ng/m^3)	UFP (#/cm^3)	PM$_{2.5}$ (µg/m^3)	BC (ng/m^3)	UFP (#/cm^3)	PM$_{2.5}$ (µg/m^3)	BC (ng/m^3)
A	Avg.	13797	10	1075	24027	12	1732	63409	17	2185
	Median	11834	9	783	12817	10	1175	41432	16	1733
	St.Dev	6650	3	850	55776	10	2090	77168	5	1854
B	Avg.	14068	56	1800	18482	62	3107	58807	106	6537
	Median	13221	56	1413	13753	60	1745	49072	103	5500
	St.Dev	5376	3	1088	14060	15	4911	36442	21	5566
C	Avg.	20568	27	1611	27613	32	2119	60752	34	3585
	Median	18632	39	1640	20868	32	1780	45996	30	3003
	St.Dev	4550	17	771	20496	9	1719	79662	24	2992
D	Avg.	10575	15	603	24419	14	3193	62141	17	3236
	Median	10406	10	496	18197	12	2075	46439	14	2933
	St.Dev	1534	10	346	17681	9	4229	44834	9	2679
E	Avg.	9882	16	795	8250	14	959	27393	16	1390
	Median	3794	16	369	4370	13	670	18874	15	922
	St.Dev	32249	3	1978	8769	4	1318	27936	5	1936
F	Avg.	22921	16	1338	24295	37	2446	85637	37	3003
	Median	14816	14	1200	15975	35	1940	48885	36	2710
	St.Dev	21821	5	1002	29560	17	1929	81752	9	1813
All	Avg.	15103	23	1210	21277	27	2237	60099	38	3311
	Median	10956	15	930	15568	17	1498	42961	24	2620
	St.Dev	18894	17	1327	29779	21	3061	64715	34	3435

Table 5. A summary of in-cabin measurements for UFP, PM$_{2.5}$, and BC without operating on-board HECA filtration system under different driving conditions in school buses.

Exp. Modes		Stationary			Local			Freeway		
Bus ID	Pollutants	UFP (#/cm^3)	PM$_{2.5}$ (µg/m^3)	BC (ng/m^3)	UFP (#/cm^3)	PM$_{2.5}$ (µg/m^3)	BC (ng/m^3)	UFP (#/cm^3)	PM$_{2.5}$ (µg/m^3)	BC (ng/m^3)
A	Avg.	4406	12	2159	7073	26	3442	22419	18	3998
	Median	4734	13	2424	3796	27	1817	14454	20	3581
	St.Dev	1232	1	590	8571	9	5809	20947	5	1342
B	Avg.	6995	22	738	25764	49	3347	24867	60	5208
	Median	6200	22	708	28172	53	3406	23836	57	5560
	St.Dev	4034	5	353	9337	18	2112	5741	16	1103
C	Avg.	NA	10	602	21310	22	1530	26512	19	3401
	Median	NA	10	542	15647	21	1835	24292	19	3465
	St.Dev	NA	0.5	300	13723	3	860	10228	2	895
D	Avg.	NA	13	248	NA	36	3591	NA	36	5282
	Median	NA	13	235	NA	37	3437	NA	36	5071
	St.Dev	NA	0.3	88	NA	6	1262	NA	5	1616
E	Avg.	5184	15	NA	15569	25	NA	28833	24	NA
	Median	4550	13	NA	14300	26	NA	21446	25	NA
	St.Dev	1640	8	NA	8811	4	NA	22624	4	NA
F	Avg.	NA	11	115	13280	41	2335	25159	28	3290
	Median	NA	11	98	5273	37	23355	20334	28	3091
	St.Dev	NA	0.6	107	16187	14	775	18668	6	1218
All	Avg.	4558	14	780	19366	33	2836	27243	30	4144
	Median	2976	13	448	13560	29	2329	23802	27	3978
	St.Dev	4151	6	805	19280	14	2898	17530	15	1516

Table 6. A summary of in-cabin measurements for UFP, PM$_{2.5}$, and BC with operating on-board HECA filtration system under different driving conditions in school buses.

Exp. Modes		Stationary			Local			Freeway		
Bus ID	Pollutants	UFP (#/cm^3)	PM$_{2.5}$ (µg/m^3)	BC (ng/m^3)	UFP (#/cm^3)	PM$_{2.5}$ (µg/m^3)	BC (ng/m^3)	UFP (#/cm^3)	PM$_{2.5}$ (µg/m^3)	BC (ng/m^3)
A	Avg.	1405	10	632	1239	11	610	1526	4	751
	Median	507	9	165	626	10	350	651	4	624
	St.Dev	2245	2	1347	1863	2	735	2091	1	531
B	Avg.	1698	14	547	2174	17	1083	5190	11	883
	Median	519	11	111	1258	15	424	4407	10	704
	St.Dev	4044	9	1308	2319	5	2442	4102	6	737
C	Avg.	12918	10	169	1855	10	849	1850	5	1201
	Median	10531	9	164	1019	9	539	121	4	308
	St.Dev	5506	4	99	3039	1	840	9516	2	1577
D	Avg.	NA	12	81	NA	15	798	NA	11	943
	Median	NA	12	42	NA	14	651	NA	11	630
	St.Dev	NA	1	119	NA	2	615	NA	2	823
E	Avg.	1763	6	NA	1043	7	NA	4595	6	NA
	Median	1060	6	NA	532	7	NA	2355	5	NA
	St.Dev	1445	1	NA	1401	1	NA	7872	2	NA
F	Avg.	NA	11	118	2182	14	420	5840	8	568
	Median	NA	11	47	443	13	360	3042	8	496
	St.Dev	NA	1	192	3725	2	309	6222	2	382
All	Avg.	2780	10	312	1614	12	734	3778	7	872
	Median	839	10	107	727	12	419	1721	6	625
	St.Dev	4551	5	866	2491	4	1219	6505	4	921

3.3 Size-resolved In-cabin UFP Reduction

Passenger Vehicle

Figure 15 shows the average particle removal efficiency as a function of particle size (10-200 nm) inside passenger vehicles. The plotted data of in-cabin UFP reduction are the averages across all field conditions (i.e., stationary, local roadway, and freeway) for the specified filtration scenario. See Appendix O for the size-resolved in-cabin UFP reduction data averaged under each driving condition. Unlike laboratory filtration efficiency tests using KCl aerosols (see Figures 3 and 4), field measurements used actual particles from different roadways. Thus, data presented in Figure 15 should be distinguished from the standardized laboratory testing that uses laboratory-generated particles under a fixed flow rate.

Across the measured size ranges, the in-cabin UFP reduction was most effective when using the HECA B filter, followed by the HECA A filter, the in-use OEM filter, and no filter. Since particle diffusion loss occurs in the ventilation system, reductions were observed even with no filter installed. Figure 15 indicates the effectiveness of in-cabin particle reduction is different across different particle sizes. For instance, the no-filter case exhibited a significant decrease of removal efficiency from 60% to 20% as the particle size decreased from 100 to 10 nm. Although the removal efficiency for the in-use OEM filter was relatively consistent at a level of 60–65% across the measured size range, it decreased considerably to 35% for particles smaller than 15 nm.

Figure 15. Comparison of in-cabin UFP reduction (%) with respect to particle diameter (Dp) for HECA B, HECA A, in-use OEM, and no-filter cases inside passenger vehicles. The plotted data are averaged from all driving scenarios. See Appendix O for the data under each driving scenario.
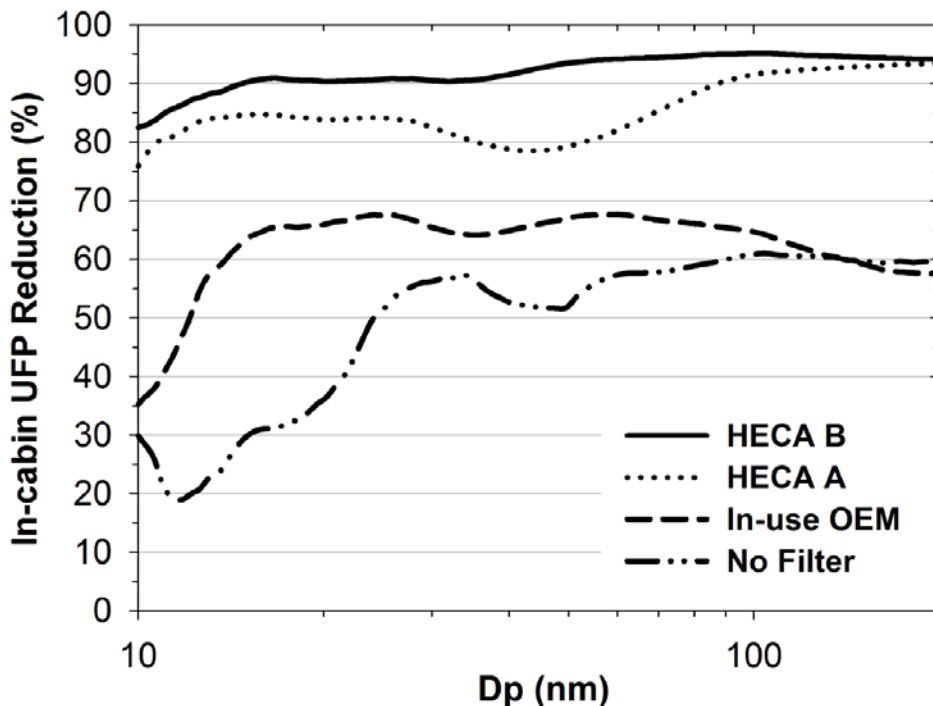
Unlike no-filter and in-use OEM filter scenarios, the removal efficiency of the HECA B filter was consistently high at approximately 95% for particle sizes down to 50 nm, with only a slight decrease to 85% for particles smaller than 50 nm. In comparison, the HECA A filter had a UFP removal of 75–93%. Both HECA filters consequently offered more consistent particle removal efficiency across the measured size range with much less variability than no filter and OEM filters. Therefore, under the field condition in this study, the in-use OEM filter could not effectively remove particles smaller than 50 nm, whereas HECA B filter provided highly effective and consistent particle removal across the measured size range. This is largely because of the diameter of fibers used for OEM filters and HECA B filters are different. As previously discussed, OEM filters have fibers with a diameter larger (2–5 μm) than HECA B filters (0.4–0.8 μm). The smaller fiber diameter of HECA B filters enhances particle collection by diffusion and interception, which is the dominant mode of particle removal especially for nucleation mode particles below 30 nm.

Different size-specific removal efficiencies in each filtration scenario also help to explain why the in-cabin UFP removal was higher on freeways (as seen in Figure 12a). The minimum filtration efficiency usually occurs around 0.1–0.3 μm (i.e., the most penetrating particle size) for conventional fibrous filters (e.g., in-use OEM filters used in this study). Thus, with the in-use OEM filter, the overall in-cabin reduction is expected to decrease for larger particles (i.e., mode diameter of ~ 80 nm) observed under stationary conditions. Conversely, more reduction can occur for smaller particles (i.e., mode diameter of ~ 30 nm) in the freeway environment even with the in-use OEM filter. In the no-filter scenario, the filtration theory for fibrous filters does not apply. Since mechanical ventilation system delivered on-road particles at higher speed in the absence of filter resistance, those particles including nucleation mode particles had less time to diffuse and deposit to the surface of the ventilation system.

Consequently, the application of HECA B filters offered consistent particle removal efficiencies across the measured particle size range and achieved an in-cabin UFP reduction by 93% on average in the field. Its performance is less affected by the on-road particle size distribution and is 2–3 times better than the in-use OEM filters. These findings also suggest that a large proportion of the measured in-cabin UFPs are in the smaller size range, even after the filtration process with in-use OEM filters. Since the deleterious health effects of UFPs are likely related to smaller particles, a consistent removal across a wide range of particle sizes is important and can be readily achievable via in-cabin HECA filters.

School Bus
Figure 16 compares size-resolved in-cabin UFP reductions under normal school bus operations (i.e., without operating the HECA filtration system, Figure 16a) and with operating the HECA filtration system (Figure 16b). The plotted data are averages of measurements from all test school buses. Appendix P provides standard deviations across different school buses.

The in-cabin UFP reductions were estimated using a measure of in-cabin UFP reduction = (1 – I/O) x 100. It is important to note that the in-cabin UFP reduction used in this study is not filtration efficiency. In-cabin UFP reduction is used here to indicate potential exposure reductions, which conflates several particle gain and loss mechanisms under realistic field conditions (e.g., self-pollution, infiltration, and surface deposition). Under normal school bus operations (i.e., without HECA filtration system), infiltration can bring on-road UFPs into the school bus cabin because of high air exchange rates through the gaps of windows and door. Particle loss naturally occurs due to diffusion during the infiltration process (Xu et al., 2010) and deposition to the interior surface (Gong et al., 2009).

Without operating the HECA filtration system (Figure 16a), the UFP reduction was relatively low, about 30–70% for particles in the size range of 7.37 to 289 nm. Under freeway driving scenarios, the in-cabin UFP reduction becomes higher for smaller particles (up to 70% below 10 nm) presumably because of particle diffusion loss. With operating the HECA filtration system (Figure 16b), the in-cabin reduction was greater than 70% under the same condition (i.e., stationary and local driving scenarios). Under the freeway driving scenario, in-cabin UFP reductions were the greatest and stayed above 87% for particles with diameter less than 289 nm. Different driving conditions did not make significant differences for the in-cabin UFP reductions as long as the HECA filtration system was operating.

Figure 16. Comparison of UFP I/O reduction (%) with respect to particle diameter (Dp) under stationary (dots), local roadway (dash), freeway (solid) scenarios inside school buses.
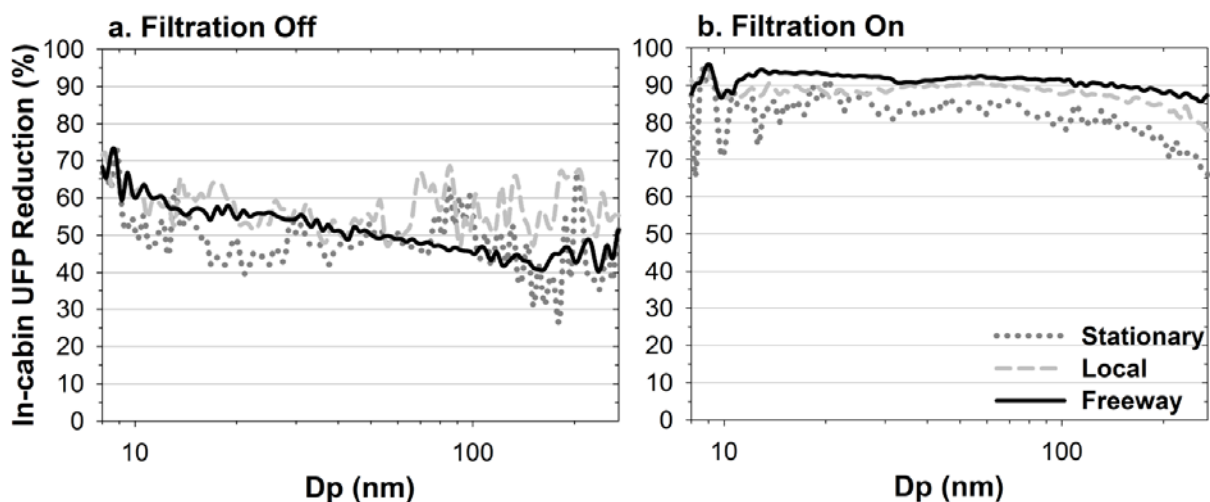
3.4 Time-Resolved UFP Reduction

Passenger Vehicle
As shown in Figure 17, the reduction of in-cabin UFPs occurs almost instantaneously when a HECA B filter was used. Time-resolved UFP size distributions measured inside (Figures 17b, 17d, and 17f) and outside (Figures 17a, 17c, and 17e) of a passenger vehicle are shown in contour plots, where x-axis presents the elapsed time at which data were collected, y-axis is the particle size in log scale, and the color intensity indicates normalized particle number concentration (dN/dLogDp) for a given size at a given time. The same concentration scale was used for all plots.

Under stationary (Figure 17a), local (Figure 17c), and freeway-driving (Figure 17e) conditions, the use of a HECA B filter (Figures 17b, 17d and 17f) offered a strong in-cabin UFP reduction throughout the measured size range. The reduction occurred immediately after a HECA B filter was installed and continued throughout the measurement period. With a HECA B filter installed, the particle size-specific reduction was approximately one order of magnitude higher across the measured size range and was especially effective for nucleation mode particles. The magnitude of particle reduction is similar to the 93% reduction of in-cabin UFP number concentrations (Figure 12) and occurred for all driving conditions.

Figure 17. Normalized particle concentrations (dN/dLogDp) are plotted with respect to time and particle diameter (Dp) for a passenger car under (a) stationary ambient, (b) stationary in-cabin, (c) local ambient, (d) local in-cabin, (e) freeway ambient, and (f) freeway in-cabin conditions. The color intensity represents dN/dLogDp. The plotted data are measurements from Honda Odyssey 2010.
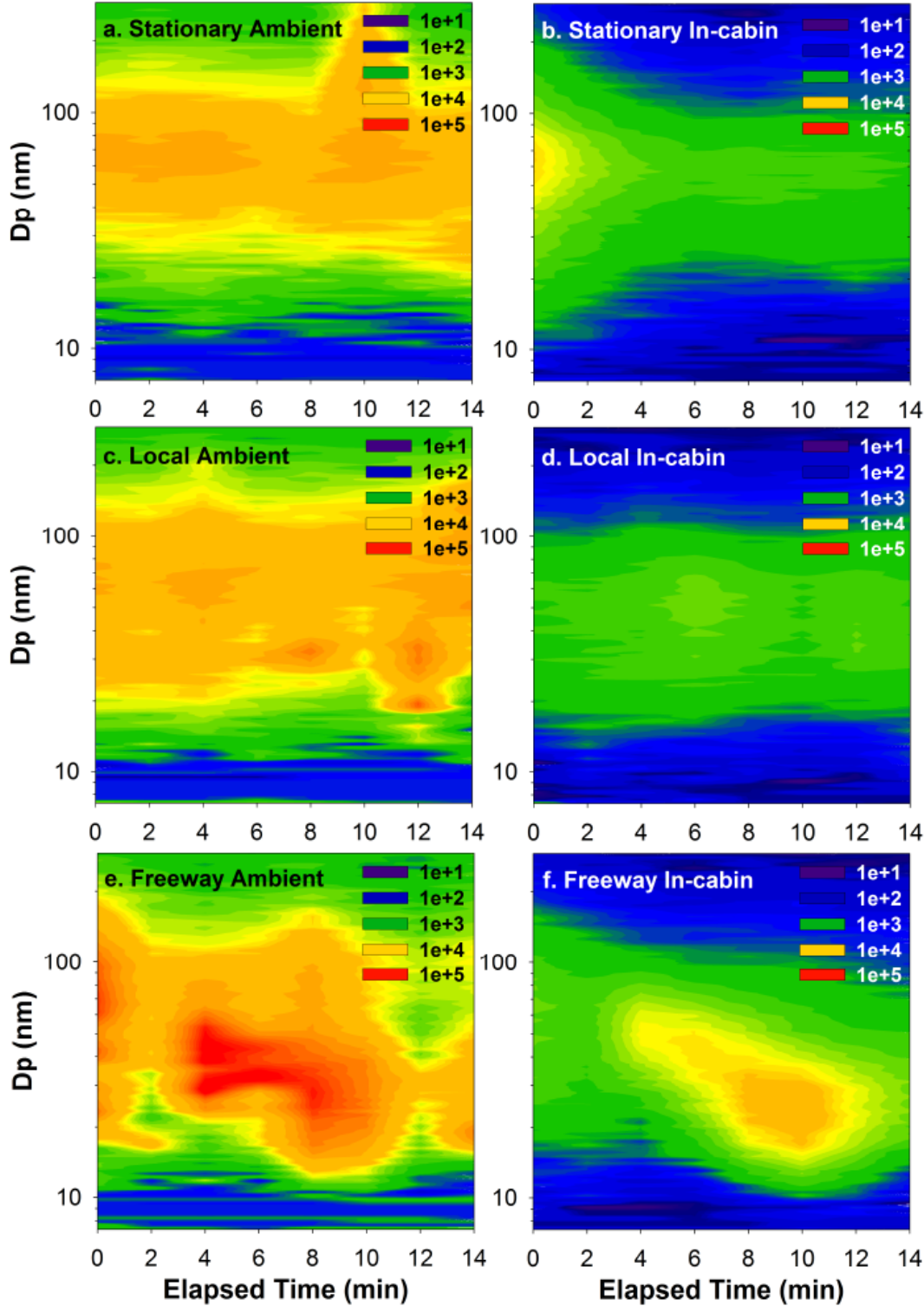
School Bus
Time-resolved UFP size distributions inside and outside of the school bus C are shown in contour plots in Figure 18. The x-axis is the elapsed time at which data were collected and the y-axis is the particle diameter in log scale. The color intensity presents the normalized particle number concentration (dN/dLogDp) for a given particle size and time. The same scale and color intensity are used for Figures 18a-d. Note that the color intensity in Figure 18 is the same as that in Figure 17. The top row panels (a) and (b) present on-road concentrations. The bottom row panels (c) and (d) show in-cabin concentrations. In-cabin concentration data were collected with (left in each panel) and without (right in each panel) operating the HECA filtration system in the bus.

As seen in Figures 18a and 18b, the on-road particle concentration changed dynamically because of surrounding traffic emissions. For instance, particle size distributions on local arterial roadways had mode diameters of 50–80 nm; whereas, on freeways, smaller mode diameters ranging from 8 to 30 nm were observed. In comparison to on-road concentrations, Figures 18c and 18d show that HECA filtration system instantaneously reduced in-cabin UFP concentrations by one or two orders of magnitude. For both local and freeway driving scenarios, the HECA filtration system effectively reduced in-cabin UFP concentrations across the measured size range (see the left-hand side of Figures 18c and 18d). In comparison, the right-hand sides of Figures 18c and 18d support this point by showing the data collected without operating the HECA filtration system. The presented data are the measurements in the school bus C and similar findings were also observed in the other five tested school buses (data not shown here).

Figure 18 also provides corroborative evidence of self-pollution inside school buses. Under normal school bus operations (i.e., without operating the HECA filtration system), UFP concentration inside the school bus became one or two orders of magnitude higher than the on-road concentration for particles smaller than 20 nm. It is particularly noticeable around the 55–80 minute period of Figure 18c, as well as the 60–80 minute period in Figure 18d. When operating the HECA filtration, normalized in-cabin particle concentrations were mostly (i.e., > 90% of time) below 100 cm^{-3} across the measured size range during the 0–60 minute period in Figure 18d. However, for particles less than 20 nm, the in-cabin normalized UFP concentrations often reached up to 10,000 cm^{-3}. Similar patterns were also observed in other tested school buses. There was no noticeable UFP emission source inside the test school bus. Freshly emitted particles from vehicle tailpipes are usually in the nucleation mode with diameter less than 20 nm. The authors did not, however, observe the same in passenger vehicles when similar HECA filters were tested. The observed increase in nucleation mode particles inside school buses is likely due to self-pollution as previously observed by other researchers (Behrentz et al., 2004; Ireson et al., 2011).

Figure 18. Normalized particle concentrations (dN/dLogDp) are plotted with respect to time and particle diameter (Dp) for the school bus C under local and freeway driving conditions. Color intensity represents dN/dLogDp. In-cabin concentration data were collected with (left in each panel) and without (right in each panel) operating the on-board HECA filtration system in school bus C.
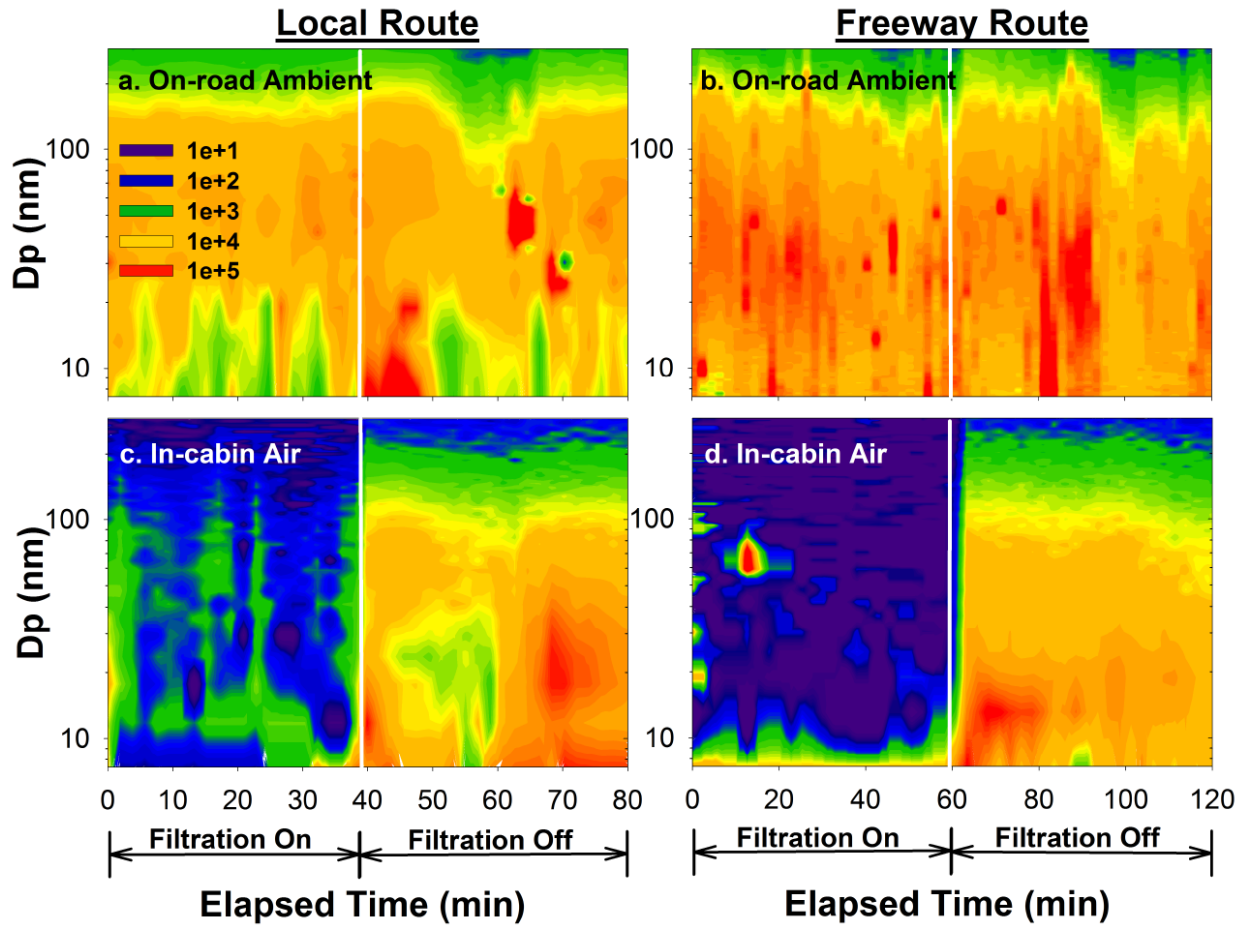
3.5 Ventilation Air-flow Rate Reduction in Passenger Vehicles

The installation of HECA filters may result in a large pressure drop that reduces the ventilation air-flow rate into the passenger cabin. Because the automotive ventilation systems primarily serve to offer thermal comfort to passengers, the reduction in the air-flow rate could become a critical limitation for in-cabin HECA filter application.

The pressure drops of HECA A and B filters were estimated as ~36 mm H_2O and ~50 mm H_2O under ASHRAE 52.2 standard MERV testing condition. However, the pressure drop can change by applied air-flow rate due to different air blower capacities in different vehicle models. The measure of ventilation air-flow rates can serve as a surrogate for pressure drop under realistic conditions which also take into account different vehicle characteristics (e.g., duct system design and blower capacity).

Figure 19 summarizes changes of ventilation air-flow rates and in-cabin UFP reductions upon retrofitting with the in-cabin HECA filters. The changes in the ventilation air-flow rates were provided in Figure 19 with respect to those measured with the in-use OEM filters under stationary conditions (as indicated by the arrow). With the in-use OEM filters under stationary conditions, the ventilation air-flow rate was averaged at 306 m^3/h with a standard deviation of ± 101 m^3/h across all test vehicles. For individual test vehicles, the changes of ventilation air-flow rates were estimated with respect to the ventilation air-flow rate with in-cabin OEM filter under stationary condition. The symbols and error bars are the averages and standard deviations of the relative changes, respectively. The presented data are the means and standard deviations of all tested vehicle models under different experimental conditions.

A non-parametric Mann-Whitney U-test was used to examine the differences of ventilation air-flow rate under various filtration scenarios. As expected, retrofitting with HECA B filters significantly reduced the ventilation air-flow rate for all driving conditions ($p < 0.01$). In comparison with the in-use OEM, the ventilation air-flow rate was reduced by 22, 12, and 7% on averages under the stationary, local, and freeway conditions, respectively. However, these reductions are unlikely to cause thermal comfort issues to passengers under realistic driving conditions. In addition, ventilation air-flow rate increases at higher driving speed due to high pressure at ventilation air intake area (i.e., passive ventilation). For that reason, the ventilation air-flow rate in Figure 19 has higher values on freeways than on local roadways or in stationary conditions. This observation was reported in a previous study, which showed that the passive ventilation significantly increases the ventilation air-flow rate when driving on freeways (Ott et al., 2008). Thus, the passive ventilation helps to overcome the additional pressure drop from the installed HECA filters.

Figure 19. Changes of the ventilation airflow rates and UFP reduction inside passenger vehicles under different driving conditions for different filtration scenarios. The symbols and the error bars are the mean and the standard deviation of the observations in different vehicle models. The arrow indicates the ventilation air flow rate with the in-use OEM filters under stationary conditions, which was at 306 ± 101 m^3/h on average across the test vehicle models.
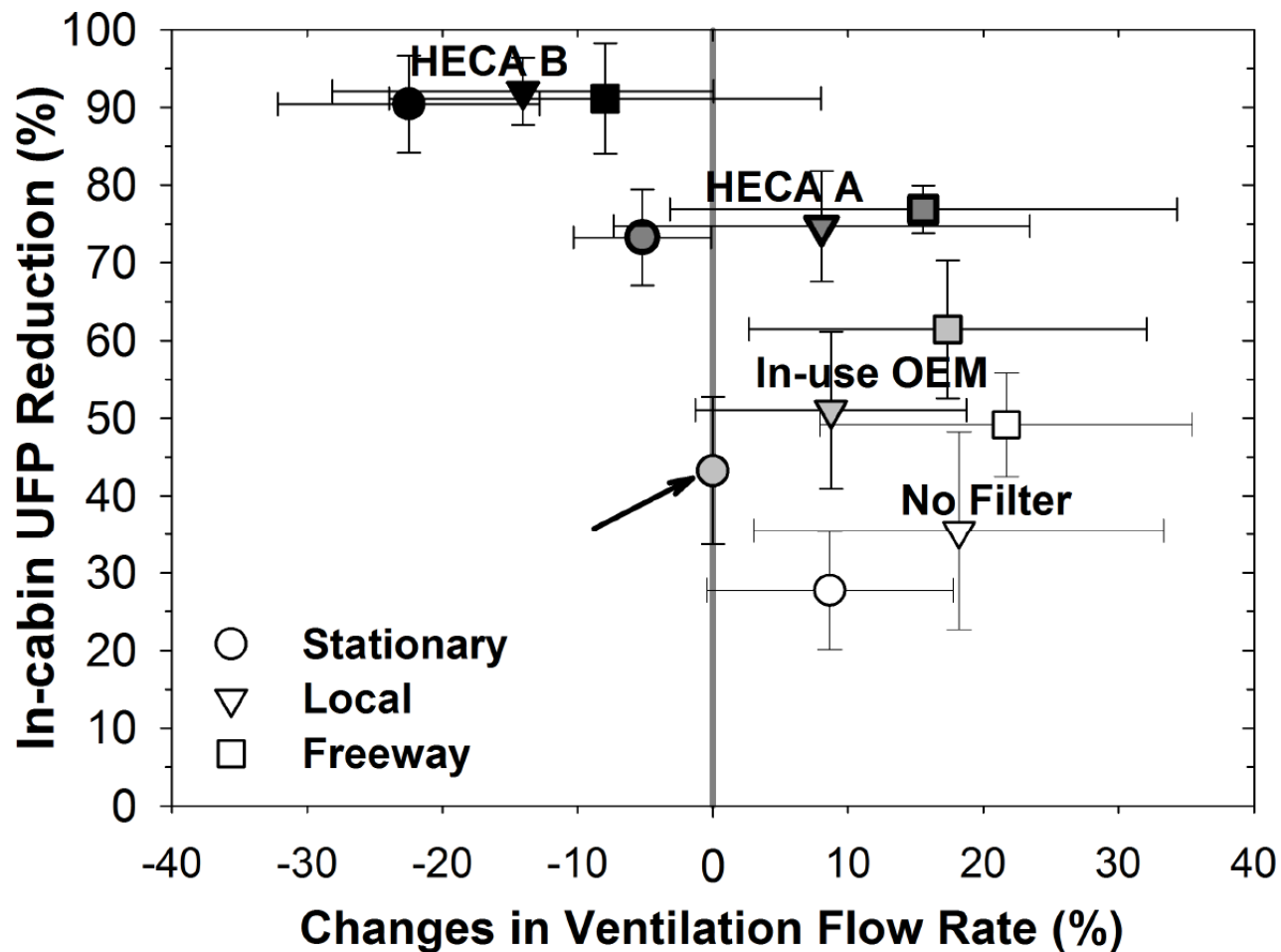
3.6 Simultaneous Mitigation of UFPs and CO_2 in Passenger Vehicles

Retrofitting the HECA filters enable a simultaneous mitigation of in-cabin UFPs and CO_2. Figures 20a and 20b show under stationary condition, the time-series of I/O estimates for UFPs with in-use OEM and HECA B filters, as well as CO_2 in OA and RC-mode, respectively. The plotted data are means and the shades are the standard deviations for all 12 test vehicles.

As shown in Figure 20b, operating vehicles in the RC mode reduced the UFP I/O down to 0.07. However, this approach also imposes the unwanted problem of passenger-exhaled CO_2 accumulation. Within 15 minutes, the CO_2 I/O tripled with 1–2 passengers (i.e., 1.3 passengers on average) inside the stationary vehicle cabin. The tripled CO_2 I/O is equivalent to a concentration of 2,500 to 4,000 ppm on average. Although the application of a HECA filter in RC mode reduced the in-cabin UFPs further than the in-use OEM filters, the problem of CO_2 accumulation still remained at a similar magnitude.

To solve this problem, the authors utilized the OA-mode ventilation system to supply HECA-filtered on-road air into the passenger cabin (Figure 20a). Under stationary OA-mode conditions with 1.3 passengers on average, the in-cabin CO_2 concentrations were maintained at a reasonable level that was ~ 20% higher than the on-road measurement. With two passengers driving on local streets and freeways, the average in-cabin CO_2 concentrations were 69% (i.e., 790 ppm) and 58% (i.e., 750 ppm) higher than the on-road concentration (i.e., ~ 470 ppm). Table 3 provides detailed data. In the meanwhile, the in-cabin UFP concentrations decreased and UFP I/O stabilized at 0.07 in the OA mode with the HECA B filter. Compared to the in-use OEM filter, which had a UFP I/O of 0.60, the application of the HECA B filter achieved a substantially lower (i.e., 0.07) in-cabin UFP I/O ratio. Regardless of the on-road concentration fluctuations under local and freeway driving conditions, the in-cabin UFP concentration in the HECA B filter scenario was an order of magnitude lower than the on-roadway level.

Figure 20. I/O ratios as a function of time for UFPs and CO_2 using the HECA B and in-use OEM filters under OA and RC modes for passenger vehicles. The plotted data are averages of data collected in all 12 passenger vehicles. The shaded areas indicate the standard deviations of the observation in different passenger vehicle models.
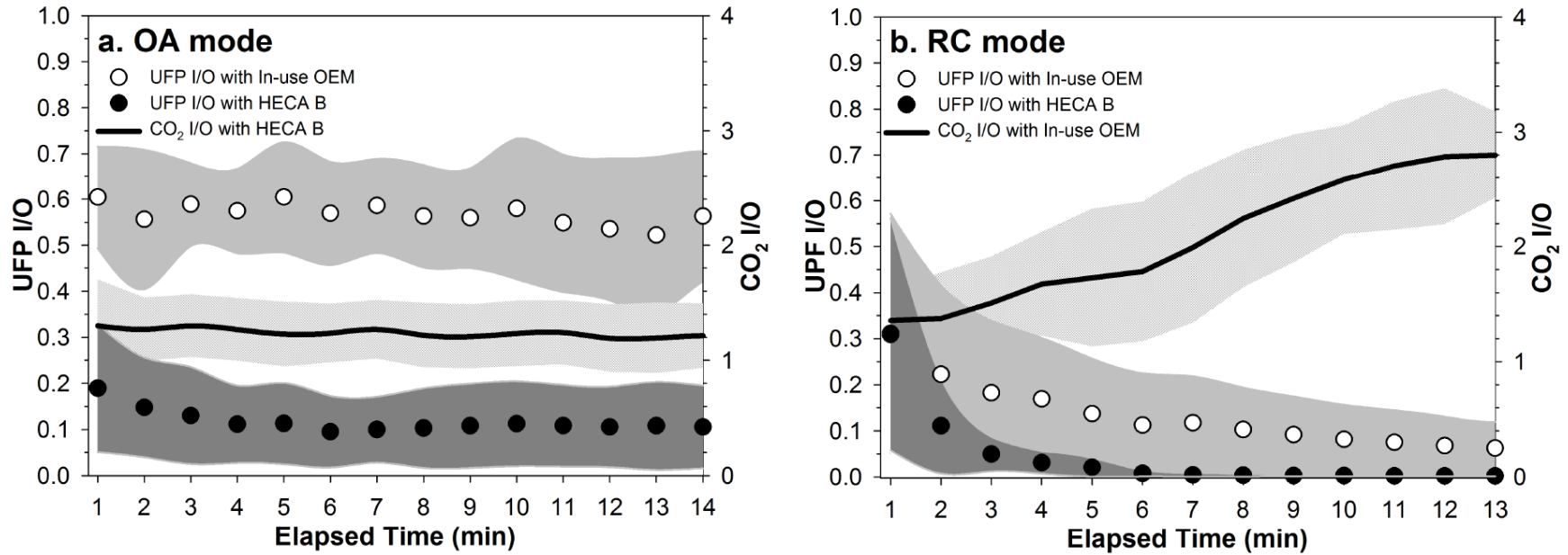
3.7 In-cabin Air Quality Improved by HECA Filtration

The HECA filtration system effectively reduced particulate pollutants (i.e., UFP, BC, and PM$_{2.5}$) inside both passenger vehicles and school buses. Typically in passenger cars, the level of exposure reduction can be expressed using the I/O ratios of pollutants, such as (1–I/O) x 100 in Equation (1). This measure works well in passenger vehicles, where no significant self-pollution problem is observed. However, self-pollution in school buses sometimes results in higher in-cabin concentration than on-road concentration (i.e., I/O > 1.0 as seen in Appendices K and L). Accordingly, the authors defined pollutant reductions by comparing two I/O ratios with and without operating the HECA filtration system. Since self-pollution occurs in both conditions (i.e., with and without operating the HECA filtration system), the I/O Reduction was estimated from $(I/O)_{HECA-On}$ normalized by $(I/O)_{HECA-Off}$, as given in Equation (2). Note that this method using Equation (2) was equally applied to the data from testing school buses and passenger vehicles in Figure 21. Note that the data shown in Figure 21b are I/O reductions estimated from Equation (2) and the data presented in Figure 12 were estimated differently for the in-cabin concentration reductions by using 1 - I/O in Equation (1).

Figure 21a summarizes average I/O Reductions with the HECA filtration system on, relative to off in school buses. The prototype HECA filtration system effectively reduced UFPs, BC, and PM$_{2.5}$ levels inside school buses. In Figure 21a, I/O Reductions were estimated by using Equation (2). The data points in Figure 21a are the means of the 1-min averaged data for each of the six test school buses under different driving conditions (i.e., stationary, local, and freeway conditions). As shown in Figure 21a, the HECA filtration system substantially reduced particulate pollutant (i.e., UFPs, BC, and PM$_{2.5}$) levels under both stationary and realistic local and freeway driving conditions inside school buses. Relative to normal school bus operations (i.e., without operating the HECA filtration system), the filtration system operation achieved I/O Reductions above 80% for UFPs and BC. The I/O Reduction ranged from 85 to 90% on average for UFPs under all driving conditions. For BC, the reductions ranged from 80 to 90% on average, and the greatest reductions were observed on freeways. The HECA filtration system was less effective (35−75% on average) for PM$_{2.5}$. Figure 21a also illustrates the I/O Reductions by the HECA filtration system under each test condition (i.e., stationary, local, and freeway). As shown in Figure 21a, the maximum I/O Reduction occurred on freeways and the minimum occurred under stationary condition. The same observation was repeated for all types of pollutants: UFPs, BC, and PM$_{2.5}$.

The I/O ratio reductions in school buses were relatively comparable to the I/O ratio reductions in passenger cars when applying the same filtration technology. In comparison with the current state of the art (i.e., OEM filters for passenger vehicles and no filtration system for school buses), HECA filtration technology improved the current level of pollutant I/O ratio by 82-88% for UFPs, 66-95% for BC, and 33-80% for PM$_{2.5}$, on averages across different passenger vehicle and school bus models. The ranges were given for different driving scenarios. One should note that some differences might result from different experimental conditions such as cabin volume size, driving speed, testing route, and on-road particle size distributions. More importantly, the application of

HECA filters was evaluated under OA mode ventilation setting in passenger vehicles. In contrast, the test school buses had neither ventilation system nor air conditioning system. Overall, the application of HECA filters and the on-board HECA filtration system achieved comparable level of pollutant reductions in both passenger vehicles and school buses. It is also important to note that sporadic door operations had insignificant impacts on UFP I/O ratios when operating the HECA filtration system inside school buses (Appendices Q and R). Similar to a typical school bus operation, the test school bus simulated door operation for 1 minute at each stop. Local and freeway roadway driving scenarios had 9 and 3 pick-up/drop-off events, respectively. While operating the HECA filtration system, the differences in UFP I/O concentration ratios were insignificant between close-door and open-door scenarios.

Figure 21. In-cabin exposure reductions by implementing HECA filtration technology in (a) school buses (i.e., with the on-board HECA filtration system) and (b) passenger vehicles (i.e., with the HECA B filter). The plotted I/O reductions are estimated by using the same measure of I/O Reduction, given in Equation (2), with respect to the current state of the art (i.e., OEM filters in passenger vehicles and no filtration system in school buses). The symbols and the error bars are the mean and the standard deviation of the averaged I/O reductions in different vehicle models.
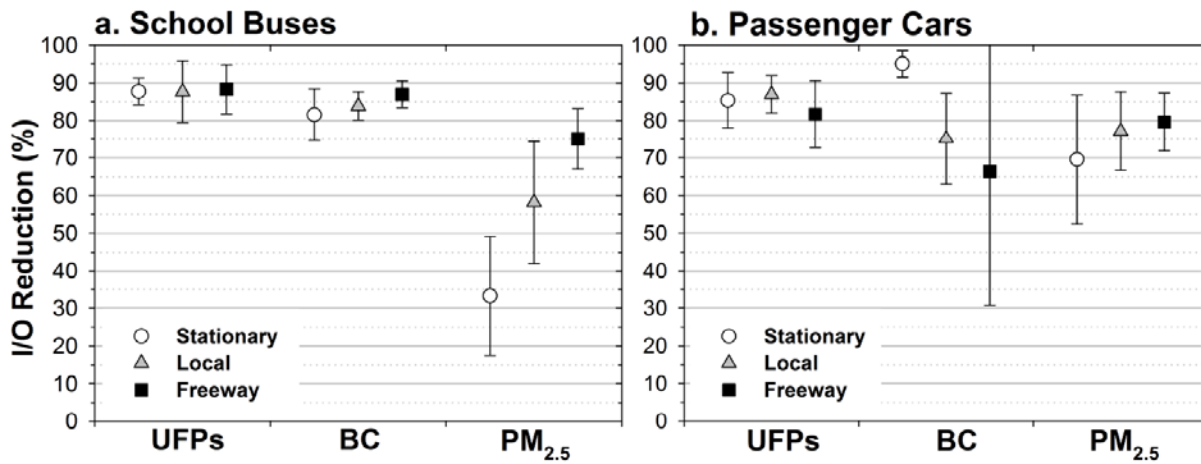
3.8 HECA Filtration Efficiency for PM$_{2.5}$

Throughout this project, the overall in-cabin exposure reduction is the greatest for UFPs, and followed by BC. The particle removal efficiency by the HECA filters seemed to be less for PM$_{2.5}$. This observation is consistent in the data from tests conducted for both passenger vehicles and school buses.

The size-dependent filtration efficiency of a filter is affected by the size of source particles. Smaller particles (e.g., UFP and BC) are removed by Brownian diffusion mechanism; whereas, larger particles are removed more likely by impaction or interception due to particle inertial. In addition, the removal efficiency for BC and PM$_{2.5}$ can be sensitive to the losses of larger particles because BC and PM$_{2.5}$ were measured in units of mass concentration whereas UFPs were measured by number concentration. The penetration of a few relatively large particles can substantially affect the measured efficiency for BC and PM$_{2.5}$.

Figure 22. The current level of in-cabin PM$_{2.5}$ exposure and potential reductions by HECA filtration in passenger vehicles and school buses. The plotted data are averages from all vehicle models. The error bars indicate the standard deviation of averaged in-cabin reductions in test vehicle models.

46
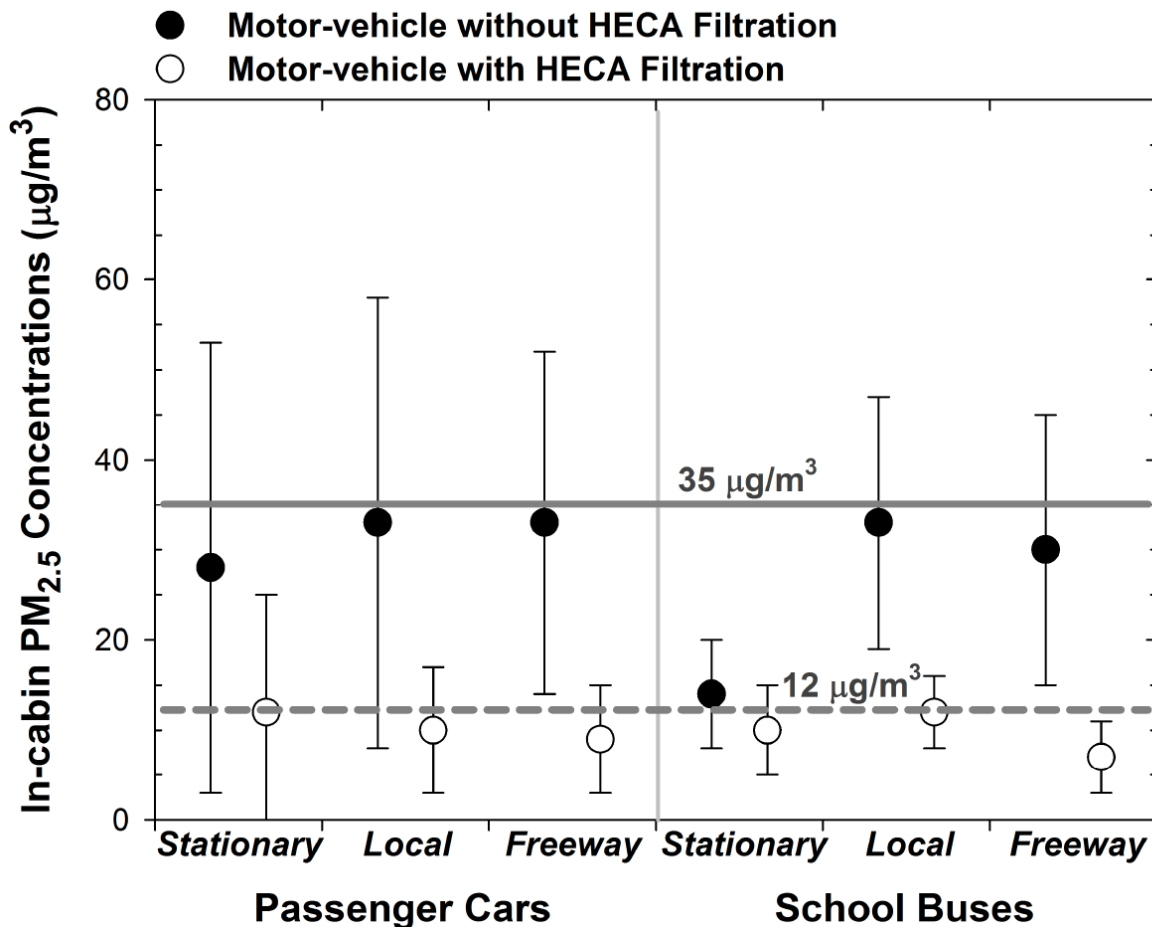
It is important to emphasize that the HECA filtration system is also effective for removing $PM_{2.5}$. Figure 22 illustrates the in-cabin $PM_{2.5}$ concentrations with and without operating the HECA filtration system in both passenger vehicles and school buses. The presented data in Figure 22 are means and standard deviations of measured $PM_{2.5}$ concentrations. Without using HECA filters and operating the HECA systems in the buses, the in-cabin $PM_{2.5}$ levels fluctuated around 35 $\mu g/m^3$. When the HECA filtration was on, the $PM_{2.5}$ level was maintained below 12 $\mu g/m^3$ on averages in passenger vehicles and school buses. Therefore, the developed HECA filters effectively reduced in-cabin $PM_{2.5}$ concentrations.

4. SUMMARY AND CONCLUSIONS

Exposures to vehicle-emitted $PM_{2.5}$, BC, and UFPs, have been associated with adverse health effects. As a potential strategy to mitigate in-cabin exposure, the authors developed a novel high efficiency cabin air (HECA) filter for passenger vehicles and a HECA filtration system for school buses. The authors evaluated the filtration efficiencies in twelve passenger vehicles and six school buses. Significant reductions of passenger exposures were observed in both passenger vehicles and school buses. In passenger vehicles, in-cabin UFP reduction was 93% on average (up to 99%) under the field conditions. The level of pollutant mitigation was slightly lower for BC (85%) and $PM_{2.5}$ (70%). The percentages of in-cabin UFP reduction were higher on the freeways than on local roadways and under the stationary condition. Using the same technology, the authors developed a novel on-board HECA filtration system for school buses and evaluated its effectiveness of reducing particulate pollutants inside six school buses. The developed on-board HECA filtration system can substantially reduce potential children's exposure to particulate pollutants while riding inside school buses. Regardless of the pollutant sources (e.g., other vehicles nearby or self-pollution), operating the on-board HECA filtration inside buses reduced UFPs and BC by 90% and 85%, respectively. Although the effectiveness of the HECA filtration system for $PM_{2.5}$ was relatively lower (i.e., ~ 60% on average and ranged from 35 to 75%) due to size-dependent filtration, it was still able to reduce in-cabin $PM_{2.5}$ levels by 33–66%, which made it below 12 µg/m^3. Sporadic door operations did not significantly change the effectiveness of HECA filtration. Overall, the developed HECA filters achieved 2–3 times greater reduction than the in-use OEM filters in passenger vehicles and typical school buses without a ventilation or air conditioning system. Using the HECA filters in passenger vehicles also kept the in-cabin CO_2 concentration at 630–920 ppm under OA-mode ventilation with two passengers driving on local streets and freeways. These concentrations are much less than in the RC mode, which could reach 2,500 to 4,000 ppm within 15 minutes. In conclusion, the HECA filters can be highly effective for the reduction of passenger exposures to UFPs under OA mode, which helps maintain CO_2 level below 1,000 ppm inside passenger vehicles. The developed on-board HECA filtration system was also effective to mitigate children's exposure to UFPs, BC, and $PM_{2.5}$ inside school buses.

5. RECOMMENDATIONS

The developed high efficiency cabin air (HECA) filtration can become a potential exposure mitigation method in passenger vehicles and school buses. However, the scope of the current study is limited because field evaluations were only conducted on new filters in a few selected vehicle models during a short period of time. This study aimed to mimic typical school bus driving patterns with pick-up / drop-off scenarios; however, it was limited by not having children on board. Involvement of children might decrease the effectiveness of on-board HECA filtration system, particularly for $PM_{2.5}$ inside school buses, because physical activity of children might lead to particle resuspension from interior surfaces of school buses.

Practical application of the HECA filter requires long-term evaluations (with children on board for school buses) under a broader range of driving conditions. The authors recommend assessing long-term performance of the developed HECA filters for a wide range of particle sizes (10 nm to 10 μm) in passenger vehicles and school buses. The assessment should focus on (1) potential degradation of filtration efficiency in time through the long-term evaluations under realistic driving conditions; (2) efficacy of HECA filters against window position and seasonal variables (e.g., temperature and humidity); (3) potential changes of fuel consumption upon retrofitting with HECA filters; and (4) potential barriers (e.g., increased cost and pressure drop) for using HECA filters inside automobile cabins. Specifically, the long-term evaluation for school buses should also address (5) potential CO_2 accumulation problems when children are on board. Results from such long-term performance evaluations of HECA filters can be used by ARB for future in-cabin air pollution exposure reduction guidelines.

VIII. REFERENCES

Apte, M.G., Fisk, W.J., Daisey, J.M., 2000. Associations between indoor CO2 concentrations and sick building syndrome symptoms in US office buildings: An analysis of the 1994-1996 BASE study data. Indoor Air-International Journal of Indoor Air Quality and Climate 10, 246-257.

ASHRAE, 2007. Standard 52.2 method of testing general ventilation air-cleaning devices for removal efficiency by particle size. American Society of Heating, Refrigerating, and Air-Conditioning Engineers, Atlanta, GA.

Behrentz, E., Fitz, D.R., Pankratz, D.V., Sabin, L.D., Colome, S.D., Fruin, S.A., Winer, A.M., 2004. Measuring self-pollution in school buses using a tracer gas technique. Atmospheric Environment 38, 3735-3746.

Chan, A.T., Chung, M.W., 2003. Indoor-outdoor air quality relationships in vehicle: effect of driving environment and ventilation modes. Atmospheric Environment 37, 3795-3808.

Chan, L.Y., Liu, Y.M., 2001. Carbon monoxide levels in popular passenger commuting modes traversing major commuting routes in Hong Kong. Atmospheric Environment 35, 2637-2646.

Fletcher, B., Saunders, C.J., 1994. Air change rates in stationary and moving motor-vehicles. Journal of Hazardous Materials 38, 243-256.

Fruin, S., Westerdahl, D., Sax, T., Sioutas, C., Fine, P.M., 2008. Measurements and predictors of on-road ultrafine particle concentrations and associated pollutants in Los Angeles. Atmospheric Environment 42, 207-219.

Fruin, S.A., Hudda, N., Sioutas, C., Defino, R.J., 2011. Predictive model for vehicle air exchange rates based on a large, representative sample. Environmental Science & Technology 45, 3569-3575.

Gilmour, P.S., Ziesenis, A., Morrison, E.R., Vickers, M.A., Drost, E.M., Ford, I., Karg, E., Mossa, C., Schroeppel, A., Ferron, G.A., Heyder, J., Greaves, M., MacNee, W., Donaldson, K., 2004. Pulmonary and systemic effects of short-term inhalation exposure to ultrafine carbon black particles. Toxicology and Applied Pharmacology 195, 35-44.

Gong, L., Xu, B., Zhu, Y., 2009. Ultrafine Particles Deposition Inside Passenger Vehicles. Aerosol Science and Technology 43, 544-553.

Hammond, D.M., Lalor, M.M., Jones, S.L., 2007. In-vehicle measurement of particle number concentrations on school buses equipped with diesel retrofits. Water Air and Soil Pollution 179, 217-225.

Hitchins, J., Morawska, L., Wolff, R., Gilbert, D., 2000. Concentrations of submicrometre particles from vehicle emissions near a major road. Atmospheric Environment 34, 51-59.

Ireson, R.G., Ondov, J.M., Zielinska, B., Weaver, C.S., Easter, M.D., Lawson, D.R., Hesterberg, T.W., Davey, M.E., Liu, L.J.S., 2011. Measuring in-cabin school bus tailpipe and crankcase PM2.5: a new dual tracer method. Journal of the Air & Waste Management Association 61, 494-503.

Klepeis, N.E., Nelson, W.C., Ott, W.R., Robinson, J.P., Tsang, A.M., Switzer, P., Behar, J.V., Hern, S.C., Engelmann, W.H., 2001. The National Human Activity Pattern

Survey (NHAPS): a resource for assessing exposure to environmental pollutants. Journal of Exposure Analysis and Environmental Epidemiology 11, 231-252.

Knibbs, L.D., de Dear, R.J., Atkinson, S.E., 2009a. Field study of air change and flow rate in six automobiles. Indoor Air 19, 303-313.

Knibbs, L.D., de Dear, R.J., Morawska, L., 2010. Effect of cabin ventilation rate on ultrafine particle exposure inside automobiles. Environmental Science & Technology 44, 3546-3551.

Knibbs, L.D., de Dear, R.J., Morawska, L., Mengersen, K.L., 2009b. On-road ultrafine particle concentration in the M5 East road tunnel, Sydney, Australia. Atmospheric Environment 43, 3510-3519.

Kroll, A., Gietl, J.K., Wiesmuller, G.A., Gunsel, A., Wohlleben, W., Schnekenburger, J., Klemm, O., 2013. In vitro toxicology of ambient particulate matter: correlation of cellular effects with particle size and components. Environmental Toxicology 28, 76-86.

Lee, E.S., Zhu, Y.F., 2014. Application of a high-efficiency cabin air filter for simultaneous mitigation of ultrafine particle and carbon dioxide exposures inside passenger vehicles. Environmental Science & Technology 48, 2328-2335.

Leung, P.L., Harrison, R.M., 1999. Roadside and in-vehicle concentrations of monoaromatic hydrocarbons. Atmospheric Environment 33, 191-204.

Li, N., Sioutas, C., Cho, A., Schmitz, D., Misra, C., Sempf, J., Wang, M.Y., Oberley, T., Froines, J., Nel, A., 2003. Ultrafine particulate pollutants induce oxidative stress and mitochondrial damage. Environmental Health Perspectives 111, 455-460.

MacKinnon, D.F., Craighead, B., Hoehn-Saric, R., 2007. Carbon dioxide provocation of anxiety and respiratory response in bipolar disorder. Journal of Affective Disorders 99, 45-49.

Marshall, J.D., Behrentz, E., 2005. Vehicle self-pollution intake fraction: children's exposure to school bus emissions. Environmental Science & Technology 39, 2559-2563.

Mohai, P., Kweon, B.S., Lee, S., Ard, K., 2011. Air pollution around schools is linked to poorer student health and academic performance. Health Affairs 30, 852-862.

Morawska, L., Ristovski, Z., Jayaratne, E.R., Keogh, D.U., Ling, X., 2008. Ambient nano and ultrafine particles from motor vehicle emissions: characteristics, ambient processing and implications on human exposure. Atmospheric Environment 42, 8113-8138.

Oberdorster, G., 2001. Pulmonary effects of inhaled ultrafine particles. International Archives of Occupational and Environmental Health 74, 1-8.

Ott, W., Klepeis, N., Switzer, P., 2008. Air change rates of motor vehicles and in-vehicle pollutant concentrations from secondhand smoke. Journal of Exposure Science and Environmental Epidemiology 18, 312-325.

Ott, W.R., Siegmann, H.C., 2006. Using multiple continuous fine particle monitors to characterize tobacco, incense, candle, cooking, wood burning, and vehicular sources in indoor, outdoor, and in-transit settings. Atmospheric Environment 40, 821-843.

Pope, C.A., Dockery, D.W., Schwartz, J., 1995. Review of epidemiological evidence of health-effects of particulate air pollution. Inhalation Toxicology 7, 1-18.

Pui, D.Y.H., Qi, C., Stanley, N., Oberdorster, G., Maynard, A., 2008. Recirculating air filtration significantly reduces exposure to airborne nanoparticles. Environmental Health Perspectives 116, 863-866.

Qi, C., Stanley, N., Pui, D.Y.H., Kuehn, T.H., 2008. Laboratory and on-road evaluations of cabin air filters using number and surface area concentration monitors. Environmental Science & Technology 42, 4128-4132.

Qian, J., Hospodsky, D., Yamamoto, N., Nazaroff, W.W., Peccia, J., 2012. Size-resolved emission rates of airborne bacteria and fungi in an occupied classroom. Indoor Air 22, 339-351.

Rim, D., Siegel, J., Spinhirne, J., Webb, A., McDonald-Buller, E., 2008. Characteristics of cabin air quality in school buses in Central Texas. Atmospheric Environment 42, 6453-6464.

Sabin, L.D., Kozawa, K., Behrentz, E., Winer, A.M., Fitz, D.R., Pankratz, D.V., Colome, S.D., Fruin, S.A., 2005. Analysis of real-time variables affecting children's exposure to diesel-related pollutants during school bus commutes in Los Angeles. Atmospheric Environment 39, 5243-5254.

Satish, U., Mendell, M.J., Shekhar, K., Hotchi, T., Sullivan, D., Streufert, S., Fisk, W.J., 2012. Is CO2 an indoor pollutant? Direct effects of low-to-moderate CO2 concentrations on human decision-making performance. Environmental Health Perspectives 120, 1671-1677.

Song, S., Paek, D., Lee, K., Lee, Y.M., Lee, C., Park, C., Yu, S.D., 2013. Effects of ambient fine particles on pulmonary function in children with mild atopic dermatitis. Archives of Environmental & Occupational Health 68, 228-234.

Strak, M., Janssen, N.A.H., Godri, K.J., Gosens, I., Mudway, I.S., Cassee, F.R., Lebret, E., Kelly, F.J., Harrison, R.M., Brunekreef, B., Steenhof, M., Hoek, G., 2012. Respiratory health effects of airborne particulate matter: the role of particle size, composition, and oxidative potential-the RAPTES project. Environmental Health Perspectives 120, 1183-1189.

Tainio, M., Tuomisto, J.T., Hanninen, O., Aarnio, P., Koistinen, K.J., Jantunen, M.J., Pekkanen, J., 2005. Health effects caused by primary fine particulate matter (PM2.5) emitted from buses in the Helsinki metropolitan area, Finland. Risk Analysis 25, 151-160.

Tian, Y., Sul, K., Qian, J., Mondal, S., Ferro, A.R., 2014. A comparative study of walking-induced dust resuspension using a consistent test mechanism. Indoor Air 24, 592-603.

Trenbath, K., Hannigan, M.P., Milford, J.B., 2009. Evaluation of retrofit crankcase ventilation controls and diesel oxidation catalysts for reducing air pollution in school buses. Atmospheric Environment 43, 5916-5922.

U.S. EPA Fuel economy database, 2012. http://www.fueleconomy.gov/feg/download.shtml (accessed Sep 7, 2012).

Weichenthal, S.A., Godri-Pollitt, K., Villeneuve, P.J., 2013. PM2.5, oxidant defence and cardiorespiratory health: a review. Environmental Health 12.

Xu, B., Liu, S., Zhu, Y., 2010. Ultrafine particle penetration through idealized vehicle cracks. Journal of Aerosol Science 41, 859-868.

Xu, B., Liu, S.S., Liu, J.J., Zhu, Y.F., 2011. Effects of vehicle cabin filter efficiency on ultrafine particle concentration ratios measured in-cabin and on-roadway. Aerosol Science and Technology 45, 234-243.

Xu, B., Zhu, Y.F., 2009. Quantitative analysis of the parameters affecting in-cabin to on-roadway (I/O) ultrafine particle concentration ratios. Aerosol Science and Technology 43, 400-410.

Zhang, Q.F., Fischer, H.J., Weiss, R.E., Zhu, Y.F., 2013. Ultrafine particle concentrations in and around idling school buses. Atmospheric Environment 69, 65-75.

Zhang, Q.F., Zhu, Y.F., 2010. Measurements of ultrafine particles and other vehicular pollutants inside school buses in South Texas. Atmospheric Environment 44, 253-261.

Zhu, Y., Fung, D.C., Kennedy, N., Hinds, W.C., Eiguren-Fernandez, A., 2008. Measurements of ultrafine particles and other vehicular pollutants inside a mobile exposure system on Los Angeles freeways. Journal of the Air & Waste Management Association 58, 424-434.

Zhu, Y.F., Eiguren-Fernandez, A., Hinds, W.C., Miguel, A.H., 2007. In-cabin commuter exposure to ultrafine particles on Los Angeles freeways. Environmental Science & Technology 41, 2138-2145.

IX. LIST OF INVENTIONS REPORTED AND COPYRIGHTED MATERIALS PRODUCED

Eon S. Lee and Yifang Zhu "Application of a high-efficiency cabin air filter for simultaneous mitigation of ultrafine particle and carbon dioxide exposures inside passenger vehicles" 2014, Environmental Science and Technology, 48 (4):2328-35. DOI: 10.1021/es404952q.

Eon S. Lee, Cha-Chen Fung, and Yifang Zhu "Evaluation of a novel high efficiency cabin air (HECA) filtration system for reducing particulate pollutants inside school buses" 2015, Environmental Science and Technology, 49 (6): 3358-3365. DOI: 10.1021/es505419m.

X. GLOSSARY OF TERMS, ABBREVIATIONS, AND SYMBOLS

Abbreviations	Descriptions
AER	Air Exchange Rate
ARB	California Air Resources Board
ASHRAE	American Society of Heating, Refrigerating and Air-Conditioning Engineers
ATCM	Airborne Toxic Control Measure
BC	Black Carbon
CO	Carbon Monoxide
CPC	Condensation Particle Counters
dN/dLogDp	Normalized Particle Number Concentration
Dp	Particle Diameter
HECA	High Efficiency Cabin Air
HVAC	Heating, Ventilating, and Air-Conditioning
I/O Ratio	In-cabin to On-roadway Concentration Ratios
MERV	Minimum Efficiency Reporting Value
NOx	Nitric Oxides
OA	Outdoor Air
OEM	Original Equipment Manufacturer
PM	Particulate Matter
PM_{10}	Particulate Matter with Diameter Equal or Less than 10µm
$PM_{2.5}$	Particulate Matter with Diameter Equal or Less than 2.5µm
RC	Recirculation
SEM	Scanning Electron Microscope
SMPS	Scanning Mobility Particle Spectrometer
UFP	Ultrafine Particle
VOC	Volatile Organic Compound

XI. APPENDICES

APPENDIX A. Changes in air exchange rate (AER) distributions by replacing the initially proposed vehicle models (i.e., BMW 3-series and Toyota 4Runner) with the substitute vehicle models (i.e., Toyota Camry and Toyota Highlander).
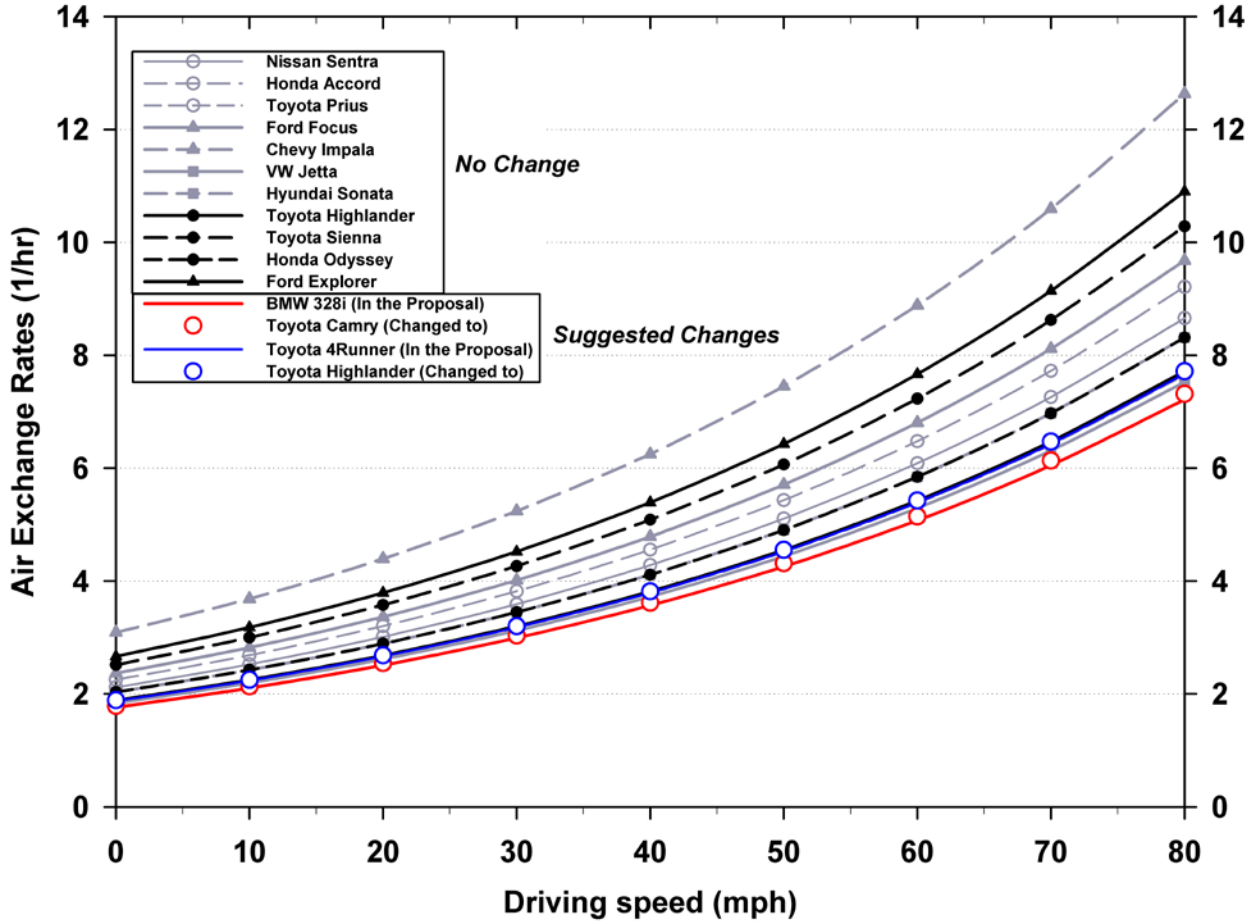
AERs were estimated for the test passenger vehicles in this study by using a previous RC-mode AER model (Fruin et al., 2011). The two substitute vehicle models are expected to serve well under the goal of this study because the AERs of the substitute vehicle models agree very well with those of the initially proposed.

APPENDIX B. Quality management project plan (Phase I. Passenger Cars).

Quality Management Project Plan

1. Summary

The objective of the Quality Management Project Plan (QMPP) is to ensure that all research findings meet the highest quality standards. The investigators are strongly committed to good science and aggressive quality management (QM) practices. The authors' commitment is documented by developing integrated QM practices for the authors' data collection, management and analysis. These activities are specifically designed to generate and process data of known and appropriate quality in a cost-effective manner. The purpose of this document is to define and describe the QM responsibilities required for the passenger vehicle portion of this project. A separate QMPP will be developed for the school bus portion of this project.

2. Project Description

In-cabin ultrafine particles have been shown to be 10 times higher than ambient levels and contribute up to 30-50% of total daily exposure for a typical California commuter. Tremendous progress has been made in reducing vehicular emissions by tightening emission standards and retrofitting buses, but the potential to further reduce exposure to vehicle-related pollutants by reducing the proportion of on-road pollutants penetrating into vehicle cabins is substantial. Previous work by various investigators has shown that setting vehicle ventilation system to recirculation on can reduce in-vehicle particles by 80-95%. However, carbon dioxide (CO_2) from exhaled breath of passengers can build up quickly and exceed Cal-OSHA exposure limits in cars when vents are set on recirculate and windows are closed (Zhu et al., 2007). Using high efficiency filters under a "vent open" scenario would reduce in-cabin particle levels and at the same time, allow sufficient air exchange which may offer a solution to the CO_2 build-up issue.

The **Overall Objective** of this study is to explore the application of high efficiency filtration during open vent conditions to reduce exposure to particles in vehicles. This study will provide data that can be used by ARB for future in-cabin air pollution exposure reduction guidelines.

3. Objectives

The specific objectives of this project are to:

1. Determine to what extent an in-cabin HEPA filter could reduce fine and ultrafine particle levels inside passenger vehicles when vents are left open.

2. Identify important factors affecting a HEPA filter's performance inside vehicles. Candidate factors include vehicle model/make, interior cabin volume, ventilation settings, mechanical air flow rate, window position, leakage characteristics, AER, driving route and driving speed.

4. Schedule

Objective (1) will be completed from April, 2012 to February, 2013
Objective (2) will be completed from January, 2013 to May, 2013

5. Experimental Design

The central hypothesis is that HEPA cabin air filter may reduce passenger exposures to high levels of particulate matter from the roadway emissions during commute with the vent open. This project will examine three different types of cabin air filters (i.e., no filter, in-use filter, and HEPA filter) on three different driving routes / conditions (i.e., stationary at 0 mph, mobile local at 30 mph, and mobile freeway at 65 mph). Based on measurements from 12 recent vehicle models representing the California vehicle fleet, this study aims to evaluate the potential reduction in passenger exposure to fine and ultrafine particles by installing HEPA cabin air filters.

Critical measurements include: (1) particle number concentration, (2) particle size distribution in the size range from 7 to 300 nm (in selected vehicles), (3) PM2.5 mass concentration, (4) black carbon concentration, (5) carbon monoxide concentration, and (6) carbon dioxide concentration. Although less critical, (7) ventilation air flow rates, (8) GPS coordinates, and (9) driving speed will also be measured concurrently.

6. Sample Handling and Custody

No physical samples are involved in this project. All samples are real-time air quality data that are concurrently measured inside passenger cabin and on roadway. The air samples will be brought into the monitors by internal pumps at instrument specified flow rates. All instruments will be synchronized before each sampling and data will be archived into a laptop computer during field measurements.

7. Sampling Methods and Equipment

Real-time concurrent measurements of in-cabin air quality include the number concentration and size distribution of UFP, $PM_{2.5}$, BC, CO, and CO_2 concentrations. A scanning mobility particle sizer (SMPS 3080, TSI Inc., St. Paul., MN) will be used to measure fine and UFP size distribution in the size range of 7 to 300 nm. A water-based condensation particle counter (WCPC 3785 and 3786, TSI Inc., St. Paul., MN) will be used to count the particle number concentrations in a size range of ~6 nm to a few

micrometers at 1-sec intervals. A TSI DustTrak photometer (Model 8520 TSI, Inc., St. Paul, MN) will be used to detect the mass concentration of $PM_{2.5}$. A TSI Q-trak indoor air quality monitor (Model 8550, TSI Inc., St. Paul., MN) will be employed to determine the concentrations of CO and CO_2 as well as temperature and relative humidity. A Magee Scientific Aethalometer model AE-42 will be used to measure the elemental carbon concentrations in near-real time (i.e., 1-min interval). The SMPS, WCPC, DustTrak, Q-trak and Aethalometer as well as two laptop computers will be powered by three deep-cycle marine batteries. The location and driving speed will be determined by a GPS data logger (Model BT-Q1000XT, QStarz, Co. Ltd., Taiwan). The selected driving routes include I-405 for freeway and Westwood or Wilshire Blvd. for local roadway to represent different driving / traffic conditions. Cabin air filters (i.e., no filter, in-use filter, and HEPA filter) will be replaced between runs to investigate their effects.

Of the twelve proposed vehicles, two (Toyota Sienna and Honda Odyssey) are in the class of mini-vans in which the SMPS systems will be used to measure particle size distribution. For the other vehicle classes only the WCPCs will be used to measure particle number concentration, due to space limitations.

7.a. Instrument Calibration

Instrument calibration will be performed to ensure accuracy and precision of the collected data. Laboratory calibration will be conducted either by Dr. David C.C. Fung or Eon Lee depending on who is responsible for conducting the upcoming experiment. Instruments will be sent to the manufacturer for calibration when needed. Detailed instrument calibration protocols are as follows:

- TSI SMPS: The SMPS system will be calibrated in the laboratory before and after the study. The sizing accuracy of the SMPS will be verified in the laboratory by means of monodisperse Polystyrene Latex spheres (PSL, Polysciences Inc., Warrington, PA). The zero response and flow rate will be checked before and after each run.

- TSI WCPC: Two WCPCs will be used in this study, one to measure in-cabin air the other to measure on-roadway air. The zero response and flow rate will be checked before and after each run. Both of the WCPCs will be co-located to collect data for at least 10 minutes before and after each run to determine their response equivalence and assess their precision.

- TSI DustTrak: The instrument is operated with the factory calibration based on Arizona road dust. The PM response will be calibrated by comparison with PM determined from filter-based mass measurements. Calibration will be performed on roadways with vehicle emission. The zero response and flow rate will be checked before and after each run.

- Aethalometer: The factory calibration will be used for this analyzer. Before and after each test run the flow rate and the response to a factory-supplied test filter

will be checked. Similar to WCPC, the two Aethalometers used to measure in-cabin and on-roadway will be collocated to collect data for at least 10 minutes before and after each run to determine their response equivalence and assess their precision.

- Q-Trak: The instrument will be calibrated before and after each test run by challenging it directly with a certified compressed gas cylinder containing CO_2 in the 300 - 5000 ppm concentration range. The calibration system is purchased from TSI and includes two gas cylinders: one of zero gas and the second is a certified gas mixture of 1000 ppm CO_2 and 30 ppm CO. Again, instrument co-location will be performed.

- Documentation: A logbook will be maintained with the instruments and all relevant calibrations, experimental procedures and observations will be recorded. Separate data sheets will be maintained for instrument QC checks.

7.b. Instrument Factory Calibration Date

Instrument Model	Serial Number	Factory Calibration Date	Notes
Qtrak (TSI 8554) A	SN 8554-12031025	2012	
Qtrak (TSI 8554) C	SN 8554-08041036	2012	
Dusttrak (TSI 8520) A	SN 85200393	2008	
Dusttrak (TSI 8520) C	SN 85202490	2012	
WCPC (TSI 3785)	SN 70526009	2012	
WCPC (TSI 3786)	SN 86030703	2012	
Aethalometer (AE42-7)	SN 781:0702	2012	
Aethalometer (AE22)	SN 887:0806	2012	

8. Key Staff Members
Yifang Zhu has overall project responsibility and will supervise project and publication progress

Yifang Zhu, Ph.D
Associate Professor
Department of Environmental Health Science
Fielding School of Public Health, UCLA
650 Charles E. Young Drive South
51-295 CHS
Los Angeles, CA 90095
Phone: (310) 825-4324
E-mail: yifang@ucla.edu

Dr. David C.C. Fung and Eon Lee have responsibility for sampling, data acquisition, data analysis, and publication preparation.

David C. C. Fung, Ph.D
Post-doc
Department of Environmental Health Science,
Fielding School of Public Health, UCLA
E-mail: fungchachen@gmail.com

Eon Lee
Doctoral Candidate
Department of Civil and Environmental Engineering,
Henry Samueli School of Engineering and Applied Science, UCLA
E-mail: eonlee@ucla.edu

9. How Quality will be Ensured

Quality is ensured by careful sampling and recording of data on the part of the investigators.   All instruments will be calibrated in the laboratory before use in the field. The two sets of instruments (i.e., one set for on-roadway and the other for in-cabin) will be co-located for 10-15 minutes before each sampling run. Data from these duplicate measurements will be used to correct one's reading to the other based on linear regression results, if needed. All data will be computer archived and can be tracked by their date and time. Data analysis by Fung and Lee will be reviewed by Zhu and vice versa. Statistical procedures, for example normality test, T-test, etc., will be performed with either SAS or SigmaStat.

10. Data Management Plan

10.a. Data Acquisition

All the instruments except for the WCPCs and SMPS have data logging functions. The raw data collected by the instruments will be downloaded to a computer after each experimental run. The WCPC/SMPS are operated with laptop computers and the raw data will store to the laptops. The raw data will be collected by Fung and/or Lee for the experimental runs.

10.b. Data Processing

The raw data will be downloaded to a single computer. Back-ups will be archived in a password protected external hard drive. The raw data will then be prepared for analysis.

10.c. Data Evaluation, Validation, and Verification

Data collected by Lee and Fung will be reviewed by Dr. Zhu and vice versa. Lee and Fung are responsible for verifying the accuracy of the original data and whether or not the data meet measurement quality objectives (see Proposal p 27, Data Validation section). Peer reviews of the design and analytical methods will be achieved through related publications.

11. Instrument Standard Operating Procedures

SMPS: Measures particle size distribution
Main Components:

Impactor: Remove particles larger than a known aerodynamic size to reduce their contribution to multiply charged aerosols. The cut size is a function of the impactor flow rate and nozzle diameter.
Electrostatic Classifier (EC): To extract a known size fraction of particles from the incoming polydisperse aerosol.

Kr-85 Bipolar Charger: exposes particles to high concentrations of bipolar ions to reach Boltzmann equilibrium.

Differential Mobility Analyzer (DMA): An electric field is created between the inside collection rod (negative voltage) and the grounded outside cylinder of DMA. Particles within a narrow range of electrical mobility exit the DMA to be counted.

Water-based Condensation Particle Counter (WCPC): The particles are detected and counted by a simple optical detector after a supersaturated water vapor condensed onto the particles, causing them to grow into larger, detectable droplets.

Aerosol Instrument Management (AIM) Software: a platform for several TSI Particle Instruments, including Aerodynamic Particle Sizer (APS), SMPS, CPC by itself, etc. Automatic data logging. File management and data export.

Operation:
Hardware:
   1.   Power should be applied to both WCPC and EC when using SMPS, otherwise WCPC. The voltage control should be set to "ANALOG Ctrl" to allow the DMA voltage to be controlled by the software.
   2.   Select flow rates from the Menu commands on the display panel. With water CPC, sampling flow rate is 1.0 lpm, sheath flow rate is 10 lpm.
   3.   Allow the WCPC to warm up. Press Drain/Prime button and then press the button a second time to select "prime growth tube", press and hold the button at least one second to active water priming function.
   4.   When the WCPC is ready, the "status" indicator will be a steady green.

5.	Select recycle mode to extend working hours between water draining.
6.	Press Drain/Prime button and scroll down to start to drain, press and hold to start draining. Apply negative pressure if necessary to the vent tubing if necessary to help water WCPC to drain.

Software:
1.	Start the AIM software.
2.	File-New to start sampling; File-Open to view existing files.
3.	Either way needs to select "files of type": ".S80" for SMPS.
4.	To sample: Give a file name, data will be automatically logged into that file. File-Properties: specify sampling hardware settings, scheduling and physical properties.
5.	Click on the green button to start sample.
6.	View button to change units (counts, dn/dlogdp, etc.), see statistics, tables, graphs etc.
7.	File-Export to export selected runs to txt files.

WCPC: Measures particle number concentration
Operation:
Hardware:
1.	Power cord should be connected to WCPC
2.	Turn on WCPC. Allow the WCPC to warm up. Press Drain/Prime button and then press the button a second time to select "prime growth tube", press and hold the button at least one second to active water priming function.
3.	When the WCPC is ready, the "status" indicator will be a steady green.
4.	Select recycle mode to extend working hours between water draining.
5.	Press Drain/Prime button and scroll down to start to drain, press and hold to start draining. Apply negative pressure if necessary to the vent tubing if necessary to help water WCPC to drain.

Software:
1.	Start the AIM software.
2.	File-New to start sampling; File-Open to view existing files.
3.	Either way needs to select "files of type": ".C85" for Model 3785 and ".C86" for Model 3786.
4.	To sample: Give a file name, data will be automatically logged into that file. File-Properties: specify sampling hardware settings, scheduling and physical properties.
5.	Click on the green button to start sample.
6.	View button to change units (counts, etc.), see statistics, tables, graphs etc.
7.	File-Export to export selected runs to txt files.

Aethalometer: Measures Particulate Elemental Carbon
Operation:

To start: Plug in and switch on. Instrument starts automatically without any operator attention. Data collection will begin after ~5 min. Instrument takes about 30 min to warm up.

To Stop: Simply switch off. Data file on disk will be current up to this time.

Flow Rate: is set by software and automatically stabilized.

To Change Settings (change date time): Power on, press STOP key, watch screen, press STOP key again. Enter "security code" of **111** to get to opening screen. Use up and down arrows to get to different menu. Press Enter to access an item.

Tape Advancing: Once EC concentration reaches a level on the filter, the instrument will automatically advances tape. No operation is needed.

To receive data: Use flash memory card adaptor to download the BCmmddyy.csv from the flash memory card.

DustTrak: Measures PM$_{2.5}$ and PM$_{10}$
Operation:
To start: Plug in and press the ON/OFF key to power the DustTrak monitor. Instrument starts automatically without any operator attention. Data collection will begin instantaneously. Instrument takes a few min to warm up.

To Stop: Simply press the ON/OFF key to switch off. Data file on disk will be current up to this time.

To Zero Check: Place a HEPA filter on the inlet and instruments should read zero. Without the HPEA filter, PM$_{10}$ should be higher than PM$_{2.5}$.

To Change to Log Mode: Press the SAMPLING MODE key to navigate to LOG1. Use the SAMPLE key to start and stop recording in LOG mode.

Flow Rate: is set by software and automatically stabilized (now is 2 lpm).

To Change Settings (change date time): Press and hold the SAMPLE key while the DustTrak monitor displays the time of day during its power-up. Release when the DustTrak monitor "beeps". Now you can view and/or change the hours, minutes, year, month, and day of month in sequence. Use the up and down arrow to change a setting. Use the SAMPLE key to store each setting and advance to the next one.

To receive data: Use a laptop and TrakPro software to 1) file-receive, 2) select the sample you want to download, 3) export the downloaded sample to tab delimited txt file.

Q-Trak: Measures CO, CO$_2$, Temperature and Relative Humidity
Operation:
To start: Use battery or plug in and press the ON/OFF key to power the Q-Trak monitor. Instrument starts automatically without any operator attention. Data collection will begin instantaneously.   Instrument takes a few min to warm up.

To Stop: Simply press the ON/OFF key to switch off. Data file on disk will be current up to this time.

To Change to Log Mode: Press the ⬏ key to navigate to the main menu. Use up and down arrow to move to LOG mode. Press ⬎ key to switch to LOG mode.

Flow Rate: Passive sampler.

To Change Settings (change date time): Press the ⬆ key to navigate to the main menu. Use up and down arrow to navigate between settings.   Press ⬎ key to switch between setting options. Use the up and down arrow to change a setting.

To receive data: Use a laptop and TrakPro software to 1) file-receive, 2) select the sample you want to download, 3) export the downloaded sample to tab delimited txt file.

Cabin Air Filter Testing Check Lists

1. The Day before the Sampling Day

List	Things to Check	Check Mark
1	Cabin air filters are ready for testing.	
2	Three marine batteries are fully charged.	
3	Fully charged batteries (AA / C) are installed in all instruments.	
4	DI water bottles in CPC are filled.	
5	CPC water reservoirs are drained.	
6	Time in all of the instruments and laptops are synchronized.	
7	Instruments:	
	• WCPC (2 ea.) or SMPS (when driving mini-van, 2 ea.)	
	• DustTrak (2 ea.)	
	• Aethalometer (2 ea)	
	• Q-Trak 8554 (2 ea.)	
	• Ventilation meter: Q-Trak 7565-x with TSI 960 probe (1 ea.)	
	• GPS data logger (1 ea.)	
	• Data logger laptop (3 ea.)	
8	Miscellaneous items:	
	• Marine battery (3 ea.)	
	• Power inverter (1 ea.)	
	• Extra battery AA type (16 ea.)	
	• Extra battery C type (8 ea.)	
	• Teflon conductive tubing	
	• WCPC communication cords (2 sets)	
	• USB-Serial adapter (2 ea.)	
	• Sealing material (Sealing strip and glue gun, 1 ea.)	
	• Multi-tab extension cords (2 ea.)	
	• Light / Heavy duty duct tape (1 ea.)	
	• Ruler (1 ea.)	
	• Cutter (1 ea.)	

2. On the Sampling Day

Date / Time: _____**Operator:**_____
_____

Vehicle Model / Year / Mileage: _____
_____

Maximum Number of Fan Settings: _____
Medium Fan Setting: _____

Before starting field sampling,

List	**Things to Check**	Check Mark
1	Load three marine batteries in the trunk and connect them to the inverter.	
2	Place all the instruments on vibration dampener in proper locations.	
3	Place ambient sampling tubes (WCPC or SMPS, DustTrak, and Aethalometer): through passenger side-door windows and seal the window gap using light-duty duct tape.	
4	Place in-cabin sampling tubes (WCPC or SMPS, DustTrak, and Aethalometer) in proper locations: in the breathing zone between driver and passenger	
5	Place the ventilation meter at the central vent outlet.	
6	Calibration for all the instruments.	
7	Double-check instrument synchronization.	
8	Connect all the instruments to the sampling tubes.	
9	Turn on the inverter and the power button on the control panel.	
10	All power cords should be connected from the battery to each outlet strip. There are in total 7 power cords including: 2 WCPCs, 3 laptops, 2 Aethalometers. Note: total of 9 power cords when using 2 SMPS.	
11	Connect two laptops to short power strip. Turn them on.	
12	Turn on the Aethalometers which needs 30 minute to warm up.	
13	Turn on the two WCPCs (or SMPS). The WCPC needs about 15 minute to warm up.	
14	Set ventilation settings to OA mode medium fan setting.	
15	Check if all windows are closed.	
	Set sampling time interval of 1 second for WCPCs, Dustraks, Q-Traks and Ventilation meter; 1 minute for Aethalometers; 2 minute for SMPS.	
16	Start logging GPS data and write down the starting time on the field log	
17	Start logging on WCPCs (or SMPS in minivan), Dustraks, Aethalometers, Q-Traks, and Ventilation meter.	
18	Confirm if all instruments are logging and working properly.	

During field sampling,

List	Things to Check	Check Mark
1	Driver will be briefed on driving protocols (see item 3) and advised to follow all California traffic regulations.	
2	Replace cabin air filters (i.e., no filter, in-use filter, and HEPA filter) every 15 minutes (carried out by the passenger). This will be done while driving if cabin filter location is accessible to the passenger from the vehicle cabin. If not, driver will be instructed to stop at safe location and then perform filter replacement.	
3	Advise the driver to maintain driving speed at 30 mph on local route and 65 mph on freeway route.	

3. Field Log Sheet

Vehicle Information

Date	Manuf.	Model	Year	Mileage (km)	VIN

Instrument Operator: _____ _____

Fan Settings

Total number of fan settings:_____   **Median fan setting:** _____

Maximum flow rates (m³/hr): _____   **Applied Flow rates (m³/hr):** ____

GPS Data Logging

GPS started logging at: _____

Stationary Mode Testing (15 minutes each)

Filter types	Started at	Finished at	Field log
No Filter			
In-use Filter			
HEPA filter			

Mobile Local Mode Testing (15 minutes each)

Filter types	Started at	Finished at	Field log
No Filter			
In-use Filter			
HEPA filter			

Mobile Freeway Mode Testing (15 minutes each)

Filter types	Started at	Finished at	Field log
No Filter			
In-use Filter			
HEPA filter			

APPENDIX C. Quality management project plan (Phase II. School Buses).

Quality Management Project Plan

1. Summary

The objective of the Quality Management Project Plan (QMPP) is to ensure that all research findings meet the highest quality standards. The investigators are strongly committed to good science and aggressive quality management (QM) practices. The authors' commitment is documented by developing integrated QM practices for the authors' data collection, management and analysis. These activities are specifically designed to generate and process data of known and appropriate quality in a cost-effective manner. The purpose of this document is to define and describe the QM responsibilities required for the school bus portion of this project.

2. Project Description

Children are more sensitive to traffic emissions because their physiological and immunological systems are still in developing stages. Children commuting on a school bus may be exposed to elevated levels of traffic emissions, in particular ultrafine particles (UFPs), due to high air exchange rate (AER) in school buses. Replacing in-cabin air filters with high efficiency filters have been shown to dramatically reduce UFPs level inside passenger vehicles. However, school buses typically do not have mechanical ventilation systems or have systems that cannot accommodate an air filter. Previous studies have found by using a stand-alone air purifier can reduce in-cabin UFP levels by 50%. The purpose of this project is to develop and test a high efficiency air filtration system to reduce UFP exposures inside school buses.

The **Overall Objective** of this study is to explore the application of high efficiency filtration systems to reduce exposure to particles in school buses. This study will provide data that can be used by ARB for future in-cabin air pollution exposure reduction guidelines.

The tasks described in this QMPP reflect updates on the originally proposed scope of work (SOW). Because the vast majority of school buses are not equipped with ventilation or air conditioning system, retrofitting AC filters is not a feasible approach. Based on the authors' discussion with IQAir and ARB staff and based on data collected during the pilot testing, the authors plan to combine Tasks # 5 and #6 in the original SOW and develop a new type of ventilation system for school bus testing. However, additional costs will be encountered using this new approach. In addition, the costs of renting the buses from Tumbleweed are higher than the authors expected. Thus, the number of school buses to be tested was reduced from six to four.

3. Objectives

The specific objectives of this project are to:

1. Proof-of-concept that incorporating a HEPA filter based filtration system could reduce fine and ultrafine particle levels inside school buses. This has been accomplished in the pilot-testing.

2. Identify important factors affecting HEPA filtration performance inside school buses. Candidate factors include bus model/make, interior cabin volume, leakage characteristics, AER, driving route and driving speed. This will be achieved by studying different buses of different model/make and interior cabin volume driving at different driving speeds on different routes. Data acquisition, validation, and archiving and data analysis are presented in the Data Management Plan section of the SOW. Briefly, the authors will calculate the I/O ratios for both on and off status of the air filtration system and conduct a paired t-test to test the hypothesis that the I/O ratios are significantly lower when the system is on than off. The authors will then quantify the system contributions to I/O ratio reduction and estimate the resultant fine and ultrafine exposure reduction during school bus commuting.

4. Schedule

Objective (1) will be completed from July, 2013 to November, 2013
Objective (2) will be completed from November, 2013 to January, 2014

Table 1 summarizes the school bus test procedure. The first and second trips of each route will be conducted back-to-back on the same day. The freeway route usually takes about 1.5 hours and local street route takes about one hour. Each bus will be tested approximately for a total of five hours on each test day.

Table 1. Overall sampling schedule for school buses

Bus ID	Bus Size	Controlled Device	Freeway Route		Local Street Route	
			1st trip	2nd trip	1st trip	2nd trip
1	L	Air filtration system	off	on	off	on
2	L	Air filtration system	off	on	off	on
3	S	Air filtration system	off	on	off	on
4	M	Air filtration system	off	on	off	on

5. Experimental Design

The central hypothesis is that high efficiency air purifier can reduce levels of UFPs inside the school bus during a commute. Various parameters can alter the effectiveness of the air purifier and experiments will be designed in order to identify them. As shown in Table 2, four buses from three different makes (Bluebird, International, and Thomas) with capacities from 22 to 78 passengers will be tested.

Table 2. Tested school buses

Test ID	Tumbleweed ID	Manufacturer	Model Year	Fuel Type	Passenger Capacity	Total Length (m)	Internal Length (m)
1	T-53	Bluebird	2010	CNG	78	11.7	9.4
2	T-180	Bluebird	2014	Propane	48	9.5	6.3
3	T-158	Thomas	2006	Diesel	22	6.3	3.9
4	T-147	International	2007	Diesel	63	11.7	9.7

Critical measurements include: (1) particle number concentration, (2) particle size distribution in the size range from 7 to 300 nm, (3) PM2.5 mass concentration, (4) black carbon concentration, (5) carbon monoxide concentration, and (6) carbon dioxide concentration. Although less critical, (7) GPS coordinates, and (8) driving speed will also be measured concurrently. School bus AER will be determined by releasing CO_2 into the bus cabin and measuring its concentration decay. AER measurements will be conducted on both freeway and local routes for each bus. GPS and speed data will be archived for future on-roadway UFP modeling work.

6. Sample Handling and Custody

No physical samples are involved in this project. All samples are real-time air quality data that are concurrently measured inside school bus and on roadway. The air samples will be brought into the monitors by internal pumps at instrument specified flow rates. All instruments will be synchronized before each sampling. Collected data will be archived into a laptop computer during field measurements.

7. Sampling Methods and Equipment

Real-time concurrent measurements of in-cabin and ambient air quality include the number concentration and size distribution of UFP, $PM_{2.5}$, BC, CO, and CO_2 concentrations. Two scanning mobility particle sizer (SMPS 3080, TSI Inc., Shoreview, MN) will be used to measure UFP size distribution in the size range of 7 to 300 nm. Two TSI DustTrak photometer (Model 8520 TSI, Inc., Shoreview, MN) will be used to detect

the mass concentration of $PM_{2.5}$. Two TSI Q-trak indoor air quality monitors (Model 8550, TSI Inc., Shoreview, MN) will be employed to determine the concentrations of CO and CO_2 as well as temperature and relative humidity. Two Magee Scientific Aethalometers (model AE-42 and model AE-22) will be used to measure the elemental carbon concentrations in near-real time (i.e., 1-min interval). The SMPS, and Aethalometer as well as two laptop computers will be powered by four deep-cycle marine batteries. The DustTrak, and Q-Trak will be powered using rechargeable batteries. In addition, a portable CPC 3007 will be located in the front of the bus to allow us to assess the pollutant spatial profile inside the buses. The location and driving speed will be determined by a GPS data logger (Model BT-Q1000XT, QStarz, Co. Ltd., Taiwan).

The selected driving routes include freeway and local streets that are typical for school pick-up and drop-off. Exact routes will be determined with discussion with Tumbleweed Transportation. Test routes are as follows:

1. 1 typical charter route (long distance route, mainly on freeways)
2. 1 typical local route (short distance, mainly on local streets with some freeway travel)

During the tests on the bus routes, pick-up and drop-off scenarios will be simulated by opening and closing the door at the designated stops. Each route will be driven through twice, once with the air purifier on and once with it off. These tests will be conducted back-to-back on the same day.

The new filtration system developed by IQAir has up to two high efficiency air purifiers fitted with the same filter media used in the passenger vehicle testing portion of this project. Depending on the bus size, either one of two air purifiers will be used in the system. The IQAir purifier uses MERV 16 equivalent filters and is wired to the existing battery of each school bus. The maximum fan setting will be used on each purifier which can supply an air flow at 680 m3/h through a jet diffuser or at 580 m3/h through an air duct. To evenly distribute the filtered air, a pair of air ducts (0.15 m in diameter and 8.4 m in length) will be used for the largest school bus (i.e., T-53 with 78 passenger capacity). The flexible duct will be attached to the roof of the bus cabin and have air outlet diffusers along its entire length. All the other test buses will use jet diffuser for air delivery. Each purifier will be placed in the last row of seats on the bus. Initial testing and calibration will be conducted by IQAir to ensure balance of the air flow through the duct.

7.a. Instrument Calibration

Instrument calibration will be performed to ensure accuracy and precision of the collected data. Laboratory calibration will be conducted either by Dr. David C.C. Fung or Eon Lee depending on who is responsible for conducting the upcoming experiment. Instruments will be sent to the manufacturer for calibration when needed. Detailed instrument calibration protocols are as follows:

- TSI SMPS: The SMPS system will be calibrated in the laboratory before and after the study. The sizing accuracy of the SMPS will be verified in the laboratory by

means of monodisperse Polystyrene Latex spheres (PSL, Polysciences Inc., Warrington, PA). The zero response and flow rate will be checked before and after each run.

- TSI DustTrak: The instrument is operated with the factory calibration based on Arizona road dust. The PM response will be calibrated by comparison with PM determined from filter-based mass measurements. Calibration will be performed on roadways with vehicle emission. The zero response and flow rate will be checked before and after each run.

- Aethalometer: The factory calibration will be used for this analyzer. Before and after each test run the flow rate and the response to a factory-supplied test filter will be checked. Similar to WCPC, the two Aethalometers used to measure in-cabin and on-roadway will be collocated to collect data for at least 10 minutes before and after each run to determine their response equivalence and assess their precision.

- Q-Trak: The instrument will be calibrated before and after each test run by challenging it directly with a certified compressed gas cylinder containing CO_2 in the 300 - 5000 ppm concentration range. The calibration system is purchased from TSI and includes two gas cylinders: one of zero gas and the second is a certified gas mixture of 1000 ppm CO_2 and 30 ppm CO. Again, instrument co-location will be performed.

- Documentation: A logbook will be maintained with the instruments and all relevant calibrations, experimental procedures and observations will be recorded. Separate data sheets will be maintained for instrument QC checks.

7.b. Instrument Factory Calibration Date

Instrument Model	Serial Number	Factory Calibration Date	Notes
Qtrak (TSI 8554) A	SN 8554-12031025	2012	
Qtrak (TSI 8554) C	SN 8554-08041036	2012	
Dusttrak (TSI 8520) A	SN 85200393	2008	
Dusttrak (TSI 8520) C	SN 85202490	2012	
WCPC (TSI 3785)	SN 70526009	2012	
WCPC (TSI 3786)	SN 86030703	2012	
Aethalometer (AE42-7)	SN 781:0702	2012	
Aethalometer (AE22)	SN 887:0806	2013	
SMPS (TSI 3080)	SN 70439119	2004	
SMPS (TSI 3080)	SN 70725210	2007	

8. Key Staff Members

Dr. Yifang Zhu has overall project responsibility and will supervise project and publication progress

Yifang Zhu, Ph.D
Associate Professor
Department of Environmental Health Science
Fielding School of Public Health, UCLA
650 Charles E. Young Drive South
51-295 CHS
Los Angeles, CA 90095
Phone: (310) 825-4324
E-mail: yifang@ucla.edu

Dr. David C.C. Fung and Dr. Eon Lee have responsibility for sampling, data acquisition, data analysis, and publication preparation.

David C. C. Fung, Ph.D
Post-doc
Department of Environmental Health Science,
Fielding School of Public Health, UCLA
E-mail: fungchachen@gmail.com

Eon Lee, Ph.D
Post-doc
Department of Environmental Health Science,
Fielding School of Public Health, UCLA
E-mail: eonlee@ucla.edu

9. How Quality will be Ensured

Quality is ensured by careful sampling and recording of data on the part of the investigators. All instruments will be calibrated in the laboratory before use in the field. The two sets of instruments (i.e., one set for on-roadway and the other for in-cabin) will be co-located for 10-15 minutes before each sampling run. Data from these duplicate measurements will be used to correct one's reading to the other based on linear regression results, if needed. All data will be computer-archived and can be tracked by their date and time. Data analysis by Dr. Fung and Dr. Lee will be reviewed by Dr. Zhu and vice versa. Statistical procedures, for example normality test, T-test, etc., will be performed with either SAS or SigmaStat.

10. Data Management Plan

10.a. Data Acquisition

All the instruments except for the SMPS have data logging functions. The raw data collected by the instruments will be downloaded to a computer after each experimental run. The SMPS are operated with laptop computers and the raw data will store to the laptops. The raw data will be collected by Dr. Fung and/or Dr. Lee for the experimental runs.

10.b. Data Processing

The raw data will be downloaded to a single computer. Back-ups will be archived in a password protected external hard drive. The raw data will then be prepared for analysis.

10.c. Data Evaluation, Validation, and Verification

Data collected by Dr. Lee and Dr. Fung will be reviewed by Dr. Zhu and vice versa. Lee and Fung are responsible for verifying the accuracy of the original data and whether or not the data meet measurement quality objectives (see Proposal p 27, Data Validation section). Peer reviews of the design and analytical methods will be achieved through related publications.

11. Instrument Standard Operating Procedures

SMPS: Measures particle size distribution
Main Components:

Impactor: Remove particles larger than a known aerodynamic size to reduce their contribution to multiply charged aerosols. The cut size is a function of the impactor flow rate and nozzle diameter.

Electrostatic Classifier (EC): To extract a known size fraction of particles from the incoming polydisperse aerosol.

Kr-85 Bipolar Charger: exposes particles to high concentrations of bipolar ions to reach Boltzmann equilibrium.

Differential Mobility Analyzer (DMA): An electric field is created between the inside collection rod (negative voltage) and the grounded outside cylinder of DMA. Particles within a narrow range of electrical mobility exit the DMA to be counted.

Water-based Condensation Particle Counter (WCPC):   The particles are detected and counted by a simple optical detector after a supersaturated water vapor condensed onto the particles, causing them to grow into larger, detectable droplets.

Aerosol Instrument Management (AIM) Software: a platform for several TSI Particle Instruments, including Aerodynamic Particle Sizer (APS), SMPS, CPC by itself, etc. Automatic data logging. File management and data export.

Operation:
Hardware:
1.   Power should be applied to both WCPC and EC when using SMPS, otherwise WCPC. The voltage control should be set to "ANALOG Ctrl" to allow the DMA voltage to be controlled by the software.
2.   Select flow rates from the Menu commands on the display panel. With water CPC, sampling flow rate is 1.0 lpm, sheath flow rate is 10 lpm.
3.   Allow the WCPC to warm up. Press Drain/Prime button and then press the button a second time to select "prime growth tube", press and hold the button at least one second to active water priming function.
4.   When the WCPC is ready, the "status" indicator will be a steady green.
7.   Select recycle mode to extend working hours between water draining.
8.   Press Drain/Prime button and scroll down to start to drain, press and hold to start draining. Apply negative pressure if necessary to the vent tubing if necessary to help water WCPC to drain.
Software:
1.   Start the AIM software.
2.   File-New to start sampling; File-Open to view existing files.
3.   Either way needs to select "files of type": ".S80" for SMPS.
4.   To sample: Give a file name, data will be automatically logged into that file. File-Properties: specify sampling hardware settings, scheduling and physical properties.
5.   Click on the green button to start sample.
6.   View button to change units (counts, dn/dlogdp, etc.), see statistics, tables, graphs etc.
7.   File-Export to export selected runs to txt files.

Aethalometer: Measures Particulate Elemental Carbon
Operation:

To start: Plug in and switch on. Instrument starts automatically without any operator attention. Data collection will begin after ~5 min. Instrument takes about 30 min to warm up.

To Stop: Simply switch off. Data file on disk will be current up to this time.

Flow Rate: is set by software and automatically stabilized.

To Change Settings (change date time): Power on, press STOP key, watch screen, press STOP key again. Enter "security code" of **111** to get to opening screen. Use up and down arrows to get to different menu. Press Enter to access an item.

Tape Advancing: Once EC concentration reaches a level on the filter, the instrument will automatically advances tape. No operation is needed.

To receive data: Use flash memory card adaptor to download the BCmmddyy.csv from the flash memory card.

DustTrak: Measures PM$_{2.5}$ and PM$_{10}$
Operation:
To start: Plug in and press the ON/OFF key to power the DustTrak monitor. Instrument starts automatically without any operator attention. Data collection will begin instantaneously. Instrument takes a few min to warm up.

To Stop: Simply press the ON/OFF key to switch off. Data file on disk will be current up to this time.

To Zero Check: Place a HEPA filter on the inlet and instruments should read zero. Without the HPEA filter, PM$_{10}$ should be higher than PM$_{2.5}$.

To Change to Log Mode: Press the SAMPLING MODE key to navigate to LOG1. Use the SAMPLE key to start and stop recording in LOG mode.

Flow Rate: is set by software and automatically stabilized (now is 2 lpm).

To Change Settings (change date time): Press and hold the SAMPLE key while the DustTrak monitor displays the time of day during its power-up. Release when the DustTrak monitor "beeps". Now you can view and/or change the hours, minutes, year, month, and day of month in sequence. Use the up and down arrow to change a setting. Use the SAMPLE key to store each setting and advance to the next one.

To receive data: Use a laptop and TrakPro software to 1) file-receive, 2) select the sample you want to download, 3) export the downloaded sample to tab delimited txt file.

Q-Trak: Measures CO, CO$_2$, Temperature and Relative Humidity
Operation:
To start: Use battery or plug in and press the ON/OFF key to power the Q-Trak monitor. Instrument starts automatically without any operator attention. Data collection will begin instantaneously. Instrument takes a few min to warm up.

To Stop: Simply press the ON/OFF key to switch off. Data file on disk will be current up to this time.

To Change to Log Mode: Press the ⬆ key to navigate to the main menu. Use up and down arrow to move to LOG mode. Press ⬇ key to switch to LOG mode.

Flow Rate: Passive sampler.

To Change Settings (change date time): Press the ⬆ key to navigate to the main menu. Use up and down arrow to navigate between settings. Press ⬇ key to switch between setting options. Use the up and down arrow to change a setting.
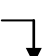
To receive data: Use a laptop and TrakPro software to 1) file-receive, 2) select the sample you want to download, 3) export the downloaded sample to tab delimited txt file.

School Bus Cabin Air Filter Testing Check Lists

1. The Day before the Sampling Day

List	Things to Check	Check
1	Cabin air filteration systems are ready for testing.	
2	Three marine batteries are fully charged.	
3	Fully charged batteries (AA / C) are installed in all instruments.	
4	DI water bottles in WCPC are filled.	
5	WCPC water reservoirs are drained.	
6	Time in all of the instruments and laptops are synchronized.	
7	Instruments:	
	• SMPS (includes WCPC 2 ea.)	
	● DustTrak (2 ea.)	
	● Aethalometer (2 ea)	
	● Q-Trak 8554 (2 ea.)	
	● Ventilation meter: Q-Trak 7565-x with TSI 960 probe (1 ea.)	
	● GPS data logger (1 ea.)	
	● Data logger laptop (3 ea.)	
	●	
8	Air Purifier Equipment	
	● Air Purifier Unit (2 ea.)	
	● Flexible duct (2 ea.)	
	● Duct connections (6 ea.)	
	● Power Cords (2 ea.)	
	● Power Inverter (1 ea.)	
	● Cords to connect to School Bus Battery	
9	Misc. Equipment	
	● Marine battery (4 ea.)	
	● Power inverter (1 ea.)	
	● Extra battery AA type (16 ea.)	
	● Extra battery C type (8 ea.)	
	● Teflon conductive tubing	
	● WCPC communication cords (2 sets)	
	● USB-Serial adapter (2 ea.)	
	● Sealing material (Sealing strip and glue gun, 1 ea.)	
	● Multi-tab extension cords (2 ea.)	
	● Light / Heavy duty duct tape (1 ea.)	
	● Ruler (1 ea.)	
	● Cutter (1 ea.)	
	● Heavy duty straps	

2. On the Sampling Day

Date / Time: _____**Operator:**_____

_____

Vehicle Model / Year / Mileage: _____

_____

Before starting field sampling,

List	Things to Check	Check
1	Load four marine batteries in bus cabin and connect them to the inverter.	
2	Place all the instruments on vibration dampener in proper locations.	
3	Place ambient sampling tubes (CPC, SMPS, DustTrak, and Aethalometer): through passenger window and seal the window gap using light-duty duct tape.	
4	Place in-cabin sampling tubes (CPC, SMPS, DustTrak, and Aethalometer) in proper locations: in the breathing zone.	
5	Calibration for all the instruments.	
6	Double-check instrument synchronization.	
7	Connect all the instruments to the sampling tubes.	
8	Turn on the inverter and the power button on the control panel.	
9	All power cords should be connected from the battery to each outlet strip. There are in total 7 power cords including: 2 WCPCs, 3 laptops, 2 Aethalometers. Note: total of 9 power cords when using 2 SMPS.	
10	Connect two laptops to short power strip. Turn them on.	
11	Turn on the Aethalometers which needs 30 minute to warm up.	
12	Turn on the two SMPS. The WCPCs needs about 15 minute to warm up.	
13	Load air purifier units onto bus and secure them to the last row seats	
14	Connect ducts to purifier units and attach ducts to ceiling.	
15	Verify connections and attachments are secure.	
16	Connect ground wires on inverter to bus.	
17	Connect inverter to bus battery.	
18	Connect power cords to inverter and air purifier units.	
19	Start bus and turn on air purifier unit to verify proper connections	
20	Check if all windows are closed.	
21	Set sampling time interval of 1 second for CPCs, Dustraks, and Q-Traks; 1 minute for Aethalometers; 2 minute for SMPS.	
22	Start logging GPS data and write down the starting time on the field log	
23	Start logging on WCPCs (or SMPS in minivan), Dustraks, Aethalometers, Q-Traks, and Ventilation meter.	
24	Confirm if all instruments are logging and working properly.	

During field sampling,

List	Things to Check	Check
1	Driver will be briefed on driving protocols (see item 3) and advised to follow all California traffic regulations.	
2	Turn on or off the air purifier unit after each trip.	
3	Advise the driver to maintain driving speed at 30 mph on local route and 65 mph on freeway route.	

3. Field Log Sheet

School Bus Information

Date	Manuf.	Model	Year	Mileage (km)	VIN

Instrument Operator: _____ _____

GPS Data Logging
GPS started logging at: _____

Stationary Mode Testing

Purifier Mode	Started at	Finished at	Field log
ON			
OFF			

Mobile Mode Testing

Route	Purifier Mode	Started at	Finished at	Field log
CHARTER	ON			
	OFF			
LOCAL	ON			
	OFF			

APPENDIX D. Air exchange rate (AER) estimated in the six test school buses. Each data point represents the estimated AER and driving speed, which the AER was estimated. Different symbols indicate different test school buses, as noted. The error bars represent standard deviations of AER and driving speed.
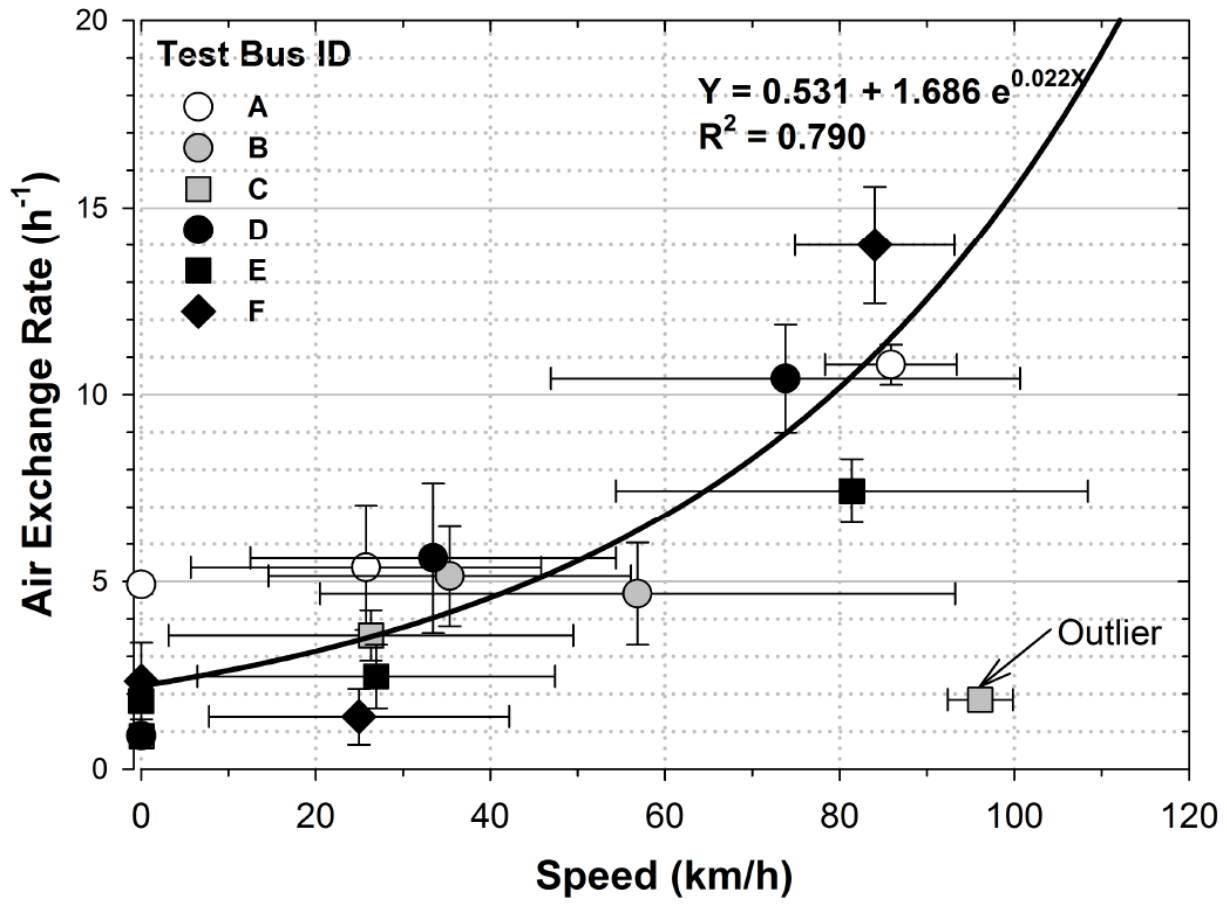
APPENDIX E. Instrument collocation data from passenger vehicle testing period

Figure E1. Instrument collocation data are plotted for (a) UFPs, (b) BC, and (c) PM$_{2.5}$.
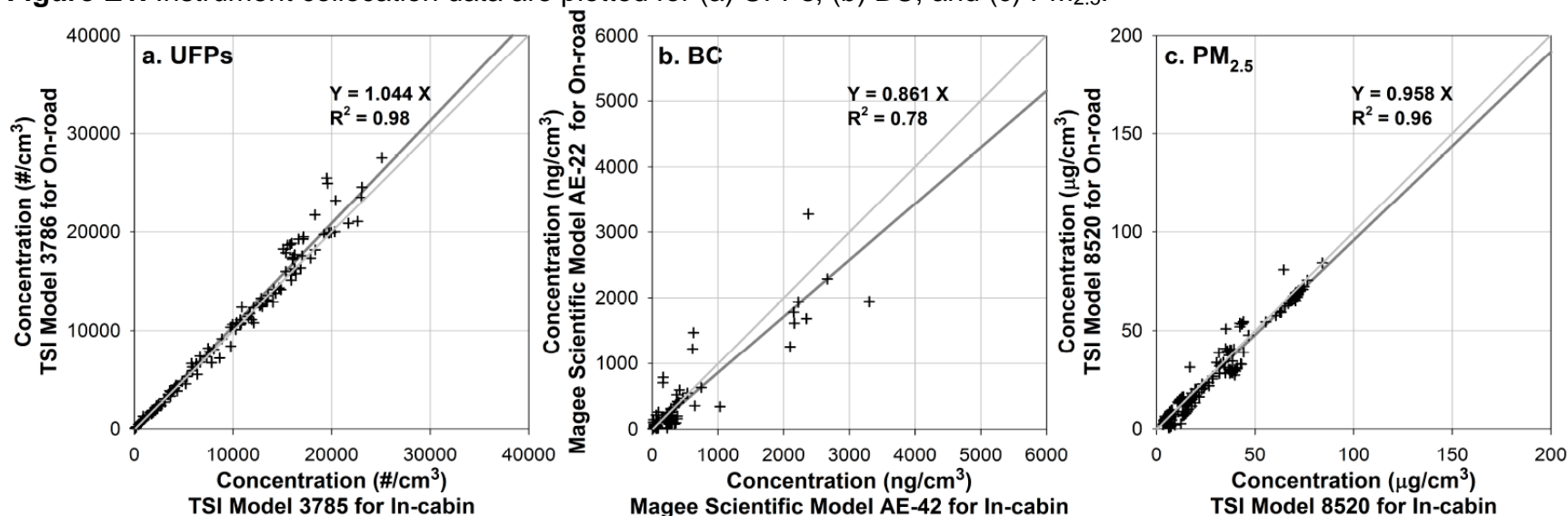
In Figures E1a and E1c, instrument collocation data provide strong correlation and little bias between the instruments used to measure (a) UFPs and (c) PM$_{2.5}$. In Figure E1b, (b) BC collocation data from two aethalometers seem to show relatively less correlation and more bias; however, this study confirmed that it occurs not because of instrument bias, but because of insufficient number of collocation data points. Please, see Figure F2a of Appendix F for more collocation data from the same aethalometers. The plotted collocation data for BC present a good correlation (R^2 = 0.93) with little bias (y = 1.09 x - 14). Therefore, no post-data processing was conducted in this study.

APPENDIX F. Instrument collocation data from school bus testing period

Figure F1. Instrument collocation data are plotted for UFP (a) TSI models 3007 unit A vs. unit B, (b) TSI models 3007 unit B vs. 3785, and (c) TSI models 3785 vs. 3007 unit A. The plotted data are 1-second raw instrument data.
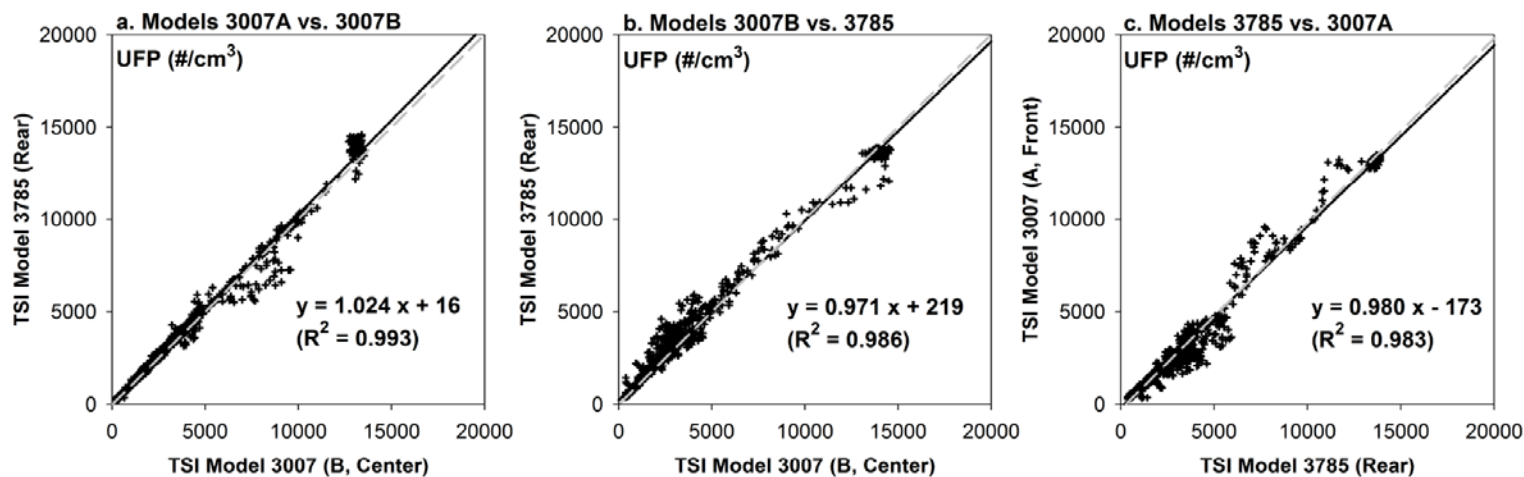
Figure F2. Instrument collocation data are plotted with 1-minute averaged data for (a) BC and (b) $PM_{2.5}$.
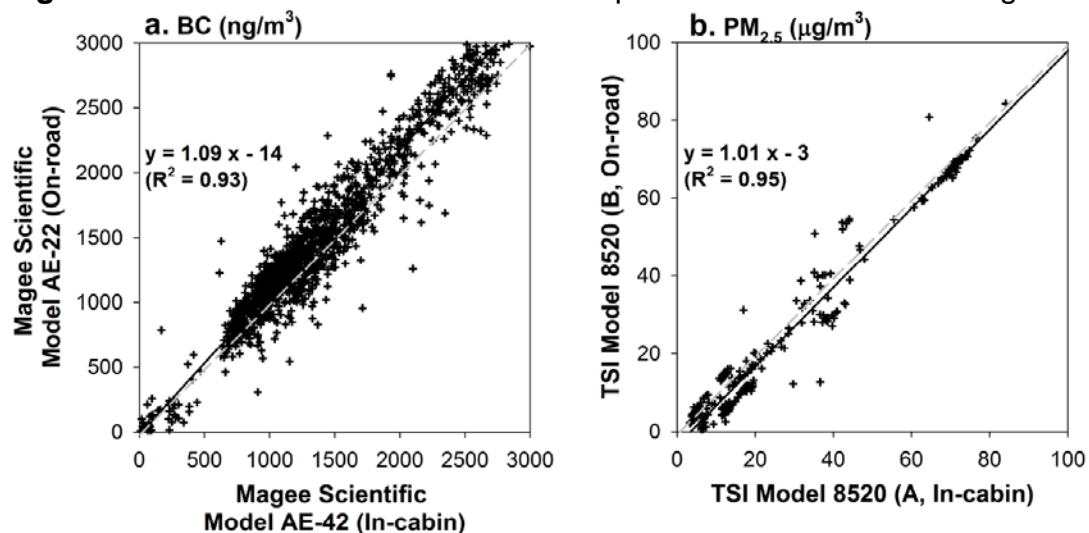
APPENDIX G. A summary of the numerical data plotted in Figure 12. In-cabin particle concentration reductions with respect to on-road particle concentration inside passenger vehicles under different scenarios. The tabulated data are estimated from the data collected in all test vehicles except for Toyota Prius and Chevy Impala, which had noticeable bypass flow around the installed filters.

Pollutants	Filtration Scenarios	Stationary			Local			Freeway		
		Average	St.Dev.	Median	Average	St.Dev.	Median	Average	St.Dev.	Median
UFP (%)	HECA B	90.42	6.25	92.02	92.08	4.32	94.01	91.13	7.11	92.81
	HECA A	73.26	6.19	75.77	74.71	7.11	74.73	76.87	3.07	76.86
	In-use OEM	43.22	9.57	42.02	51.05	10.13	49.39	61.44	8.86	63.12
	No Filter	27.73	7.63	25.11	35.46	12.81	33.59	49.17	6.67	50.05
BC (%)	HECA B	89.40	12.12	93.66	81.73	11.38	84.06	77.21	18.40	81.79
	HECA A	68.55	22.66	75.08	75.32	7.68	78.51	72.13	18.15	76.74
	In-use OEM	17.11	14.70	10.97	35.73	16.86	36.59	34.40	13.30	31.91
	No Filter	17.81	6.37	16.92	28.62	17.35	23.01	24.86	12.60	23.91
PM$_{2.5}$ (%)	HECA B	65.53	26.45	70.26	65.62	28.53	73.06	71.56	26.90	80.24
	HECA A	61.53	22.03	66.10	68.57	24.74	78.27	63.48	29.04	72.57
	In-use OEM	26.08	15.63	33.24	30.32	24.05	22.98	27.61	19.34	21.02
	No Filter	21.42	12.87	25.75	23.56	16.65	14.78	23.09	13.85	26.41

APPENDIX H. In-cabin UFP reductions in individual passenger cars tested. In-cabin UFP reductions under four filtration scenarios: HECA B, HECA A, in-use OEM, and no filters. The data are provided for stationary, local roadway, and freeway conditions.
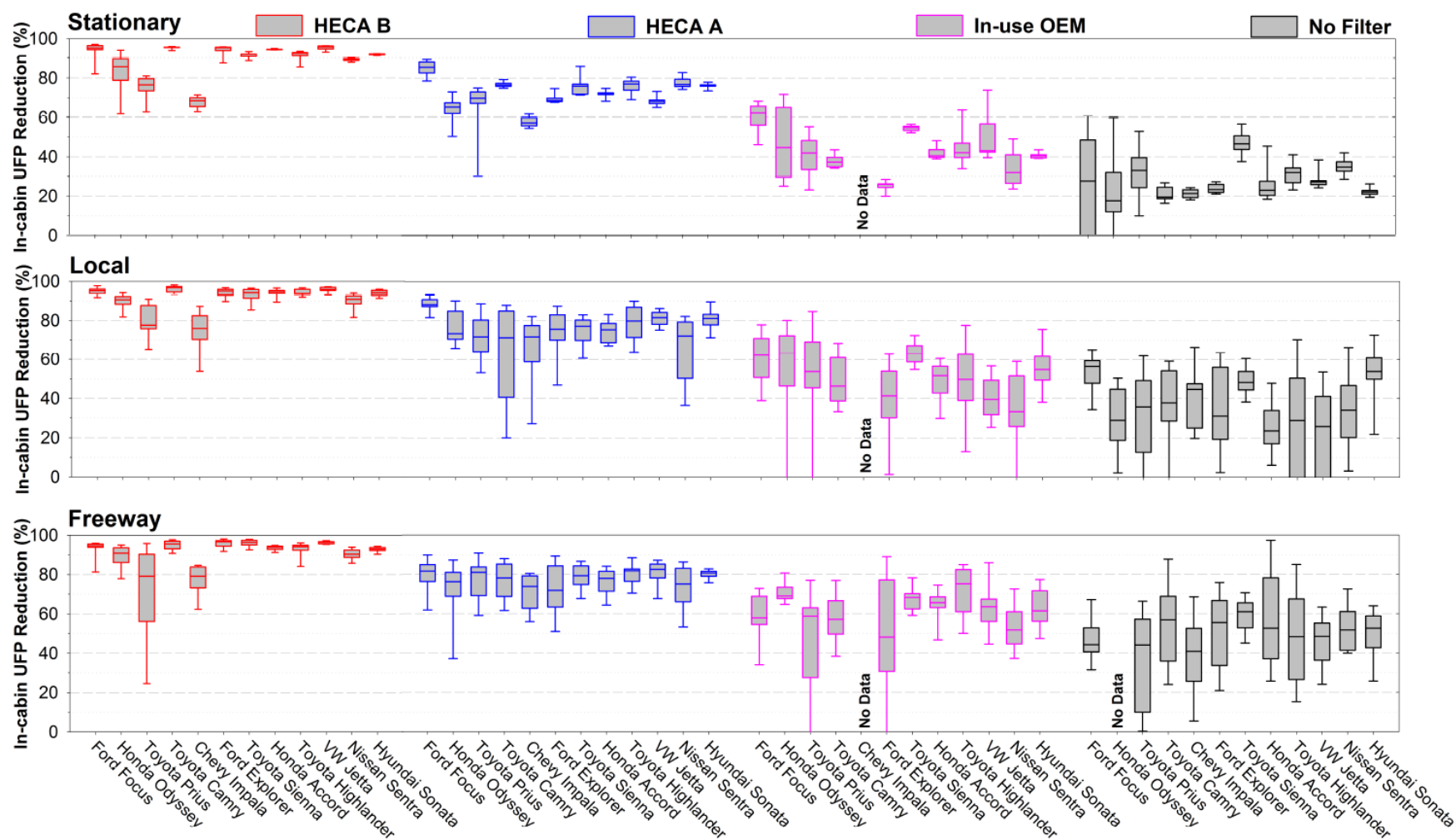
No data were collected because the test vehicle was not equipped with any cabin air filter for the in-use OEM filter scenario in Chevy Impala and instrument mal-function occurred during freeway sampling in Honda Odyssey.

APPENDIX I. A summary of in-cabin reductions (%) for UFP (data presented in Appendix H), PM$_{2.5}$, and BC in individual passenger cars tested.

.

Filtration Modes	Vehicle Models	Stationary			Local			Freeway		
		UFP	PM$_{2.5}$	BC	UFP	PM$_{2.5}$	BC	UFP	PM$_{2.5}$	BC
HECA B	Focus	93.52	NA	NA	94.88	NA	NA	92.85	NA	NA
	Odyssey	82.60	70.26	NA	89.60	89.75	NA	88.99	86.81	NA
	Prius	75.10	NA	NA	79.84	31.02	72.05	69.76	NA	73.54
	Camry	95.41	6.97	NA	96.30	8.84	76.19	94.40	15.56	39.20
	Impala	67.99	48.13	64.97	74.92	23.16	61.92	77.00	28.51	69.54
	Explorer	94.02	85.36	94.19	94.25	72.56	93.31	95.76	85.69	90.54
	Sienna	91.21	NA	93.14	92.95	NA	70.06	95.90	NA	70.22
	Accord	94.52	94.14	94.21	94.08	95.03	89.15	93.48	94.38	NA
	Highlander	91.49	82.78	NA	94.25	82.81	NA	92.38	90.10	NA
	Jetta	95.44	60.85	97.81	95.71	71.30	79.30	96.28	82.85	94.22
	Sentra	89.27	82.01	NA	89.56	83.03	NA	90.08	77.32	NA
	Sonata	92.02	59.25	92.07	94.01	73.57	92.35	92.77	76.74	90.34
HECA A	Focus	84.88	NA	NA	88.26	NA	NA	79.66	NA	NA
	Odyssey	64.19	72.90	NA	76.39	84.07	NA	71.48	90.71	NA
	Prius	64.67	NA	NA	71.16	NA	61.62	76.87	11.29	73.55
	Camry	76.77	23.53	NA	62.56	79.45	NA	76.18	11.27	29.96
	Impala	57.73	39.85	64.69	64.65	2.44	66.14	70.65	42.41	68.45
	Explorer	69.51	65.34	75.01	72.55	56.99	73.73	72.60	72.57	72.10
	Sienna	76.05	NA	25.55	74.84	NA	79.58	78.67	NA	82.59
	Accord	71.95	86.52	80.48	74.62	84.99	78.00	76.16	89.29	NA
	Highlander	75.77	77.74	NA	79.17	77.08	NA	80.02	85.86	NA
	Jetta	68.48	39.50	75.15	81.04	67.68	80.82	80.48	82.99	85.44
	Sentra	77.63	82.33	NA	65.56	80.35	NA	73.45	69.84	NA
	Sonata	75.97	66.10	90.39	80.67	71.87	79.02	79.97	68.26	85.00

In-use OEM	Focus	60.12	NA	NA	60.70	NA	NA	58.09	NA	NA
	Odyssey	45.70	33.24	NA	54.20	55.46	NA	71.09	50.66	NA
	Prius	41.42	NA	NA	49.30	NA	40.62	41.24	NA	34.21
	Camry	37.93	NA	NA	49.48	78.18	NA	56.42	61.80	30.15
	Impala	NA	7.87	3.54	NA	9.43	41.82	NA	7.16	31.91
	Explorer	25.19	NA	NA	37.70	NA	72.67	45.13	NA	43.73
	Sienna	54.54	38.75	7.07	63.34	39.40	22.75	67.13	43.07	NA
	Accord	42.02	36.84	NA	48.62	32.03	NA	64.05	37.61	NA
	Highlander	44.69	2.89	39.04	48.10	3.74	36.59	71.25	22.41	10.33
	Jetta	49.41	21.18	10.97	40.87	17.20	23.57	62.99	19.63	58.99
	Sentra	33.67	41.76	24.91	33.06	14.46	23.34	52.80	10.63	31.50
	Sonata	40.73	NA	NA	55.62	22.98	17.54	63.24	14.34	41.89
No Filter	Focus	21.75	NA	NA	53.61	NA	NA	47.26	NA	NA
	Odyssey	22.67	25.75	NA	30.14	37.71	NA	NA	40.02	NA
	Prius	32.19	9.07	NA	31.15	NA	31.03	37.21	NA	20.22
	Camry	20.92	NA	NA	35.55	55.95	NA	54.03	26.41	NA
	Impala	21.28	NA	NA	40.51	NA	42.70	38.79	NA	43.64
	Explorer	24.03	3.08	16.01	32.65	8.68	39.79	51.04	13.84	27.60
	Sienna	46.67	NA	27.06	48.81	NA	66.74	59.11	NA	41.15
	Accord	26.19	28.16	12.46	25.47	31.76	22.21	51.44	37.35	NA
	Highlander	31.66	28.92	NA	20.88	12.04	NA	47.49	27.71	NA
	Jetta	28.30	NA	17.83	11.03	NA	9.59	45.00	1.18	15.92
	Sentra	34.82	15.00	10.30	34.53	15.45	20.91	51.55	15.13	9.38
	Sonata	22.31	39.97	23.19	51.40	14.12	23.80	49.07	NA	13.21

APPENDIX J. In-cabin particle reductions (%) averaged across different passenger cars under all driving conditions. The tabulated data are estimated from the data collected in all test vehicles except for Toyota Prius and Chevy Impala, which had noticeable bypass flow around the installed filters.

| Pollutants	UFP (%)				BC (%)				PM$_{2.5}$ (%)			
Filtration Scenarios	HECA B	HECA A	In-use OEM	No Filter	HECA B	HECA A	In-use OEM	No Filter	HECA B	HECA A	In-use OEM	No Filter
Average	89.79	74.20	50.60	36.59	80.87	71.36	30.82	25.46	66.38	63.69	28.91	23.21
St. Dev.	7.78	6.52	11.49	12.48	15.00	16.61	16.84	14.47	27.70	25.61	19.52	14.15
Median	92.90	75.87	49.41	34.82	89.15	75.08	31.50	22.21	77.03	72.22	22.98	25.75

APPENDIX K. A summary of the numerical data plotted in Figure 13. I/O ratio reductions (%) when operating the on-board HECA filtration systems under different scenarios inside school buses. The tabulated data are estimated from the data collected in all test vehicles except for Toyota Prius and Chevy Impala, which had noticeable bypass flow around the installed filters.

Pollutants	Stationary		Local		Freeway	
	Average	St.Dev.	Average	St.Dev.	Average	St.Dev.
UFP (%)	87.73	3.57	87.62	8.2	88.25	6.54
BC (%)	81.53	6.87	83.86	3.8	86.95	3.53
PM$_{2.5}$ (%)	33.29	15.86	58.17	16.2	75.13	8.07

APPENDIX L. I/O reductions (%) averaged across all six school buses under all driving conditions. The I/O reduction represents the cabin air quality improvement by operating the on-board HECA filtration system.

Pollutants	UFP (%)	BC (%)	PM$_{2.5}$ (%)
Average	87.77	84.33	55.38
St. Dev.	5.86	5.01	22.28
Median	88.33	84.55	55.82

APPENDIX M. I/O ratio in the six school buses tested (A through F). I/O changes are shown for each test school bus with (white) and without (grey) operating HECA filtration systems. The data also present the differences in I/O ratios for UFPs, PM$_{2.5}$, and BC under stationary, local roadway, and freeway conditions.
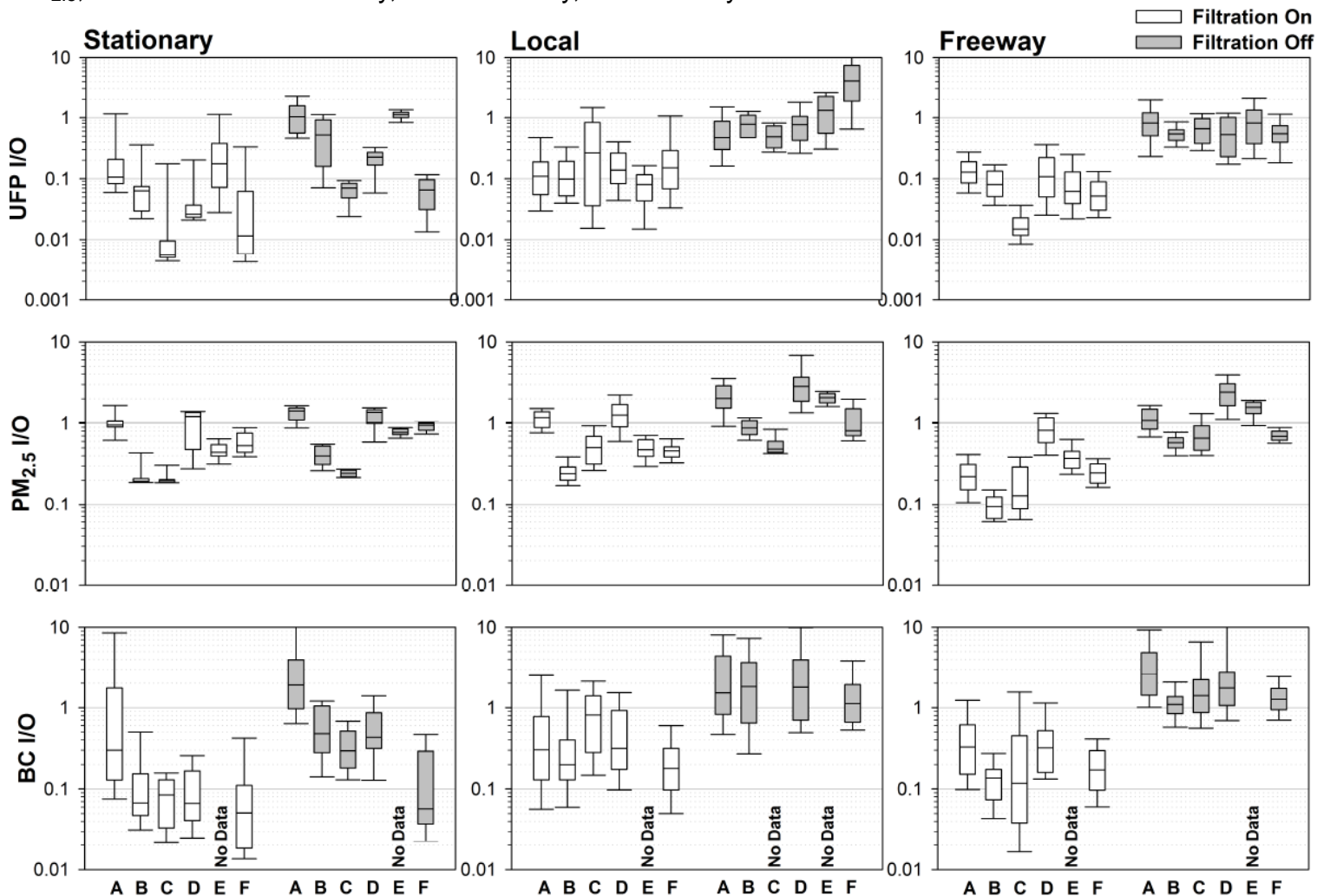

No data were collected because instrument mal-function occurred.

APPENDIX N. A summary of the I/O ratios in individual school bus tested (the data presented in Appendix M).

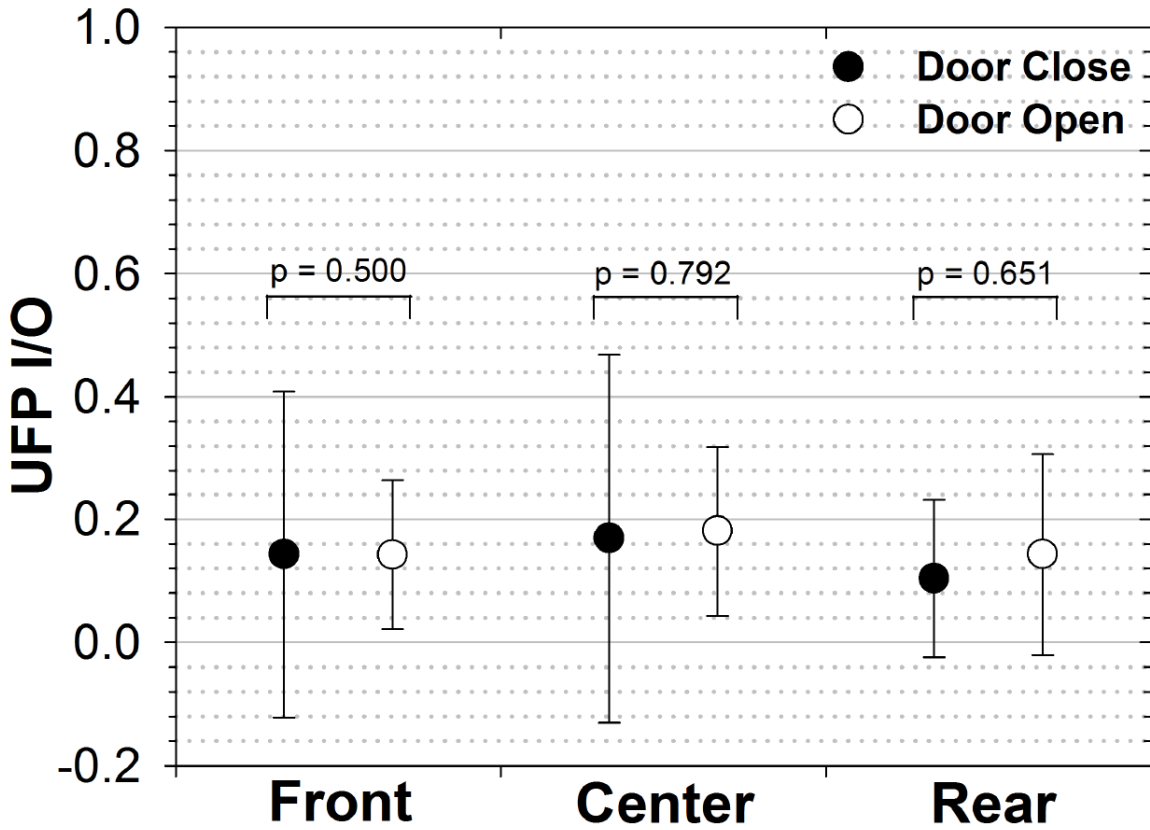| Location	ID	HECA Filtration System On						HECA Filtration System Off					
		UFP		PM$_{2.5}$		BC		UFP		PM$_{2.5}$		BC	
		Average	St.Dev.	Average	St.Dev.	Average	St.Dev.	Average	St.Dev.	Average	St.Dev.	Average	St.Dev.
Stationary	A	0.35	0.77	1.03	0.38	1.84	3.88	1.15	0.64	1.32	0.29	3.75	4.50
	B	0.10	0.14	0.25	0.16	0.15	0.19	0.55	0.37	0.40	0.11	0.59	0.39
	C	0.05	0.13	0.22	0.09	0.09	0.06	0.07	0.03	0.24	0.02	0.34	0.21
	D	0.06	0.09	0.97	0.45	0.10	0.08	0.22	0.08	1.24	0.33	0.57	0.41
	E	0.30	0.35	0.47	0.12	NA	NA	1.17	0.37	0.79	0.15	NA	NA
	F	0.07	0.13	0.60	0.21	0.12	0.22	0.07	0.05	0.92	0.11	0.14	0.17
Local	A	0.19	0.28	1.16	0.31	1.47	4.38	0.61	0.42	2.20	1.03	3.88	6.74
	B	0.15	0.16	0.26	0.08	0.66	1.89	0.75	0.42	0.88	0.25	3.28	6.22
	C	0.55	0.62	0.54	0.27	1.47	4.46	0.53	0.21	0.55	0.16	0.00	0.01
	D	0.19	0.14	1.32	0.57	2.05	9.43	0.87	0.60	3.31	1.97	4.70	11.53
	E	0.09	0.06	0.51	0.15	NA	NA	1.41	0.92	2.05	0.38	NA	NA
	F	0.37	0.60	0.48	0.14	0.35	0.88	4.96	3.97	1.10	0.58	1.94	2.58
Freeway	A	0.15	0.10	0.24	0.12	1.22	5.71	1.02	0.85	1.14	0.38	5.01	7.80
	B	0.10	0.09	0.11	0.08	0.16	0.19	0.55	0.19	0.58	0.16	1.19	0.60
	C	0.02	0.01	0.18	0.13	0.47	0.83	0.67	0.32	0.74	0.35	3.29	8.13
	D	0.16	0.13	0.86	0.36	0.50	0.70	0.60	0.40	2.45	0.96	58.97	452.95
	E	0.10	0.11	0.38	0.14	NA	NA	0.96	0.71	1.51	0.38	NA	NA
	F	0.06	0.04	0.26	0.08	0.21	0.17	0.60	0.35	0.71	0.13	1.57	1.30

APPENDIX O. Comparisons of size-resolved in-cabin UFP reduction data collected inside passenger vehicles under (a) stationary, (b) local, (c) freeway scenarios. Different line symbols represent averaged in-cabin UFP reductions with different filter types (i.e., HECA B, HECA A, In-use OEM, and No Filter).
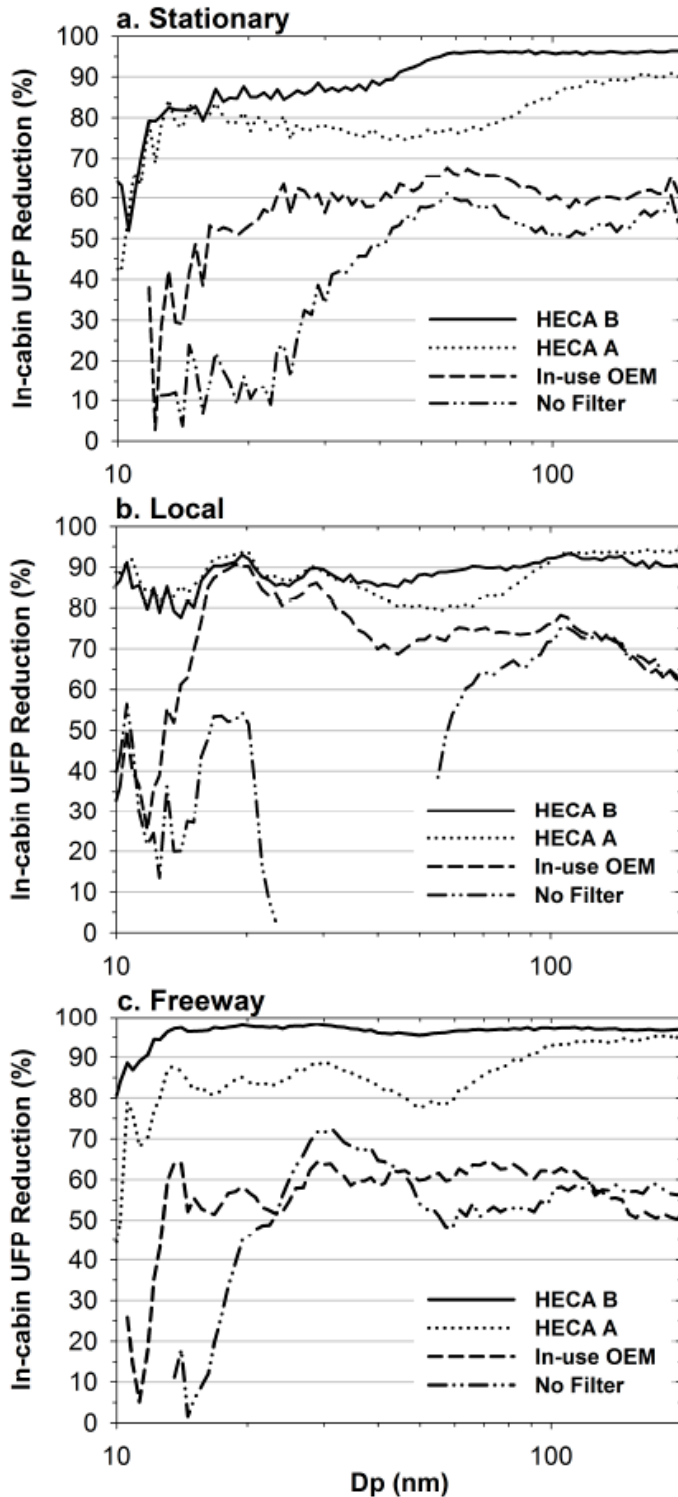
APPENDIX P. Comparisons of size-resolved in-cabin UFP reductions inside school buses without (panels a, c, and d) and with (panels b, d, and f) operating the on-board HECA filtration system under stationary (dots), local roadway (dash), freeway (solid) scenarios. The in-cabin UFP reductions with respect to on-road concentrations are plotted as a function of particle diameter (Dp). Line symbols and error bars are means and standard deviations of measurements from all six school buses, respectively.
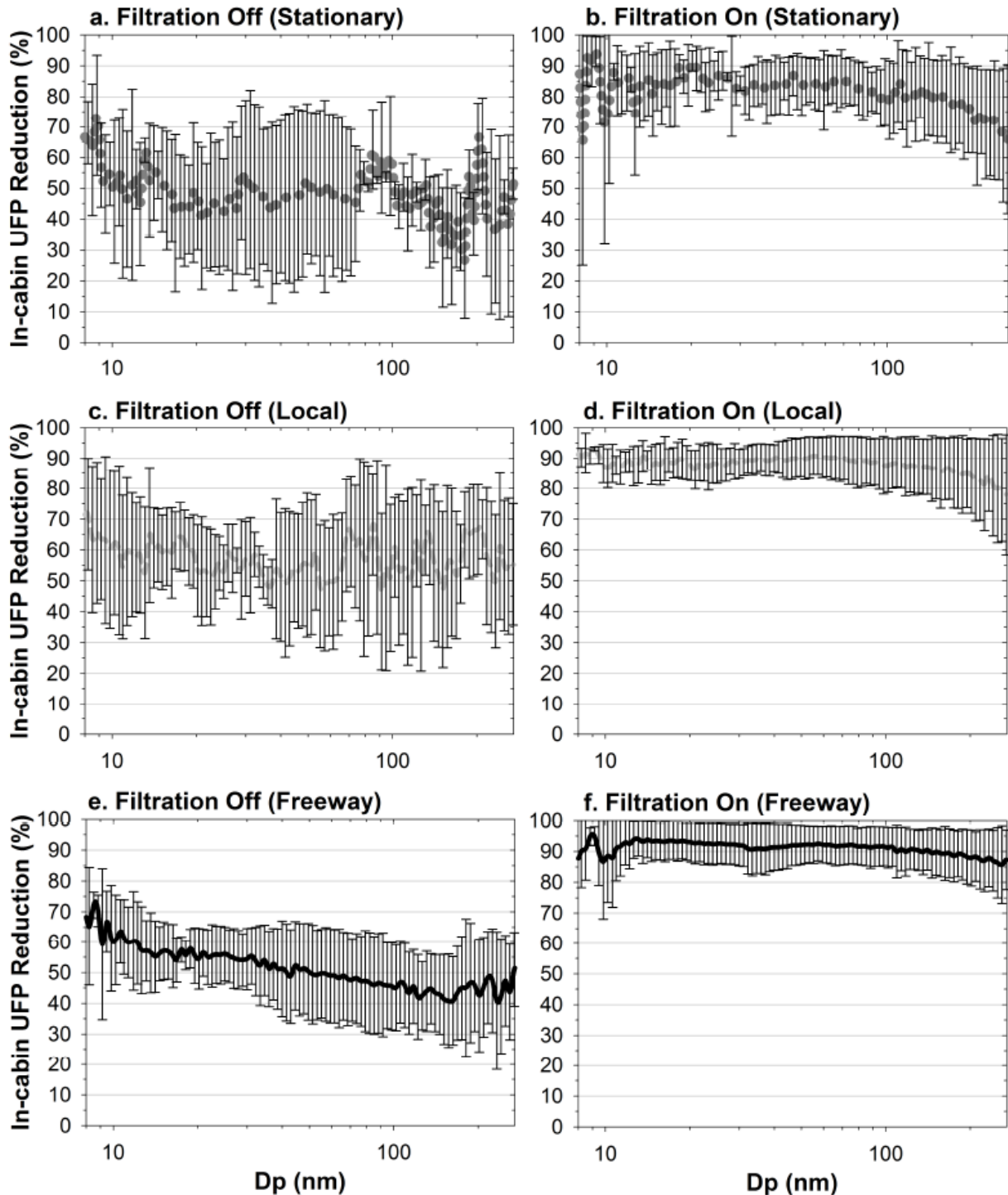
APPENDIX Q. UFP I/O Ratio at three in-cabin locations during door-operations of school buses. The circle symbols are the averaged UFP I/O ratios at different locations inside school buses when closing the door and opening the door under HECA filtration system operation. The error bars represent the standard deviation of the observation.

APPENDIX R. A time-series plot of UFP I/O measured in school bus F with closed door (white) and with open door (black) while operating HECA filtration systems. Similar findings were observed in the other school buses tested in this study.